UNITED STATES DEPARTMENT OF THE INTERIOR

GEOLOGICAL SURVEY

GENESIS OF A ZONED GRANITE STOCK, SEWARD PENINSULA, ALASKA

By

Travis Hudson

TABLE OF CONTENTS

	Page
LIST OF FIGURES	vi
LIST OF PLATES	ix
LIST OF TABLES	x
ABSTRACT	xi
ACKNOWLEDGMENTS	xiv
Chapter	
I. INTRODUCTION	1
Location	1
Methods of Study	3
Physical Setting	4
Previous Work	8
II. GEOLOGY	10
Metamorphic Rocks	10
Gneissic Rocks	11
Paragneiss	13
Orthogneiss	14
Graphitic Metasediments	15
Banded Hornfels	17
Dark-Gray Hornfels	18
Phyllitic Schist	19
Metasiltite	20
Mica-Quartz Schist	22
Chlorite-Muscovite-Quartz Schists	24
Carbonate Rocks	26
Carbonate Rocks Within Graphitic Metasediments	28
Marble in Isolated Masses	29
Thermal Metamorphism	31
Structure	34
Folds	34
Faults	35
Age of Structural Features	37
Igneous Rocks	38
The Granite Complex	38
Age	42
Contact Relations	42

Chapter | Page

Depth of Emplacement 45
Peripheral Dikes 47
Rocks of Zone 1 49
Facies 1A--Medium-grained Equigranular Granite 51
Facies 1B--Coarse-grained, Approximately Equigranular Granite 52
Facies 1C--Semiporphyritic Granite 53
Rocks of Zone 2 54
Facies 2--Porphyritic Granite 54
Rocks of Zone 3 57
Facies 3A--Seriate Granite 58
Facies 3B--Composite-textured Granite 60
Rocks of Zone 4 65
Facies 4A--Fine- to Medium-grained Equigranular Granite 67
Facies 4B--Leucocratic Granite 68
Microscopic Textures 69
Subsolidus Albite 69
Myrmekite 72
Fringed Biotite 75
Graphic Intergrowths 75
Megascopic Structures 79
Foliations 79
Dikes 81
Cavities 85
Inclusions 89
Joints 92
Deuteric Features 93
Plagioclase Composition 95
Modal Composition 98
Variation of Modal Averages 99
Chemical Composition 101
Variation of Major Oxides 101
Variation of Trace Elements 110
Variation of Trace Elements in Biotite . . . 114
Trace Elements in Pocket Muscovite 118
Comparison with Average Compositions of Granite and Biotite 119
Crystal Populations 125
Geometry of the Complex 130
External Form 130
Crystallization of the Granite Complex 134
Stage 1--Crystallization of Facies 1A 135
Stage 2--Crystallization of Facies 1B, 1C, and 2 139
Stage 3--Emplacement and Crystallization of Facies 3A 143
Stage 4--Emplacement and Crystallization of Facies 3B 147
Stage 5--Crystallization of Facies 4A and 4B 150

Chapter Page

Alternative Interpretations 154
Economic Geology 156
Geochemical Surveys 157
Alluvial Materials 157
Bedrock Materials 158
Spatial and Structural Controls 159
Similarities to Other Tin-Mineralized Areas 161
Origin of Mineralization 163

III. IMPLICATIONS OF THE STUDY 165

Crystallization of Zoned Granitic Complexes 165
Origin of Tin-Bearing Granites 167
The Concept of Metallogenetic Provinces 169
Timing of Fracturing, Final Crystallization, and Mineralization 172
Importance of Depth in Environments of Tin Mineralization 176

REFERENCES 182

LIST OF FIGURES

Figure		Page
1.	Location of the Serpentine Hot Springs area, Seward Peninsula, Alaska	2
2.	View of rolling tundra-mantled hills west of Serpentine Hot Springs	5
3.	View looking east across the southern part of the granite complex	7
4.	Hand specimens of biotite-plagioclase-quartz paragneiss and granite orthogneiss	12
5.	Outcrop of strongly deformed chlorite-muscovite-quartz schist	25
6.	Photomicrograph showing complex deformation features in chlorite-muscovite-quartz schist	27
7.	Distribution of tin-granite plutons, Seward Peninsula, Alaska	39
8.	Plot of modal Pl:Q:Or ratios for samples collected from all parts of the granite complex	40
9.	Generalized section across eastern contact of the granite complex illustrating the negative topographic expression of the granite-country rock contact	44
10.	Plot of normative Q:Ab:Or:SiO_2 ratios for facies 4B rocks	46
11.	Representative specimens of the textural facies in zone 1	50
12.	Representative specimens of zone 2	55
13.	Representative specimens of textural facies 3A	59
14.	Representative specimens of textural facies 3B	62
15.	Exposed contact between facies 3A and facies 3B	63
16.	Representative specimens of textural facies 4A and 4B	66

Figure		Page
17.	Photomicrographs of subsolidus albite	70
18.	Photomicrograph of interstitial myrmekite	73
19.	Photomicrograph of a fringed biotite crystal	76
20.	Photomicrograph of a graphic intergrowth of quartz in potassium-feldspar	77
21.	Mineral segregations in facies 3A rocks	80
22.	Discontinuous and interconnected aplite dikes in facies 3A rocks	83
23.	Composite, 3 ft wide, aplite-pegmatite dike	84
24.	Quartz-feldspar pegmatitic pod in facies 3A rocks	86
25.	Vuggy replacement selvage along walls of 2 ft wide pocket in facies 3A rocks	88
26.	Pipelike swarm of inclusions in facies 2 rocks	91
27.	Plagioclase compositions in the textural facies of the granite complex as determined optically	97
28.	Variation of modal averages through the facies sequence	100
29.	Variation of major oxides with percent SiO_2	107
30.	Variation of major oxides through the facies sequence	109
31.	Variation of selected whole-rock trace elements through the facies sequence	112
32.	Variation of selected trace elements in biotite through the facies sequence	115
33.	Schematic illustration showing possible relations within the granite stock soon after emplacement	137
34.	Schematic illustration showing possible relations within the granite stock near the end of stage 2 crystallization	140
35.	Schematic illustration showing possible relations within the granite stock after stage 3 crystallization	145

Figure Page

36. Schematic illustration showing possible relations within the granite stock after stage 4 crystallization 148

37. Schematic illustration showing possible relations within the granite stock after complete crystallization 152

LIST OF PLATES

Plate

1. Geologic map and generalized cross section of the Serpentine Hot Springs area, Seward Peninsula, Alaska . . in pocket

LIST OF TABLES

Table		Page
1.	Analytical data for K-Ar age determinations	43
2.	Whole-rock major oxide compositions of selected samples of the granite complex in weight percent	102
3.	Whole-rock trace-element composition of selected granite samples in ppm	103
4.	Results of semiquantitative spectrographic analysis of biotite separates from the granite complex	104
5.	Results of quantitative spectrographic analyses for selected trace elements in biotite separates from the granite complex	105
6.	Whole-rock trace-element composition of five selected samples of the granite complex	106
7.	Average and calculated bulk major-oxide composition of the granite complex and other granite averages in weight percent	120
8.	Average trace-element composition of the granite complex and of low Ca granites in ppm	122
9.	Average and range of trace element abundances in biotites from some felsic intrusive rocks in the western United States and from the Serpentine Hot Springs area	123
10.	Dimensions and calculated volumes of the granite complex based on a cylindrical shell model for zones 1 through 4	133
11.	Results of semiquantitative spectrographic analyses of composite grab samples of soil, altered rock, and gossan fragments collected along fault zone containing fine-grained dike	160

ABSTRACT

A composite epizonal stock of biotite granite has intruded a diverse assemblage of metamorphic rocks in the Serpentine Hot Springs area of north-central Seward Peninsula, Alaska. The metamorphic rocks include amphibolite-facies orthogneiss and paragneiss, greenschist-facies fine-grained siliceous and graphitic metasediments, and a variety of carbonate rocks. Lithologic units within the metamorphic terrane trend generally north-northeast and dip moderately toward the southeast. Thrust faults locally juxtapose lithologic units in the metamorphic assemblage, and normal faults displace both the metamorphic rocks and some parts of the granite stock. The gneisses and graphitic metasediments are believed to be late Precambrian in age, but the carbonate rocks are in part Paleozoic. Dating by the potassium-argon method indicates that the granite stock is Late Cretaceous.

The stock has sharp discordant contacts, beyond which is a well-developed thermal aureole with rocks of hornblende hornfels facies. The average mode of the granite is 29 percent plagioclase, 31 percent quartz, 36 percent K-feldspar, and 4 percent biotite. Accessory minerals include apatite, magnetite, sphene, allanite, and zircon. Late-stage or deuteric minerals include muscovite, fluorite, tourmaline, quartz, and albite.

The stock is a zoned complex containing rocks with several textural facies that are present in four partly concentric zones. Zone 1 is a discontinuous border unit, containing fine- to coarse-grained biotite

granite, that grades inward into zone 2. Zone 2 consists of porphyritic biotite granite with oriented phenocrysts of pinkish-gray microcline in a coarse-grained equigranular groundmass of plagioclase, quartz, and biotite. It is in sharp, concordant to discordant contact with rocks of zone 3. Zone 3 consists of seriate-textured biotite granite that has been intruded by bodies of porphyritic biotite granite containing phenocrysts of plagioclase, K-feldspar, quartz, and biotite in an aplitic groundmass. Flow structures, pegmatite and aplite segregations, and miarolitic cavities are common in the seriate-textured granite. Zone 4, which forms the central part of the complex, consists of fine- to medium-grained biotite granite and locally developed leucogranite. Small miarolitic cavities are common within it.

Eight textural facies have been defined within the complex, and mineralogic, petrographic, modal, and chemical variations are broadly systematic within the facies sequence. Study of these variations shows that the gradational facies of zones 1 and 2 systematically shift toward more mafic compositions inward within the complex. Seriate-textured rocks of zone 3 are similar in composition to those of zone 2, but porphyritic rocks of zone 3 and rocks of zone 4 mark shifts to more felsic compositions. These late-crystallizing felsic rocks are products of an interior residual magma system. This system was enriched in water and certain trace elements including tin, lithium, niobium, lead, and zinc. The complex as a whole has higher concentrations of these elements than many other granites. The nature of this geochemical specialization is particularly well demonstrated by the trace-element composition of biotite.

The crystallization history of the pluton was complex. The available data suggest that this history could have included: (1) chilling and metasomatic alteration adjacent to the contact, (2) *in-situ* crystallization in several marginal facies accompanied by some transfer of residual constituents toward interior parts of the pluton, (3) slight upward displacement of magma that was subjacent to the crystallized walls, accompanied by disequilibrium crystallization and local vapor saturation, (4) upward displacement of part of the residual water-rich interior magma, accompanied by rapid loss of a separated vapor phase, and (5) displacement of the margins of the pluton by normal faults, accompanied by loss of an exsolved vapor phase from the residual core of the pluton.

The vapor phase that escaped along crosscutting faults during the end stages of crystallization produced tin-mineralized zones in country rocks adjacent to the granite complex. The general geologic environment of the area is similar to that of other tin-mineralized areas, and the results of the study are applicable to an understanding of tin-deposit genesis as well as to problems of granite origin and crystallization.

ACKNOWLEDGMENTS

This work was suggested and supported by C. L. Sainsbury, who provided help both as the project chief of the U. S. Geological Survey's Seward Peninsula Project and as a friend during four summers of geologic investigations on the Seward Peninsula. Colleagues of the U. S. Geological Survey who have provided material and personal support are Henry Berg, George Gryc, George Plafker, and Bruce Reed. Lowell Kohnitz photographed the hand specimens and Norman Prime assisted in the taking of photomicrographs.

Richard H. Jahns, Konrad B. Krauskopf, Robert C. Compton, and William C. Luth of Stanford University gave helpful suggestions and discussions during various parts of this study. Jahns visited the Serpentine Hot Springs area in 1970, and he and Krauskopf have been major sources of guidance and direction throughout the investigation. Eugene Foord, John Lufkin, David Mustart, Jeffrey Steiner, and James Whitney participated in many helpful discussions concerning problems of ore genesis and magmatic processes.

During the summer of 1968, C. L. Sainsbury, Reuben Kachadoorian, and Thomas Richards participated in the field work as part of the regional investigations of the Seward Peninsula Project. Clifford Weyiounna was an excellent field assistant during the 1969 season and did much of the systematic sampling of the granite complex. In 1970, field assistance was provided by Tom Hayward who did most of the outcrop point counting. The 1969 field work was partially funded by

a Penrose Bequest Research Grant from the Geological Society of America.

I am thankful to many friends on the Seward Peninsula for their help during various stages of the field work. Special thanks go to the Tweet families of Teller who, while operating their mine near Taylor on the Kougarok River, were my closest neighbors. They made substantial efforts to help retrieve and repair disabled track vehicles, and their kindnesses and friendly hospitality will always be appreciated.

Finally, I am deeply grateful for the personal support given by Christine Allen through several years of this work and especially during the summer of 1969. Her contributions and sacrifices to the study far exceed what I can acknowledge here.

CHAPTER I

INTRODUCTION

The purpose of this study was to map and describe the geology of the Serpentine Hot Springs area of the Seward Peninsula, Alaska, to outline the crystallization history of the granite complex within it, and to discuss possible relationships between magmatic processes and the origin of tin mineralization in the area. Mapped lithologic and structural relations and the results of extensive laboratory investigations have been integrated in the study. The findings and conclusions probably are applicable to several areas of similar geology on the Seward Peninsula, and also to other areas characterized by the association of tin mineralization with biotite granite.

Location

The Serpentine Hot Springs area, in the north-central part of the Seward Peninsula, Alaska (fig. 1), is a 70 sq mi area in the Bendeleben D-6 and D-5 quadrangles and lies 120 mi north-northeast of Nome, the largest community on the peninsula. A maintained gravel road extends from Nome to points about 40 mi south of Serpentine Hot Springs, and from this road the area can be reached by track vehicle or light aircraft. The Arctic Circle is 45 mi to the north and Bering Strait, separating North America from Siberia, is 98 mi to the west (fig. 1).

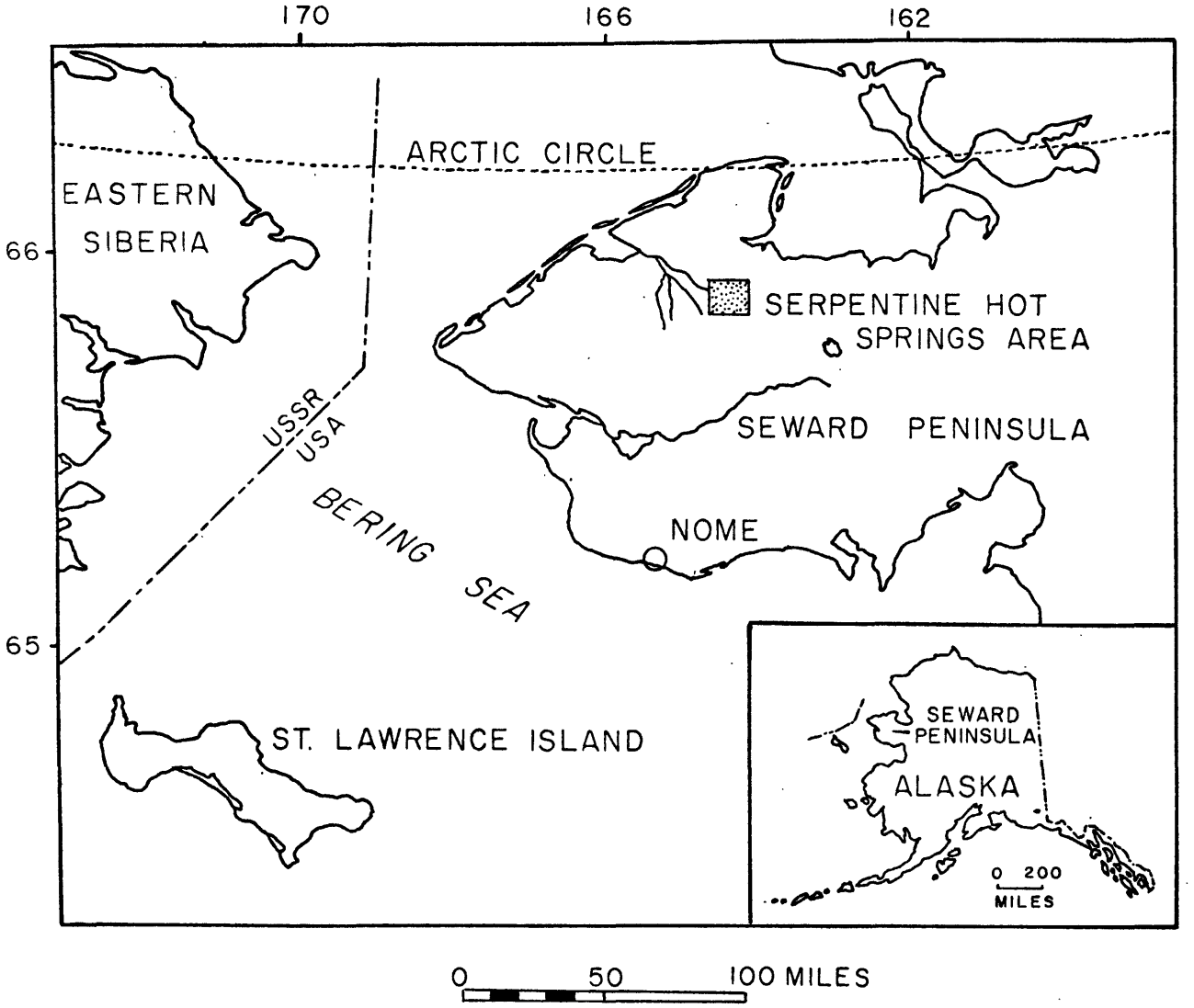

Figure 1. Location of the Serpentine Hot Springs area, Seward Peninsula, Alaska.

Methods of Study

Much of the field work was done from a base camp established in a large wood frame cabin at Serpentine Hot Springs. A track vehicle served as a mobile camp for work in outlying parts of the area. The geology was mapped by foot traverse on topographic maps at a scale of 1:63,360 and larger, and representative samples of rocks were collected throughout the area. Many outcrop relationships were documented by photographs. The field investigations were made during the periods June 25 to July 22, 1968, June 16 to August 23, 1969, and August 10 to August 27, 1970. The 1968 work was part of a regional mapping project with principal emphases upon studies and sampling of mineralized areas (Sainsbury and others, 1970), but during this time the margin of the granite complex was also outlined. The major lithologic units were defined, mapped, and sampled in 1969, when systematic sampling of the granite complex, on a 3/8-mi spacing, also was completed. In 1970, important structural features within the complex were studied, and a transparent plastic overlay with grid points spaced 1 1/4 in. apart was used to determine modal phenocryst populations in several of the rock types. The transparent grid was taped to flat outcrop surfaces for the counting of more than 1000 points at each of 23 localities.

Thin sections and hand specimens were systematically examined and described in the laboratory. Detailed examination of granite specimens was facilitated by the staining of K-feldspar on sawed slabs (Norman, 1974). The stained surfaces were point counted with transparent plastic grid overlays; maximum spacing of points was 2.5 mm, and 800 to more than 1000 points were counted on each slab. Plagioclase compositions

were determined optically by the a-normal method with reference to curves published by Deer, Howie, and Zussman (1966, p. 333). Some mineral identifications were made by means of X-ray diffraction powder patterns, and compositions and structural states were determined for a few K-feldspars according to the method of Wright (1968). Mineral separates were made through use of magnetic separators, heavy liquids, and polished metal vibrating tables.

Chemical data were obtained from the Branch of Analytical Laboratories, U. S. Geological Survey. The major oxide compositions of whole-rock samples were determined by procedures described by Shapiro and Brannock (1962), and semiquantitative trace element analyses of whole-rock samples and mica separates were made chiefly by procedures described by Meyers and others (1961). Normative mineral compositions were calculated by computer according to the C.I.P.W. method. Potassium-argon dating of two biotite separates was done by techniques described in Dalrymple and Lanphere (1969).

Physical Setting

The Serpentine Hot Springs area is located near the head of the Serpentine River, a stream with a tightly meandering, serpent-like channel. This part of the Seward Peninsula is in the Intermontane Plateau of Alaska (Wahrhaftig, 1965) and is characterized by a landscape with elongate, rounded ridges and hills that are in large part mantled by tundra (fig. 2). Where surface materials are exposed, they are dominantly frostriven rubble. Bedrock outcrops are scarce.

The study area straddles a north-trending ridge that reaches an elevation of 2592 ft within the area and a maximum of 2720 ft at

Figure 2. View of rolling tundra-mantled hills west of Serpentine Hot Springs.

Midnight Mountain 3 mi to the south. These are the highest points for many miles, and they contribute to an increased variability of local relief and an unusual degree of exposure of both surface materials and bedrock (fig. 3).

In areas underlain by granite, the ridges display spectacular pinnacle outcrop forms. In other areas, the summits and higher slopes have well-developed altiplanation terraces. Nonterraced slopes are convex except where talus rubble is abundant. The uplands are cut by ravines and sharp V-shaped avenues of drainage on steeper slopes. These merge at lower elevations into small valleys occupied by streams.

The area has an annual rainfall of 7 to 15 in. and receives 30 to 34 in. of snow (Hopkins and others, 1955). Permafrost is essentially continuous except locally along larger streams, in the vicinity of hot springs, and in places where the surficial cover is thin or absent, lacks vegetation, or is well drained. The vegetation is dominated by herbaceous tundra (Sigafoos, 1958), although shrub tundra and thick, brushy willows are locally abundant along streams.

Weathering, together with discontinuities in bedrock types, has produced some land forms specially characteristic of the area and environment. These include the negative topographic expression of the granite margin, pinnaclelike outcrops of granite, and talus and solifluction features. The trace of the contact between granite and country rocks lies on slopes that face inward toward the central parts of the granite complex. The relatively rapid rate of granite weathering and the more resistant nature of the surrounding zone of hornfels evidently have combined to produce this relationship.

Figure 3. View looking east across the southern part of the granite complex, showing altiplanation terraces developed in metamorphic rocks beyond. Distance to the far ridgeline is 6 mi.

The prominent outcrops of granite reflect frost action and preferential weathering along joint sets. Some of the outcrops are tens of feet high and are visible for many miles as highly anomalous irregularities in the landscape. These outcrops and their exfoliation features were first described and photographed by Collier (1902).

Talus slopes are common along margins of the steeper sided ridges and altiplanation terraces. In areas underlain by metamorphic rocks, these slopes are the places where outcrops are most likely to be found; elsewhere the bedrock is effectively mantled by rubble. In places where finer grained material occurs on the steeper slopes, well-developed solifluction lobes are present.

The streams, the larger of which are braided, are frozen during the winter except at places where they are warmed by hot springs. Thermal springs occur in alluvial materials of lower Hot Springs Creek at two localities (pl. 1). The spring waters are moderately mineralized and reach temperatures of 171^{o}F. A small undrained thaw lake, located 0.5 mi northeast of Serpentine Hot Springs, is the only standing body of water in the area.

Alluvial deposits are fairly extensive along lower Hot Springs Creek, especially at its juncture with the major tributary entering from the east where the flood plain is bounded by banks 10 to 20 ft high. Terrace gravels are exposed along these banks, which gradually become lower in an upstream direction.

Previous Work

Earlier field studies on the Seward Peninsula were generally of a reconnaissance nature or were directed to specific mineral deposits.

Those reports pertinent to the Serpentine Hot Springs area include overviews of the regional geology by Collier (Collier and others, 1908) and Sainsbury (1975), discussions of tin occurrences throughout the peninsula by Knopf (1908) and Steidtman and Cathcart (1922), and a detailed description of the geology of the central York Mountains by Sainsbury (1969). Results of an aeromagnetic survey have been reported by Johnson and Sainsbury (1974), and a regional Bouguer anomaly map has been published by Barnes (1971). Regional investigations of granitic rocks in western Alaska have been made by Miller (1970) and by Csejtey and others (1971).

A brief visit to the Serpentine Hot Springs area was described by Collier (1902), who later drew attention to the potential there for tin mineralization (1904a) and mentioned an unconfirmed report of lode tin in the area (1904b). Knopf (1908) confirmed the presence of placer cassiterite on Humbolt Creek. Moxham and West (1953) visited the area in search of deposits of radioactive minerals, Sainsbury and others (1968) described placer concentrates containing cassiterite from Humbolt Creek, and Sainsbury and others (1970) provided a preliminary description of the geology and the results of a more detailed investigation of mineralized areas. Some data on the thermal springs in the area were included in a report by Miller and others (1975).

CHAPTER II

GEOLOGY

The Serpentine Hot Springs area contains a diverse assemblage of metamorphic rocks that are in part intruded by an epizonal and composite stock of biotite granite. The metamorphic rocks comprise three different general assemblages, each of which can be divided into distinct lithologic units. The stock also comprises differing units, the mapped distribution of which reveals considerable complexity within the igneous complex and provides important data concerning structural relationships in the surrounding terrane.

Despite the poor exposures, it has been reasonably well established that thrust faulting, which antedated intrusion of the granite stock, was responsible for the juxtaposition of certain lithologic units, and that normal faulting, in part at least, followed the major part of crystallization of the stock. Tin and related mineralization was structurally controlled by normal faults southeast of the granite complex. Cassiterite occurs with gold in the placer deposits of Humbolt Creek, which has its headwaters in the mineralized area.

Metamorphic Rocks

The bedrock surrounding the granite stock consists entirely of metamorphic rocks. These rocks are late Precambrian and Paleozoic in age, of greenschist and amphibolite facies regional metamorphic grade, and together comprise three general lithologic assemblages:

(1) gneissic rocks, (2) graphitic metasediments, and (3) carbonate rocks. Gneissic rocks extend northward from a segment of the granite contact, graphitic metasediments are widespread and almost completely surround the pluton, and carbonate rocks occur locally within the graphitic metasediments and as discrete larger masses in the eastern map area.

Each of the general lithologic assemblages can be subdivided into two or more distinct lithologic units. These units have been mapped (pl. 1), but poor bedrock exposure commonly prevents a clear understanding of the nature of the contacts between them. The distribution of various lithologies probably reflects original sedimentary layering, but the structural and tectonic history of the area is so complex that unrecognized structural complications are probably present. Adjacent to the granite stock, the regionally metamorphosed rocks have been recrystallized in a well-developed thermal aureole.

Gneissic Rocks

The gneissic rocks, which extend northward from the north-central granite contact, include both paragneiss and orthogneiss. The two lithologies can be readily distinguished (fig. 4), and their separate distributions have been mapped. These amphibolite-facies rocks are texturally and mineralogically the highest grade regionally metamorphosed rocks of the area. Similar rocks, biotite-rich paragneiss and granitic orthogneiss, have been found elsewhere on the Seward Peninsula only in the heart of the Kigluaik Mountains, 76 mi southeast of the Serpentine Hot Springs area (Sainsbury, 1972). The gneisses in the Kigluaik Mountains have been dated radiometrically as late

Figure 4. Hand specimens of biotite-plagioclase-quartz paragneiss (right) and granite orthogneiss (left).

Precambrian (730 m.y.); a similar age is inferred for the gneisses of the Serpentine Hot Springs area.

The gneisses do not crop out, but the two kinds are not extensively intermixed in the surface rubble and the location of the contact between them is reasonably distinct. The nature of this contact has not been determined, but in the Kigluaik Mountains orthogneiss is intrusive into paragneiss (Sainsbury, 1972). The sharp break in metamorphic grade between the gneisses (amphibolite facies) and the immediately adjacent graphitic metasediments (greenschist facies), combined with the apparent absence of conglomerates and other expressions of a depositional contact, suggests that the graphitic metasediments have been structurally juxtaposed against the gneisses.

Paragneiss

Paragneiss is found adjacent and to the north of the stock. It is mottled light brownish gray in color and fine to medium grained. Thin concentrations of fine-grained biotite are discontinuous along the foliation and outline light-colored lenses and bands rich in quartz or plagioclase. The lenses and bands are discontinuous and ordinarily are less than 0.75 cm in thickness. The essential minerals in order of decreasing abundance are quartz, plagioclase, and biotite. Minerals present in minor amounts include chlorite, calcite, muscovite, green amphibole, opaques, apatite, and zircon(?).

The thin sections that were examined are from samples collected near the granite margin and show effects of thermal metamorphism. Quartz is unstrained and forms mosaics of anhedral, subequant grains with simple boundaries. Plagioclase ($An_{\geq 15}$) is consistently fine

grained and anhedral. It commonly is twinned and forms complexly interlocking aggregates with simple to sutured grain boundaries. Commonly it is poikilitic, and ovoid quartz is the most abundant inclusion. Biotite is pleochroic from straw yellow to dark brown, virtually inclusion free, undeformed, and with cleavages oriented both parallel and oblique to the trace of the foliation. The less abundant minerals include the accessories and such secondary minerals as chlorite, calcite, muscovite, and some iron hydroxides. Chlorite is interleaved with biotite, as is muscovite to a lesser extent. Muscovite more commonly occurs with calcite in fine-grained patchy aggregates of generally diversely oriented grains that replace plagioclase. Filmy, reddish iron hydroxides occupy fractures and grain boundaries adjacent to other secondary minerals.

Commonly associated with the paragneiss are fine-grained, lineated, well-foliated, dark greenish-gray amphibolites that may represent originally intercalated mafic volcanic rocks or dikes. Samples collected from near the northern granite contact contain granular clouded sphene, fine-grained granoblastic plagioclase, and green hornblende.

Orthogneiss

Orthogneiss is present in the northernmost part of the map area. It is a muscovite-plagioclase-quartz-microcline gneiss equivalent to granite in modal composition. The plagioclase:quartz:K-feldspar ratio is approximately 20:35:45. The color is a mottled light orange to gray, with the orange shades primarily due to iron hydroxide staining on mineral surfaces. It is dominantly fine grained except for some microcline grains that exceed 1 mm in maximum dimension. Muscovite and

lesser biotite are strongly oriented within segregations along the foliation. In contrast to the paragneiss, the felsic minerals do not occur in well-defined, compositionally segregated lenses and bands but are more homogeneously distributed.

In thin section the quartz grains are seen to be anhedral and the larger ones are elongate and oriented parallel to the foliation. Undulose extinction is moderately well-developed, and grain boundaries are simple to moderately complex. The plagioclase ($An_{\geq 15}$) is anhedral and angular, with poorly developed twinning that is hazy and distorted. The extinction is irregular, and some larger grains have ovoid quartz inclusions. Microcline is fine to medium grained, anhedral with interstitial boundaries, and in part semipoikilitic, including both quartz and plagioclase. Muscovite forms fine, intergranular grains or aggregates and is strongly oriented parallel to the trace of the foliation. Biotite is pleochroic from light tan to dark green brown, and is finer grained and much less abundant than the muscovite. Minerals present in minor amounts include very fine-grained granular opaque materials and subequant but anhedral zircon. Iron hydroxide is common as hazy films along nearly all fractures and grain boundaries.

Graphitic Metasediments

Rocks of the graphitic metasediment assemblage are the most abundant of the metamorphic rocks in the map area. Many different lithologies are present but in a general way the sequence is characterized by its fine grain, its dark color, its content of graphite, and its metamorphic structures that indicate a history of multiple deformation. These rocks are products of greenschist-facies regional metamorphism of fine-grained,

variably sorted, thin-bedded, and generally quartz-rich sediments. They include many layers of calcareous schists and some thin, dark-gray marble interbeds and light-gray marble lenses. Adjacent to the granite stock thermal recrystallization has produced rocks of hornblende hornfels facies.

The graphitic metasediments are part of a thick sequence which has been identified throughout the Seward Peninsula. The sequence was originally called the Kuzitrin Series in the central Seward Peninsula, and was correlated with similar but lower grade metasediments in the York Mountains by Brooks (Brooks and others, 1901). Most aspects of this correlation have been accepted by later workers, but the formal name, Kuzitrin Series, has been dropped and the sequence as a whole has become informally referred to as "slates of the York region" (Sainsbury, 1972) or simply "York Slate" (Sainsbury, 1975). In the York Mountains, Sainsbury (1969) described a conformable transition from lower Ordovician limestone downward through a thick unfossiliferous section of argillaceous calcareous rocks into these slates. Based on this relationship, he concluded that the graphitic sediments of the York Mountains are late Precambrian in age and, because these can be traced eastward to the Serpentine Hot Springs area, that the similar but higher grade metasediments in this area are also late Precambrian (Sainsbury and others, 1970, p. H6).

Variations in composition, texture, and response to thermal metamorphism, combined with marginally adequate exposures, allowed mapping of lithologically distinct units within the graphitic metasediments east of the granite complex. Their mapped distribution shows that they form a series of roughly north-south-trending bands parallel to the

regional structure. The separately identified lithologic units are: (1) banded hornfels, (2) dark-gray hornfels, (3) lineated phyllitic schist, (4) dark-gray metasiltite, (5) mica-quartz schists, and (6) strongly deformed chlorite-muscovite-quartz schists.

Banded Hornfels

Banded hornfels has been mapped in a zone along part of the eastern margin of the granite complex and in a parallel zone approximately 1400 ft farther east. The first zone contains hornfels throughout but the second grades into schistose rocks to the south. Overall the hornfels is medium light gray, but commonly it is somewhat mottled light to medium dark gray with variably distributed brown or green tints. Banding is conspicuous in most hand specimens and is defined by color, compositional, and textural variations. Individual bands are commonly less than 0.2 in. in width. The darker ones have a schistose foliation, whereas those that are lighter colored have a more sugary texture. In irregularly banded rocks the general fabric is more evenly schistose, with discontinuous stringy aggregates of mafic minerals concentrated along the foliation. Also present are some light-gray marble beds and somewhat coarser calc-silicate schists containing variable proportions of diopside, idocrase, calcite, and plagioclase.

The thermally recrystallized schists and hornfels are diopside-quartz-amphibole-plagioclase rocks that also contain red-brown biotite, chlorite, sphene, calcite, zircon, granular opaque materials and cordierite. Quartz forms aggregates of anhedral grains with irregular but simple interlocking boundaries. The largest grains are poikilitic plagioclase porphyroblasts that are as much as 0.6 mm across. The por-

phyroblasts are subequant, have irregular boundaries, and lack twinning whereas smaller nonpoikilitic plagioclase displays simple twinning. Both diopside and amphibole occur intergranularly between the generally larger quartz and plagioclase grains. Of the other minerals, biotite is the most common. It is diversely oriented and restricted to individual bands, as is chlorite, but the chlorite has a preferred orientation parallel to the foliation and is generally intergrown with amphibole and biotite. Dark pleochroic halos are present in some of the mafic minerals. The compositional variation between bands is dominantly the result of the preferred distribution of diopside, amphibole, and biotite.

Dark-Gray Hornfels

Dark-gray hornfels occurs between the two zones of banded hornfels. It is typically a schistose biotite-cordierite-quartz hornfels characterized by its uniformly fine grain size and medium dark-gray color. Most of these rocks are hard and break irregularly across schistosity. Those south of Hot Springs Creek weather to flaggy fragments that are as much as 2 or 3 ft across and tabular parallel to the foliation. Lithologies present in lesser amounts are dark-gray, fine-grained marble with isoclinally folded quartz stringers and green, fine-grained, schistose mafic dikes that are also thermally recrystallized.

Quartz occurs in aggregates of anhedral, angular, simply bounded grains that generally lack undulose extinction. The aggregates are elongate lenses that are oriented parallel to the foliation but also fill in "pressure shadows" adjacent to cordierite porphyroblasts. Cordierite occurs as subequant to elongate, very irregularly shaped grains oriented along the foliation and riddled with inclusions of

biotite, dusty to granular opaque materials, and quartz. Subequant cross-sections reach 0.5 mm across and in part deflect the adjacent foliation. Biotite, the only mineral readily identified in hand specimen, is dark red-brown in color. It has a bimodal preferred orientation parallel and approximately perpendicular to the foliation. Other minerals that are present include muscovite, associated with biotite, and disseminated opaque material that is dominantly pyrrhotite. The pyrrhotite has a tendency towards idiomorphic forms and is both subequant and elongate. In the latter case, the length is oriented parallel to the foliation.

Phyllitic Schist

Phyllitic schist occurs about halfway between the granite contact and Hill 2592. It is typically somewhat lustrous, medium- to medium dark-gray, calcite-albite-quartz-muscovite rock that weathers to platy and tabular fragments as much as 2 or more ft across. Megascopically it is fine grained, graphitic, locally porphyroblastic, and strongly lineated. The even and pervasive schistosity is very finely crenulated, producing a strong lineation parallel to the microfold axes. Oblique to this is a second lineation produced by broader spaced folds with wave lengths between 1/4 and 1/2 in. An incipient second foliation has developed along the axial planes of these broader folds.

Muscovite occurs as felted, dense aggregates forming bands parallel to the foliation, and elsewhere as intergranular, oriented grains or smaller aggregates. The denser aggregates display tight crenulations with the strong microfold lineation evident in hand specimens. Quartz is subequant and elongate, less than 0.35 mm across, and forms some

inclusions in albite porphyroblasts. The inclusions are ovoid in cross-section and intergranular grains have simple but irregularly angular boundaries. Albite, some with simple twinning, occurs intergranularly with quartz or as subequant porphyroblasts to 1 mm across. The porphyroblasts are generally poikilitic with included grains, dominantly quartz, that form strings, aggregates, or elongate individuals oriented parallel to the foliation. The porphyroblasts are rounded in outline, have boundaries that are smooth and continuous, and are commonly mantled by muscovite aggregates. Locally, intergranular, subequant calcite grains to 0.8 mm across make up 10 to 15 percent of the rock. Pale chlorite with greenish-gray interference colors forms aggregates or individual grains interleaved with muscovite, and may comprise 5 percent of a specimen. Other minerals that are present include dull-brown biotite, dusty graphite, granular disseminated opaque material that is dominantly hematite, and a minor amount of disseminated, euhedral tourmaline.

In summary, this schist was originally a thinly bedded argillaceous and quartz-rich rock. It is now characterized by the presence of graphite and abundant phyllosilicates, microscopic compositional banding, and well-developed metamorphic structures of two distinct generations.

Metasiltite

The most distinctive (but not dominant) lithology within the graphitic metasediment assemblage throughout the Seward Peninsula is a dark-gray, very fine-grained metasiltite that weathers to brittle, rectangular fragments less than a foot across. It consists almost wholly of quartz. Throughout the Serpentine Hot Springs area this lithology has been mapped separately and, although the nature of all

contacts has not been determined, it is possible that there is more than one dark-gray metasiltite unit within the graphitic metasediment sequence.

Rocks located on the west side of Hill 2592 are typical of this lithology. They are medium to dark gray, weather to platy and tabular fragments, and contain 80 to 95 percent quartz. The even grain size is less than 0.3 mm and commonly around 0.1 mm. Metamorphic structures, not everywhere obvious, include very thin banding, a strong lineation due to intense crenulation, and a thinly spaced regular schistosity. Where the metamorphic structures are well-developed, these rocks are graphite-quartz schists. The schists commonly have combinations of structures indicating a polydeformational history.

Quartz typically forms equant, angular grains in interlocking aggregates. Muscovite and lesser chlorite occur along quartz grain boundaries, and graphite forms disseminated dusty grains. Other minerals include tourmaline, plagioclase (some as porphyroblastic albite), epidote, and apatite.

Thermal metamorphism and physical deformation near thrust faults have produced two important textural variations. Within the thermal aureole of the granite complex, the metasiltite coarsens in grain size to a maximum of about 0.3 mm, banding becomes better developed because opaque material and phyllosilicates are concentrated along the foliation, and the quartz grains become semirectangular with very simple grain boundaries and elongation parallel to the foliation. Minerals that are locally developed within the hornfels zone include cordierite, brown biotite, and porphyroblastic anhedral andalusite. If the metasiltite has been deformed, usually in the vicinity of thrust faults,

the quartz has strong undulose extinction and complexly sutured grain boundaries. Crenulation of the principal foliation is common, and a strong lineation parallel to microfold axes is developed.

Among other variants known in the map area is a light-gray weathering metasiltite found near the headwaters of Humbolt Creek. In thin section, the lighter colored parts of these rocks differ from the normal dark-gray parts only in that they lack disseminated dusty opaque material. Apparently, the opaque material has been removed in some manner.

White quartz segregations and large veins are common in the metasiltite, especially in deformed zones or near the contact with the granite. Brecciated metasiltite, encrusted with rust-colored iron hydroxides, is locally common in the surface rubble of the metasiltite unit mapped at the head of Humbolt Creek.

Mica-Quartz Schist

Mica-quartz schists occur in a relatively wide belt that extends along strike from the granite complex across the headwater of Ferndale Creek and past Hill 2592. This unit, which displays more lithologic variations than others in the sequence, includes chlorite-muscovite-quartz schists, mica-tremolite-plagioclase-quartz schists, and, in zones of thermal metamorphism, biotite-rich schists. These schists are typically faintly brownish medium light gray, and are lineated, fine grained, and equigranular. A strong lineation is parallel to the axes of microfolds, and thin compositional layering can be seen in hand specimen but is usually more obvious in thin section. Locally these schists are calcareous and contain disseminated pyrite. Oxidation of pyrite leaves limonite spots and patches along the foliation. Thin

marble interbeds and lenses are relatively common, and near the granite complex greenish calc-silicate rocks, formed from impure calcareous interbeds, contain diopside with less abundant sphene and labradorite.

In thin section, these rocks are aggregates of many different minerals of variable size and distribution. As a result, they have a dirty or cluttered appearance. Quartz is equant, anhedral, and has simple to sutured grain boundaries. Tremolite, where present, is the next most abundant mineral and forms prismatic, faintly greenish, irregularly terminated, and variably oriented grains less than 0.2 mm long. Phyllosilicates commonly compose 40 percent of individual specimens and include chlorite with gray to deep-blue interference colors, muscovite, and biotite. Chlorite and muscovite generally occur in stringers and aggregates parallel to the foliation but biotite, less than 0.1 mm long and amber, light tan, or moderate red brown in color, is variably oriented, inclusion free, and in places interleaved with chlorite or muscovite. Both biotite and tremolite appear to be products of thermally induced recrystallization. Plagioclase forms anhedral, equant, semiporphyroblastic grains with inclusions of mica and quartz. Twinning is obscure to absent. Granular pyrite and other opaque materials are common, and individual grains, some to 0.1 mm across, tend to be angular and subidiomorphic. Other minerals include small euhedral tourmaline crystals, very fine-grained epidote, intergranular calcite, and trace amounts of apatite and subhedral zircon.

Hornfels textures are well developed in some of these rocks adjacent to the granite complex. In these, porphyroblastic cordierite(?) and andalusite(?) accompany biotite, plagioclase, and quartz. The quartz

is coarser than elsewhere in this unit and forms angular, equant grains with simple boundaries and even extinction.

Chlorite-Muscovite-Quartz Schists

The chlorite-muscovite-quartz schists have been severely deformed during thrust faulting and are texturally and structurally distinct from other parts of the graphitic metasediment sequence. They occur in two klippen, one on the summit and eastern side of Hill 2592 and the other on a small spur on the east side of Hill 2592. In general, they are greenish gray and weather to very irregular fragments. Megascopic structures are complex, characterized by lensoid white quartz segregations that are severely contorted and isoclinally folded (fig. 5). They are composed of quartz and muscovite in subequal amounts and less abundant chlorite. Minerals present in minor amounts are dusty to granular opaque material, epidote, albite, and tourmaline.

Some quartz is fine grained and irregularly angular to rectangular with simple grain boundaries, but more generally it is strongly strained with complex, granulated to sutured grain boundaries. Muscovite is fine to medium grained and occurs in deformed aggregates which outline distorted compositional banding. It is complexly microfolded and has elongate stringers of opaque material along cleavages and grain boundaries. Chlorite is a moderate grass-green color and is concentrated in layers or in dense aggregates which form sporadically distributed patches. Individual grains within these patches are bent and strained. Small opaque grains with square and rectangular outlines occur as inclusions in chlorite.

Figure 5. Outcrop of strongly deformed chlorite-muscovite-quartz schist with complexly folded white quartz segregations.

Of the other minerals present, fine-grained opaque material, probably graphite, is the most abundant. This material commonly is associated with muscovite in thin stringers that sharply outline the complex crenulations resulting from deformation. Albite forms small subequant, anhedral grains with irregular boundaries but it also commonly forms large grains that verge on being porphyroblastic. Tourmaline occurs as small rods along the axes of microfolds.

As a whole, this unit is compositionally similar to other parts of the graphitic metasediment sequence, but texturally and structurally it is much more complexly deformed. Megascopic and microscopic structures vary in complexity but they clearly reflect at least two episodes of deformation. A strong foliation is parallel to compositional banding defined by variations in chlorite, quartz, and muscovite concentrations. It has been intensely crenulated, variously folded, and displaced along axial plane shears (fig. 6).

Carbonate Rocks

Carbonate rocks occur as thin interbeds and small lenses as much as a few hundred feet long within the graphitic metasediment sequence and as larger, isolated marble masses with complex structural relations to surrounding metamorphic rocks. The carbonate rocks intercalated in the graphitic metasediments occur throughout the sequence in minor amounts but are most common within the mica-quartz schists and similar rocks found in the eastern part of the map area. The larger, isolated marble masses occur along the ridge east of Humbolt Creek. They do not support vegetation well, and stand out as light-colored knobs, mounds, and hills.

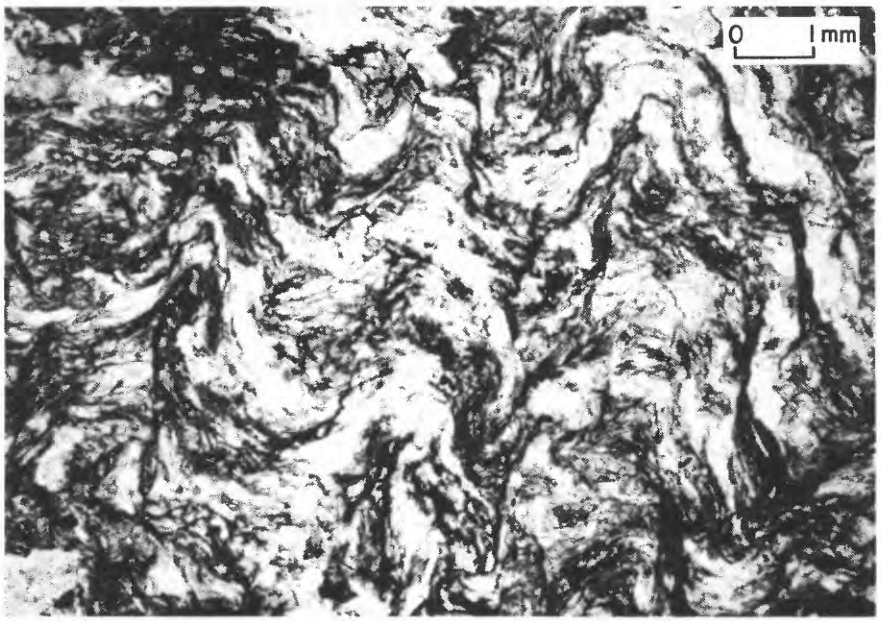

Figure 6. Photomicrograph showing complex deformation features in chlorite-muscovite-quartz schist. Plane polarized light; dark dusty and granular opaque materials in part outline crenulations.

Carbonate Rocks Within Graphitic Metasediments

The carbonate rocks intercalated in the graphitic metasediment sequence include calcareous schists and interbeds and lenses of marble. They have been mapped separately only in the area north of lower Ferndale Creek.

Marble interbeds are commonly less than 2 ft thick, dark gray, fine to medium grained, graphitic, and equigranular. The coloration of weathered surfaces is similar to that of fresh surfaces. Weathering does accentuate thinly spaced color banding and some specimens have thin, tightly folded, quartz bands that stand out conspicuously on weathered surfaces. More impure interbeds are medium dark gray to medium gray and micaceous.

The largest of the marble interbeds occurs in a klippe of chlorite-muscovite-quartz schist 3/8 mi south of Tin Mountain. Here a medium-gray marble band is approximately 10 ft thick, dips in general 5 to 10 degrees eastward, and crops out for more than 1/4 mi in an east-west direction.

Carbonate lenses, commonly less than 100 ft in length, are generally a thinly cleaved, medium-gray, thinly banded marble that weathers to platy fragments. Near the granite complex the lenses are recrystallized to more massive, splotchy medium-gray, variably grained marbles with coarse white calcite segregations. Impure layers in these thermally metamorphosed rocks have been converted to rust-stained, brown-green calc-silicate bands that are a combination of diopside, idocrase, plagioclase, calcite, and garnet.

Calcareous schists and associated marble are mapped separately north of lower Ferndale Creek. Here buff-orange weathering graphitic

muscovite-calcite schists grade upward into medium-gray, semiplaty marble. The relation of these rocks to underlying chlorite-muscovite-quartz schists is not clear, bur foliation attitudes in closely spaced outcrops of the two schists are nearly the same and the sequence may be entirely transitional.

Marble in Isolated Masses

East of Humbolt Creek are the largest carbonate bodies in the map area. They form nonvegetated hills, knobs, and mounds on which outcrops are limited and the surface is usually an accumulation of frost-riven rock fragments. The largest mass is exposed over about 1 sq mi and forms the northern end of the ridge east of Humbolt Creek. Other similar but smaller bodies occur farther south along this ridge and on its east flank.

The marble in these masses weathers to chunky, irregular fragments that are a fairly uniform medium gray in color. It is variably colored light and medium gray on fresh surfaces, fine to medium grained, and massive to thinly banded. The banding is defined by changes in the darkening of gray coloring and is caused primarily by variation in graphite content. Impurities other than graphite are uncommon.

Small-scale lithologic, textural, and structural variations are common. Calcite may be fine and medium grained in a single specimen, white calcite-cemented marble breccias can be found in some places, and fractures containing iron hydroxides are locally abundant. Individual calcite crystals more than 1 ft across and large boulders of milky-white quartz were found in the surface rubble of the northernmost body. Fragments of dark-gray, very fine-grained schist have

been found in surface rubble of the body south of elevation 1808. In the mass nearest elevation 1320, strongly deformed, dark-colored, graphitic calcite schists with small quartz segregations and veinlets are interbedded and interfolded with massive, buff-orange weathering, medium-gray, fine-grained dolomite.

One mile east of elevation 1320, adjacent to the eastern margin of the map area, abundant remnants of Paleozoic spaghetti corals (probably Silurian or Devonian, according to Charles Merriam, 1973, verbal commun.) were found in one of these bodies. Here the marble is massive and variable gray in color. The coral remnants are white calcite spots and short rods in a much finer grained, dark-gray, graphitic calcite matrix. These are the only fossils that have been found in the map area and serve to help identify this and similar isolated carbonate masses as significantly different in age from surrounding graphitic metasediments.

The contact relations of these marble masses to surrounding metasediments are complex and generally structural in nature. Imbricate thrust faulting is a dominant aspect of the regional structure of the Seward Peninsula (Sainsbury, 1969). The restriction of the marble masses to the higher elevations of the north-south-trending ridge east of Humbolt Creek, combined with their isolated nature as indicated by their mapped distribution and form, suggests that they are the remnants of a once larger thrust sheet that juxtaposed them against the graphitic metasediments. This possibility is also supported by the age discrepancy that is indicated by the fossil corals in some of the marbles, the variability of deformation and recrystallization within the marbles, the complex folding that is evident in the outcrops just east of elevation

1320 (Sainsbury, 1969). Normal faulting apparently has downdropped the northernmost thrust remnant and in places is responsible for the development of local brecciated zones.

In summary, the larger, isolated marble masses are Paleozoic in age and they are probably the remnants of a once larger thrust sheet. The Paleozoic marble masses differ from carbonate bodies intercalated in the graphitic metasediments in that they have more uniform weathering characteristics, a more conspicuous variability of small-scale lithologic, textural, and structural features, are less schistose or thinly cleaved, contain graphite as the principal impurity, and tend to be larger in size.

Thermal Metamorphism

The granite complex is sharply discordant and is surrounded by a well-developed thermal aureole. This aureole varies in horizontal width and is widest in the southeast part of the map area (pl. 1). Rocks within the aureole have been metamorphosed to hornblende hornfels and albite-epidote hornfels facies (Turner, 1968). Rocks of albite-epidote hornfels facies have complex textures and mineral assemblages gradational between those of the regionally metamorphosed greenschist facies rocks and the more extensively recrystallized rocks of hornblende hornfels facies. In general, incipient thermal metamorphism is indicated by the development of biotite and textural adjustments of quartz grain boundaries.

Biotite is present locally and replaces previous phyllosilicates. It is light colored and pleochroic in various shades of tan and yellow. In some samples it has a preferred distribution and is either spatially

associated with other mineral grains, such as opaque material, or is concentrated in definite compositional bands. Increasing temperature conditions are indicated by a darkening of the color to red-browns and/or increased grain size. In the higher grades, biotite tends to develop a bimodal orientation of the cleavage traces both parallel and perpendicular to the trace of the foliation.

Quartz grain boundaries are another sensitive indicator of thermal gradients in the lower grade rocks. Quartz boundaries in rocks that have not undergone thermally induced recrystallization are characterized by complex textural relations that in general include sutured grain boundaries, variable grain size, and undulose extinction. Upon recrystallization, there is a gradational change from these relations to one where the quartz boundaries have developed granoblastic textures. Incipient recrystallization is evidenced by boundary adjustments that tend to occur in individual zones or domains where quartz is the dominant mineral (essentially monomineralic domains). Here the initial changes are increases in the length of individual grain boundary segments, a homogenization of grain size, and a decrease in the degree of internal straining. These initial textural adjustments may be present in rocks having only greenschist facies mineral assemblages. As metamorphism proceeds, quartz grains throughout the specimen become recrystallized so that granoblastic textures are well developed. These granoblastic textures are unlike those described by Spry (1969), in that the triple points tend to be orthogonal rather than equiangular. This seems to be due to the influence of original banding and layering on the scale of one grain size in width. The advanced stage of textural adjustments in the siliceous metasediments is reached when individual quartz grains

become rectangular in outline and form layers one to a few grains in width that are separated by thin, discontinuous, oriented mica-rich segregations.

Gradational assemblages between those of greenschist and hornblende hornfels facies are most obvious in rocks that were originally argillaceous and compositionally inhomogeneous. In these, thermal recrystallization tends to be incomplete and disequilibrium assemblages and complex (dirty) textures develop. Disequilibrium assemblages are characterized by mineral compositions that vary and the coexistence of greenschist and hornblende hornfels facies minerals. Both plagioclase and amphibole (tremolite-actinolite-hornblende) can have a range of compositions within an individual specimen.

The characteristic minerals of the more extensively recrystallized rocks of the thermal aureole are andalusite and cordierite. Staurolite was observed in one thin section of hornfels. Andalusite tends to occur as subhedral porphyroblasts oriented parallel to the foliation, where cordierite occurs dominantly as very irregular, elongate, poikilitic porphyroblasts that create weblike textures in which oriented inclusions of mica are very abundant.

In summary, the granite complex is surrounded by a distinct thermal aureole in which rocks of hornblende hornfels facies have been formed. The contact relations and thermally induced assemblages are characteristic of an epizonal plutonic environment, and the temperature gradient between the pluton and the surrounding rocks evidently was steep. The greater horizontal width of the thermal aureole along the southeast margin of the pluton is probably a reflection of the shallow dip of the granite body in that direction.

Structure

The structural relations and features discussed in this section are principally developed in the metamorphic rocks of the area. The graphitic metasediments strike north-south to slightly northeast and have a low to moderate dip to the east. Isoclinal overturned folding may have affected parts of the metasediment sequence, high-angle faults are abundant in the southeast map area, and thrust faults are present in three areas. The thrust faults are part of the Collier thrust belt (Sainsbury, 1969), a thrust terrane that includes the entire Seward Peninsula and is characterized by imbricate, complicated faulting.

Folds

It was hoped that mapping of different lithologic units within the metasediments would help clarify structural relations, and it has done so with respect to some high-angle faults. But the question of the importance of large-scale isoclinal folding has not been resolved. Such folding is suspected because of the presence of a relatively small overturned anticline near the south-central boundary of the map area, that plunges to the south and has an amplitude of a few hundred feet. This anticline is in fine-grained, lineated and banded, quartz-calcite-albite-muscovite schists containing some biotite. These schists are mapped as part of the banded hornfels as they apparently grade into such rocks along strike to the north. Repetition of apparently similar units of banded hornfels, or related rocks was noted in the south-central map area between the small anticline and the granite contact and may

be an indication of larger isoclinal folding. The stratigraphy is so poorly known that the presence of such folds can only be suspected.

Faults

The presence of thrust faulting in three separate areas has been mentioned earlier in the discussion of the metasedimentary units. These areas include: (1) the gneiss-metasiltite contact in the north-central map area, (2) the klippen of highly deformed chlorite-muscovite-quartz schist and associated marble overlying the graphitic metasediments in the southern map area, and (3) the discontinuous marble masses located along the ridge east of Humbolt Creek.

In the area north of the granite the principal evidence for thrust faults is the marked discrepancy in metamorphic grade between the metasiltite and gneisses, the lack of features that would characterize a depositional contact between them, and the low dipping attitude of the mapped gneiss-metasiltite contact. Two such contacts have been recognized, and the mapped relations indicate that they dip in opposite directions. This suggests that the original contact may have been broadly warped.

Thrust faulting in the southern map area is evidenced by the severe deformation of the chlorite-quartz-muscovite schists (figs. 5, 6) and by their mapped distribution, which defines relatively thin and shallow dipping plates that were probably once connected. The almost flat-lying attitude of these plates is in sharp contrast to the strong north-south continuity of the other lithologic units that have been mapped in the graphitic metasediments.

On the ridge east of Humbolt Creek, isolated masses of Paleozoic marble overlie the graphitic metasediments and a thrust relation is

suspected because: (1) the mapped distribution of isolated masses indicates that they could have once been part of a continuous sheet, (2) silicification is localized at the base of the marble mass that is immediately east of the placer workings on Humbolt Creek, (3) dolomitization and complex folding are present in the second mass east of the placer workings on Humbolt Creek, and (4) the apparent age discrepancy between the underlying rocks, believed to be late Precambrian, and the Paleozoic (probably Devonian) overlying marbles. Silicification and dolomitization at and near the base of such marble masses is considered by Sainsbury (1969) to be indicative of thrust zones in the Collier thrust belt.

High-angle faults are the most widespread and easily recognized of the structures found in the area. Individual faults are evidenced by topographic discontinuities, linear zones of alteration or deformation, and offset of lithologic units. Where offsets have been recognized, the sense of displacement is normal. They are best developed in the metasediment sequence southeast of the granite complex and near or within the eastern margin of the granite.

Several apparently preferred orientations for the high-angle faults were recognized by Sainsbury and others (1970, p. H7-H8). The most conspicuous faults are those that trend northeast and northwest. Commonly, fault intersections are at high angles and the faults define rectangular to irregular fault bounded blocks. The granite margin is offset in many localities by steep faults, and one relatively large structure extends into the interior of the complex where it terminates as a series of hydrothermally altered splays in Zone 4. The somewhat regularly oriented faults concentrated within the granite complex near

its eastern margin are large-scale primary joints along which differential vertical displacements and local offset of the granite contact have occurred. The distribution of high-angle faults in the metamorphic rocks south and east of the granite is important because these structures, particularly those that trend northwest, have localized cassiterite and sulfide mineralization.

Age of Structural Features

The relative age of various structures can be determined in part, but the only absolute age reference is the 68 to 69 m.y. K-Ar age date for the granite complex. The deformation and metamorphism of the metasediments took place before emplacement of the granite complex, and folding within the graphitic metasediments may have preceded or accompanied thrust faulting. Microfolding in the graphitic metasediments is common, and as the axial planes are oblique to the primary schistosity, the microfolds may indicate that two periods of deformation affected these rocks. However, much microfolding could be related to local tectonic deformation associated with thrust faulting. The thrust faults themselves may have been warped, as suggested by the opposite dips of the gneiss-metasiltite contact north of the granite. The thrusting and possible warping of the thrust sheets predates granite emplacement. The high-angle faults may be of at least three ages. From older to younger these are: (1) northeasterly trending structures apparently conforming to regional structural trends, (2) northwesterly to westerly trending structures that displace the granite margin and some thrust sheets, and along which mineralization commonly is localized, and (3) somewhat regularly oriented primary joints near the eastern

margin of the granite, along which differential vertical movement has occurred but mineralization is not known to be localized.

Igneous Rocks

The igneous rocks of the area are all related to a Late Cretaceous epizonal stock of biotite granite. This stock is one of several very similar granite plutons that occur in a northeasterly trending belt across northern Seward Peninsula (fig. 7). All these plutons are related to tin mineralization and are informally referred to as "tin-granites." The granite stock in the Serpentine Hot Springs area is exposed over a larger area and to deeper levels than any of the other tin-granites in the belt and it is therefore best suited for the study of the magmatic processes that were operative during their crystallization.

The Granite Complex

The granite complex of the Serpentine Hot Springs area is a texturally and compositionally zoned intrusion exposed over an area of about 26 sq mi, roughly oval in plan except for a bulge in the northeast direction. The complex is composed of varieties of biotite granite and minor leucogranite. The overall felsic nature of the pluton is illustrated by the modal ratios plotted in figure 8. The average mode for the essential minerals, determined from samples collected from all parts of the complex, is 29 percent plagioclase, 31 percent quartz, 36 percent K-feldspar, and 4 percent biotite. Accessory minerals, amounting to less than 1 percent, include apatite,

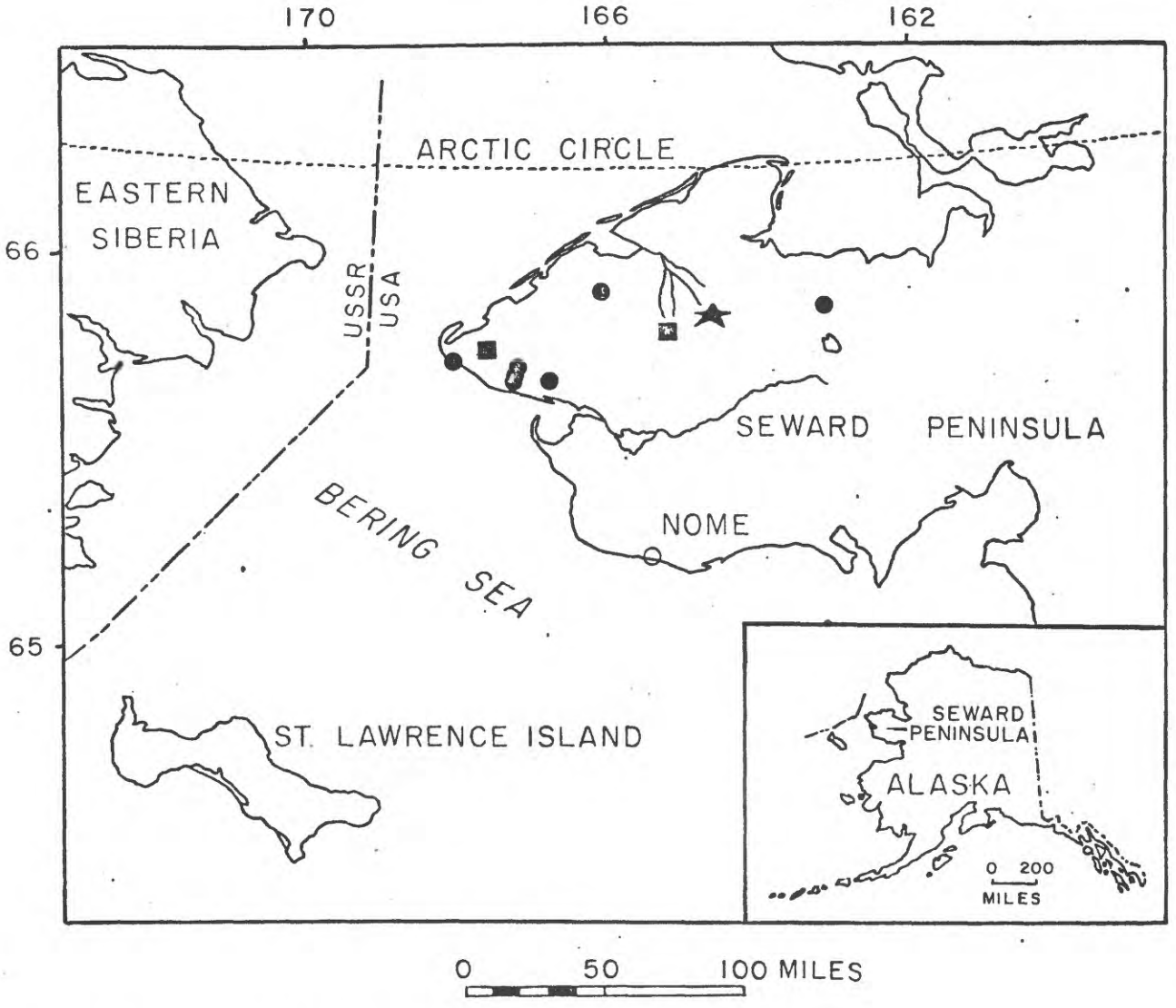

Figure 7. Distribution of tin-granite plutons, Seward Peninsula, Alaska (●, exposed; ■, inferred at depth; ★, granite complex of the Serpentine Hot Springs area).

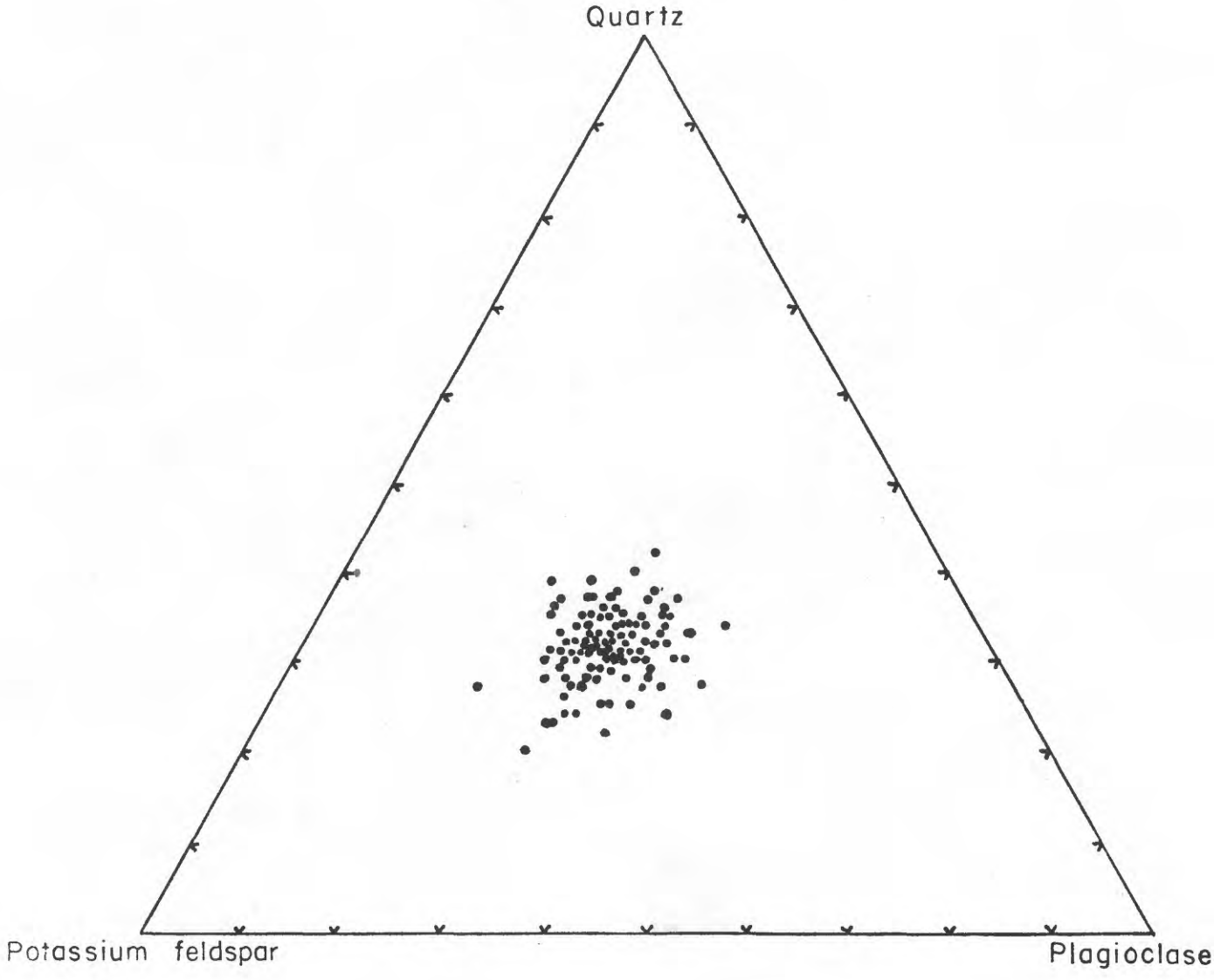

Figure 8. Plot of modal Pl:Q:Or ratios for samples collected from all parts of the granite complex.

magnetite, zircon, sphene, allanite, and monazite(?). Late-stage or deuteric minerals include muscovite, fluorite, schorl, quartz, and albite.

The complex is composed of several different textural facies that are part of four principal zones (pl. 1). Some of the facies are texturally and compositionally gradational with one another, but some form distinctly crosscutting intrusions. A sequence of the textural facies is defined by their mutual field relationships and by important shifts in major and trace-element compositions, modal ratios, mineral compositions, and petrographic relations. Study of these variations shows that the initially emplaced magma probably underwent fractional crystallization and evolved a residual magma system that was saturated with respect to an aqueous phase. A coexisting aqueous phase probably was also present at the contact upon initial crystallization and locally when some interior parts of the complex were almost totally crystallized. The evolved aqueous phase was enriched in tin and certain related elements. Final crystallization of the complex accompanied the localization of this tin-bearing fluid along late-formed fault structures that transect the pluton. These faults presumably represent the dynamic adjustments that took place within the complex as it neared complete solidification.

In the following sections, the field and petrologic characteristics of each zone and textural facies are described, with emphasis on those parameters that show variability from one facies to the next. The textural, structural, compositional, and spatial relations that are best studied in the context of the pluton as a whole are treated separately in latter sections. In the last section, the available data are integrated into an evolutionary model of the crystallizing pluton.

Age

A Late Cretaceous age is assigned to the granite complex on the basis of two K-Ar radiometric age determinations, provided by Marvin A. Lanphere of the U. S. Geological Survey, on biotite separates from samples representative of facies 1C (69 AH 283) and facies 3B (69 AH 228). The analytical data are shown in table 1. These dates help substantiate correlations with other bodies of biotite granite to the west (Collier and others, 1908; Sainsbury and others, 1968), one of which also has been dated by the K-Ar method and found to be 75.1 ± 3.0 m.y. old (Sainsbury, 1969, p. 61).

Contact Relations

The granite complex is in sharp and discordant contact with adjacent country rocks. In general, the trace of the principal contact is easily identified on air photos or on the ground, and is continuous and regular. The contact is in many places topographically expressed by changes in surface slopes between bordering country-rock areas and marginal areas within the pluton. These slopes face towards the interior areas of the pluton and are generally steeper in the country rocks than in the immediately adjacent parts of the pluton (fig. 9). Rocks of hornblende hornfels facies are present in the country rocks adjacent to the contact with granite, and their resistance to weathering compared to that of the granite is in large part responsible for the topographic relations between them. On a local scale, the granite-country rock contact can be very irregular, and diking into the country rocks is common. The dikes, discussed in more detail in a later section, can be several hundred feet long and in many places are clearly direct

TABLE 1.--Analytical data for K-Ar age determinations.

Field No.	Mineral	Location Lat(N) Long(W)	Percent K_2O	Ar^{40}_{rad} (Moles/gm)	$\frac{Ar^{40}_{rad}}{Ar^{40}_{Total}}$	Apparent Age (millions of years)
69AH 228	Biotite	65°50' 164°35' (Zone 1)	8.495	8.624×10^{-10}	0.90	67.5± 2
69AH 283	Biotite	65°51' 164°42' (Zone 2)	9.155	9.563×10^{-10}	0.90	69.4±2

(Argon analyses and age calculations by J. C. Von Esson; potassium analyses by L. B. Schlocker; decay constants for K^{40}: $\lambda_\beta = 0.585 \times 10^{-10}$ year^{-1}; $\lambda_\beta = 4.72 \times 10^{-10}$ year; atomic abundance of $K^{40} = 1.19 \times 10^{-4}$.)

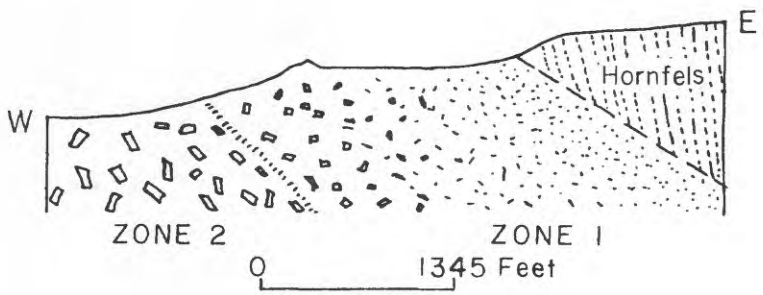

Figure 9. Generalized section across eastern contact of the granite complex illustrating the negative topographic expression of the granite-country rock contact.

offshoots of the granite complex. The principal contact gains additional irregularity where it is offset by high-angle faults.

Depth of Emplacement

A shallow environment for emplacement of the pluton is indicated by the nature of the contact relations, the presence of many open voids within it, and a tentative correlation with experimentally determined compositional relations for vapor-saturated parts of the haplogranite system. The development of rocks of hornblende hornfels facies within the thermal aureole indicates maximum lithostatic pressures on the order of 2 or 3 kbar (Hietanen, 1967). The many miarolitic cavities in facies 1A, 3B, 4A, and 4B rocks, including an open pocket 1.5 ft across, suggest that total confining pressures may well have been less than the maximum pressures indicated by the contact metamorphic mineral assemblages. For parts of the pluton that crystallized under vapor-saturated conditions and have bulk compositions that can be nearly completely defined within the haplogranite system ($NaAlSi_3O_8$-$KAlSi_3O_8$-SiO_2-H_2O), a possible indicator of depth is the relation of the observed bulk composition to the trend of successive isobaric minima for the haplogranite system (Duffield and Jahns, 1975). The only rocks that satisfy the requirements of being water saturated and of simple bulk composition are those of zone 4. The plot of normative Q:Ab:Or ratios for the analyzed rocks of facies 4B fall close to the isobaric minimum for a confining pressure of 1 kbar (Tuttle and Bowen, 1958, p. 75), as shown in figure 10. This suggests an emplacement depth of about 4 km if the confining pressure was totally lithostatic but, as is shown later, facies 4B rocks probably formed under conditions in which the

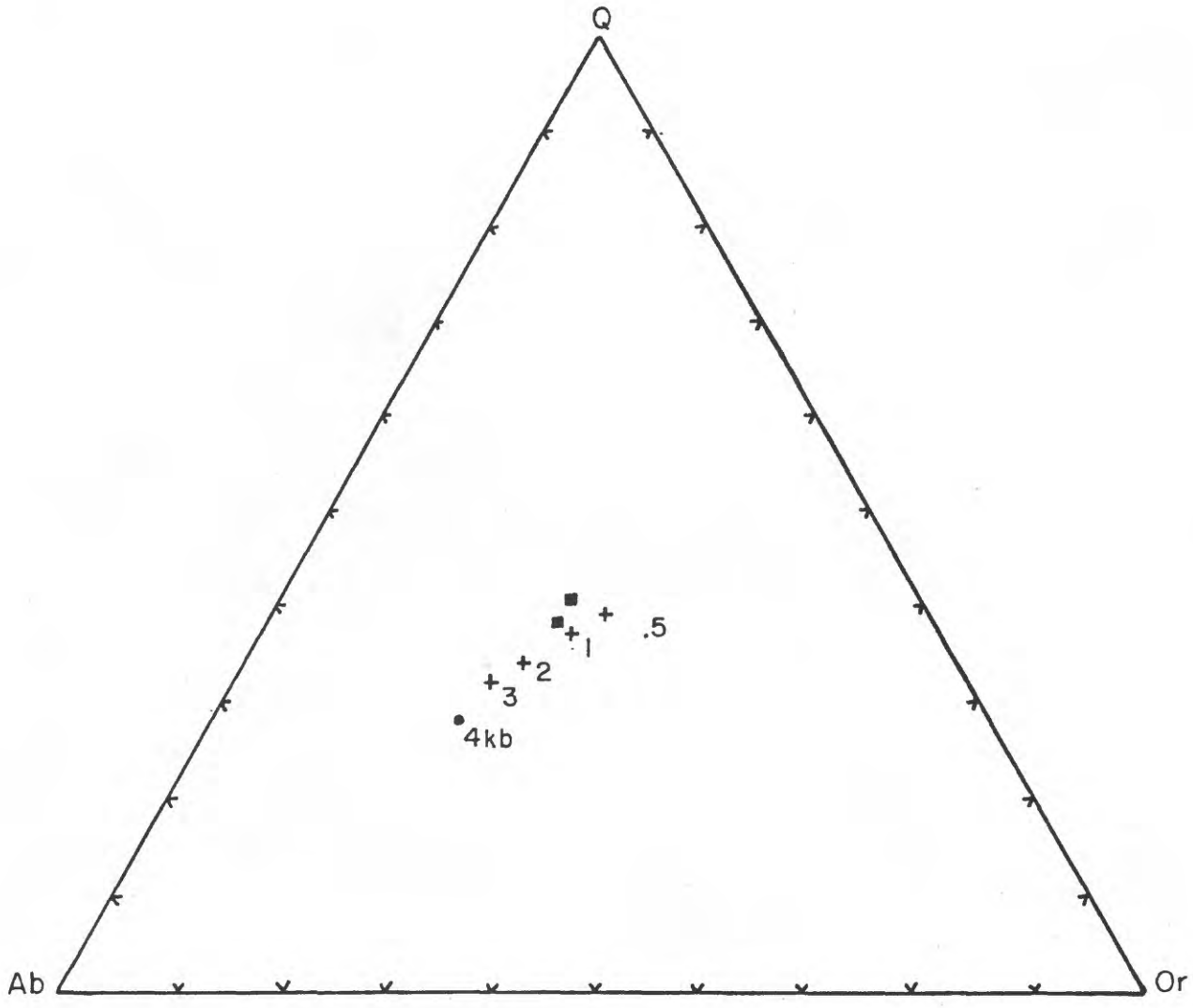

Figure 10. Plot of normative Q:Ab:Or:SiO_2 ratios for facies 4B rocks (■) in relation to the trend of successive isobaric minima determined by Tuttle and Bowen (1958, p. 75) for the system $NaAlSi_3O_8$-$KAlSi_3O_8$-SiO_2-H_2O.

pressure regime was complex and not necessarily totally lithostatic. For this reason, the 1 kbar confining pressure probably should be considered a minimum pressure, and the depth of emplacement is therefore thought to have been between 4 and 8 km.

Peripheral Dikes

Granitic dikes in the country rocks surrounding the granite complex include direct offshoots of the complex, isolated quartz porphyry dikes, and foliated dikes whose relationship to the granite complex is not well defined.

The dikes that are clearly direct offshoots of the granite complex occur peripherally to it throughout the area. These dikes are as much as a few hundred feet long, of differing width but commonly less than 5 ft across, and display no systematic orientation. They are very light gray in color, fine grained, and wholly or partly allotriomorphic equigranular in texture. Seriate hypidiomorphic textures and relatively abundant graphic and myrmekitic intergrowths are characteristic of some. The essential minerals include quartz and unzoned, variably twinned plagioclase in about equal proportions, somewhat less abundant perthitic microcline, and less than 5 percent mica which is dominantly biotite or muscovite. Accessory minerals are not abundant but locally include a few grains of allanite and more abundant schorl. The schorl is fine to medium grained and occurs as subhedral intergranular grains, irregular interstitial grains, and in small vugs. Vugs are relatively common, especially so in the more altered specimens. Alteration is the result of replacements, locally extensive, by muscovite. Oxidation

has caused discoloration and filming of grain boundaries by iron hydroxides together with chloritization of biotite.

Quartz porphyry dikes have been found in the peripheral zones of the thermal aureole southeast of the granite complex. These dikes intrude rocks of the graphitic metasediment assemblage, and at the present surface are not connected directly with the granite pluton. They are very fine grained, very light gray to white in color, and contain rounded-appearing megacrysts of gray quartz to 1 mm across, disseminated and commonly oxidized euhedral pyrite, and pervasive fine-grained muscovite. Some specimens contain numerous small vugs that in part display mica concentrations and secondary iron staining. Some of these dikes are apparently localized along high-angle fault structures, and at least one of them has been affected by postintrusion faulting (locality C, pl. 1). Soil samples collected along this dike contain anomalous metal values (see table 11).

An area with abundant diking borders part of the northern granite complex and has been identified separately on the geologic map. The dikes here include typical offshoots of the pluton, but more commonly they differ in that they are foliated and oriented in a general north-south direction. This orientation is parallel to the general strike of the metamorphic host rocks, and the dikes may actually be sills. They are found in association with both paragneiss and graphitic metasediments.

In general, the foliated dikes are light to medium gray and fine grained. In hand specimen, the foliation is defined by discontinuous segregations of oriented biotite (less commonly muscovite) and strung-out aggregates of quartz. Sugary textures are common and some gradations

from coarser, more obviously foliated, border zones into finer grained, sugary interiors have been observed. Some specimens are porphyritic, with individual plagioclase and perthitic K-feldspar phenocrysts that reach 5 mm in length. In thin section, the foliated dike rocks are dominantly allotriomorphic and contain, in decreasing order of abundance, quartz, plagioclase, perthitic K-feldspar, biotite, and muscovite. Secondary mineral development is common, consisting of minor to extensive chloritization of biotite and replacements by muscovite and sericite. Oxidation produces discoloration due to iron staining.

Rocks of Zone 1

Zone 1 is a discontinuous border zone that was mapped in the field on the general basis of its characteristic nearly hypidiomorphic equigranular textures and K-feldspar crystals that are clearly light gray to white in color. These characteristics distinguish Zone 1 rocks from those that are transitional inward from them, i.e., the rocks of Zone 2 that are porphyritic and have large pinkish K-feldspar crystals. Within Zone 1 the rocks systematically increase in grain size and show important textural shifts inward from the contact. These inward changes permit convenient subdivision into three different textural facies. From the contact inward, these facies are referred to as facies 1A, 1B, and 1C, and representative examples of each are shown in figure 11. In addition to the regular increase in grain size, both the K-feldspar and quartz populations show important transitional textural changes inward. K-feldspar changes from small anhedral grains that are not generally connected to one another (facies 1A) to those that are slightly above average in grain size, distinctly less interconnected in nature, and with better defined crystal morphology (facies 1C). In this same

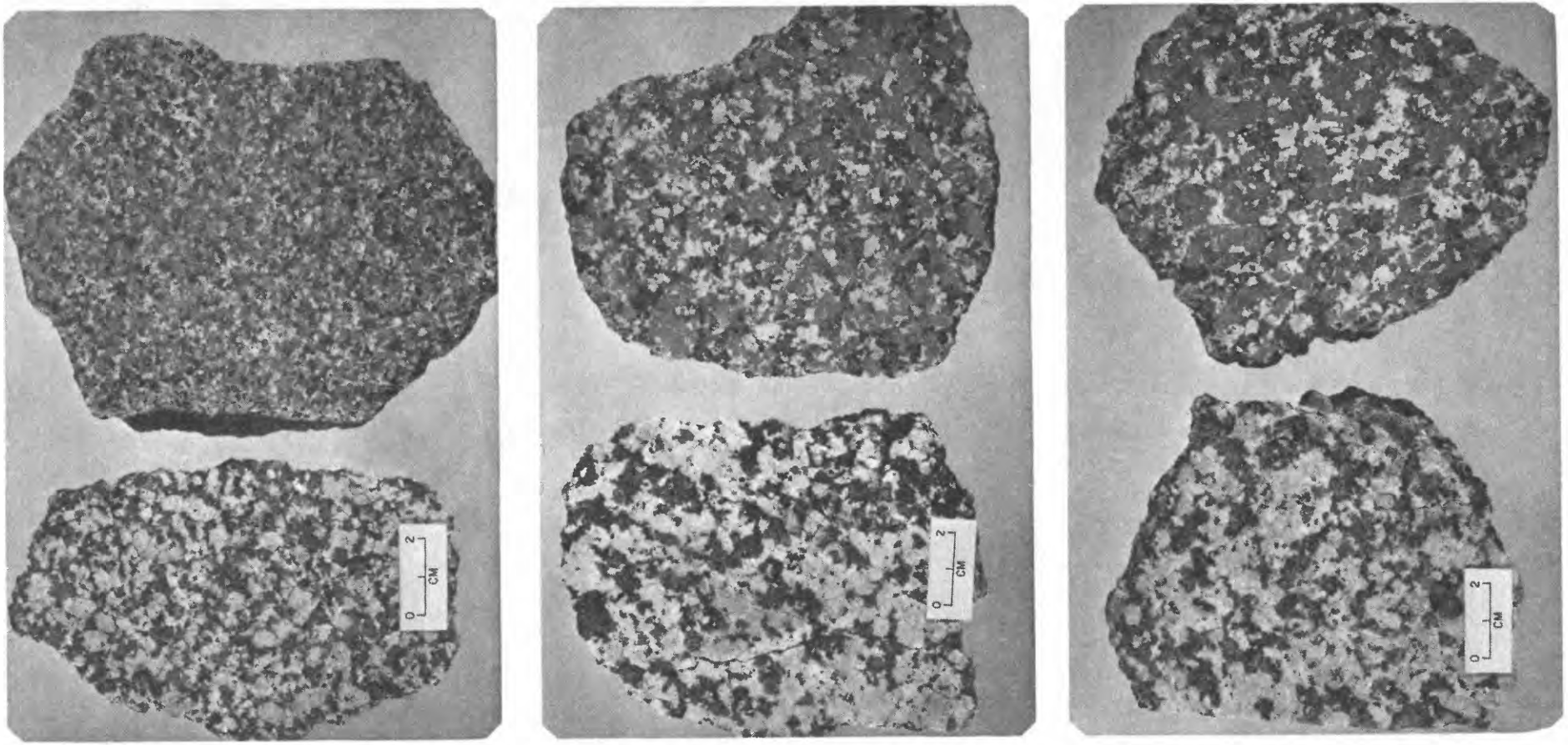

Figure 11. Representative specimens of the textural facies in Zone 1. From left to right: facies 1A, 1B, and 1C. Potassium-feldspar stained yellow.

sequence quartz changes from equant and generally unconnected grains to partially aggregated clusters of anhedral grains, and thence to totally aggregated clusters of anhedral grains.

Facies 1A--Medium-grained Equigranular Granite

Rocks of facies 1A are medium-grained, hypidiomorphic, and equigranular biotite granite. They are found adjacent to the contact and for a short but unknown distance inwards. They are similar to the peripheral dikes that are direct offshoots of the pluton. The essential minerals occur as individual equant, subhedral to anhedral grains that are dominantly 0.3 mm in size. Small, generally open miarolitic cavities are common but in some places they are larger and contain tourmaline, muscovite, and fluorite. Local inhomogeneity is caused by graphic intergrowths, domains a few centimeters across of quartz or feldspar concentration, and a few fine-grained intergrowths of plagioclase and biotite with some hornblende. In a few places muscovite extensively replaces some of these rocks.

Plagioclase displays a wide range of composition (An_8-An_{27}) and a characteristically even extinction. A few scattered, apparently unzoned phenocrysts of plagioclase are present in the finest grained parts of this facies. Zoning is uncommon and, where present, is not well developed. The zoned crystals have cores with even extinction and narrow normally zoned rims. In a few larger grains, faint oscillations are present in the rims. The compositional heterogeneity of the plagioclase exists between crystals in one specimen as well as between specimens. The zoned crystals and phenocrysts commonly have higher anorthite contents, but the composition of more typical crystals cannot be predicted within the overall range of composition.

Some K-feldspar is euhedral but most is anhedral, has undulose extinction and obscure grid twinning, and is string or stringlet microperthite. It is characteristically very clouded by minute inclusions of clay(?) minerals. Some quartz grains contain small inclusions of plagioclase, muscovite, and biotite whereas elsewhere in the complex small muscovite grains are usually the only inclusion. Biotite is fine grained, variable in pleochroism (moderate brown, root-beer brown, dark red brown, olive, and dark green brown), and contains abundant pleochroic halos. The accessory minerals include zircon, magnetite, and monazite(?). They occur characteristically as small inclusions in biotite, generally too small for optical identification. A tabular, high-relief mineral with high birefringence and inclined extinction may be monazite; it has not been observed elsewhere in the complex.

Facies 1B--Coarse-grained, Approximately Equigranular Granite

The biotite granite of facies 1B is transitional inward from that of facies 1A and occurs within a few hundred feet of the contact and into the medial parts of zone 1. The rocks are characterized by a texture in which linearly seriate, anhedral, and interconnected grains of K-feldspar occur with dominantly equigranular plagioclase and quartz. As a whole the rocks are coarse grained but the seriate K-feldspar, which is up to 2 cm across, has a median grain size generally greater than the average for quartz and plagioclase. Quartz is light to medium light gray and displays a variable degree of aggregation; clusters of two or more grains are common, but isolated subequant grains are also present. Xenoliths(?) of fine-grained plagioclase and biotite, up to 3 cm but commonly less than 1 cm across, are present in more than

half of the specimens studied. Other inhomogeneities include small concentrations of quartz and K-feldspar.

Plagioclase ($An_{\simeq 20}$) grain interiors display patchy extinctions, some localized or oriented seriate replacements, and narrow rims normally zoned to albite. Some larger grains have well-developed fine oscillatory zoning, but with little overall composition change outward to the rim. Twinning follows combinations of Carlsbad and albite twin laws. The K-feldspar is vein microperthite, commonly grid twinned, and locally has small plagioclase inclusions that outline growth boundaries. Biotite is dark reddish brown and is coarser and contains much fewer pleochroic halos (1 per every 4 or 5 grains) than that in facies 1A. The accessory minerals are intergranular allanite, sphene, magnetite, and zircon. Apatite, characteristically occurring as oriented small, euhedral inclusions in biotite, first appears in this facies.

Facies 1C--Semiporphyritic Granite

Biotite granite of facies 1C is transitional inward from that of facies 1B and makes up about the inner half of zone 1. The characteristic texture is one in which subhedral K-feldspar, coarser on the average than other minerals, occurs with coarse-grained plagioclase and quartz; the quartz is anhedral and almost totally aggregated into clusters containing two or more grains. The K-feldspar is seriate but has a skewed grain size distribution such that more than half of the grains are larger than the middle value in the K-feldspar grain size range. The interconnected nature of K-feldspar is significantly diminished compared to that in facies 1B. Quartz, darker colored than in facies 1A and 1B, commonly is medium light gray. As a whole, plagioclase and

quartz form an equigranular hypidiomorphic population with an average grain size of 0.4 to 0.5 cm. As the median K-feldspar grain size is commonly 1.5 times greater than this, facies 1C is considered to be semiporphyritic.

Plagioclase (An_{19-24}) grains have distinct central cores with patchy zoning, and marginal normal zoning with thin and somewhat faint oscillations. The K-feldspar is vein and patch perthite, has well-developed grid twinning, and is marked by growth boundaries defined by both plagioclase inclusions and thin albite lamellae. Biotite and the accessory minerals are similar to those in facies 1B except that idiomorphic development and grain size increase inwards.

Rocks of Zone 2

Rocks of zone 2 are texturally transitional inwards from those of zone 1. The contact between these zones was identified in the field on the basis of K-feldspar. The rocks of zone 2 contain pinkish-gray K-feldspar that is conspicuously coarser grained than other minerals. The transition from typical facies 1C rocks to those typical of zone 2 takes place over a distance of a few hundred feet. Rocks of zone 2 are texturally the most homogeneous in the entire complex and are considered to represent one textural facies, facies 2.

Facies 2--Porphyritic Granite

Representative specimens of facies 2 are shown in figure 12. Typically, the rocks are porphyritic with large (commonly to 3 or 4 cm long), light pink-gray K-feldspar phenocrysts in an approximately equigranular and coarse-grained groundmass of white to very light-gray plagioclase and medium-light-gray to medium-gray, anhedral quartz

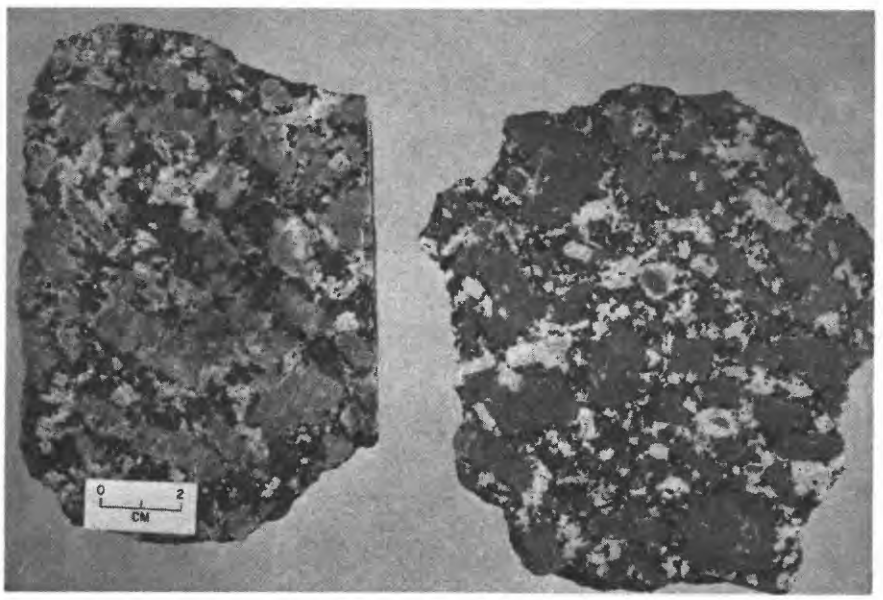

Figure 12. Representative specimens of Zone 2 (textural facies 2).

that is totally aggregated into clusters of two or more grains. The K-feldspar is dominantly euhedral and at least two times the average grain size of quartz and plagioclase. Considerable range in grain size exists, however, and some specimens contain medium- to fine-grained, subhedral to anhedral grains that are in part interstitial. The boundaries of large K-feldspar grains are irregular on a small scale, and the grains have interstitial offshoots and partly include adjacent grains. Preferred orientation of the phenocrysts is common and, combined with the variable aggregation of quartz and plagioclase, produces a small degree of local inhomogeneity.

The plagioclase (An_{18-26}) is distinctly zoned. Grain interiors are generally homogeneous but some display patchy extinction or marked optical discontinuity with surrounding material. Marginal bands with strong oscillatory normal zoning in which the oscillations are relatively sharp are wider than in rocks of the marginal facies. K-feldspar is well twinned, vein and patch perthite with a high proportion of inclusions, mostly plagioclase but also quartz and biotite. Included plagioclase generally outlines growth boundaries. Biotite is euhedral, commonly greater than 2 mm across, pleochroic to dark brown, and contains relatively few pleochroic halos. In some specimens biotite shows a preferred distribution, with concentration in a zone adjacent to large K-feldspar phenocrysts. Sphene, allanite, zircon, and magnetite are commonly euhedral, intergranular, and coarser grained than in more marginal facies. Allanite, for example, forms crystals as much as 1.5 mm long. Magnetite and biotite are more abundant in this facies than in any other.

Rocks of Zone 3

Zone 3 was originally mapped as a separate unit because it is much less consistent in lithology and structure than other parts of the complex. In general it is concentric with respect to zones 1 and 2 but the northeastward bulge of the pluton is due primarily to the intrusive emplacement of parts of this zone along the northeast contact of the original, pre-zone 3 pluton. The contact of zone 3 with earlier crystallized zones is relatively sharp, especially if compared to the highly transitional zone 1-zone 2 contact. The intrusive character of the zone 3 contact is clearest along the east-central and northeastern margins of the pluton, where zone 3 rocks have been emplaced into adjacent country rocks and now separate what probably once were continuous parts of zones 1 and 2. Along the western boundary of zone 3 the contact is concentric, with earlier zones indicating that displacement of the central zone 3 magma was relatively minor. This part of the contact is best seen about 1000 ft north of the mouth of McAble Creek. It is not well exposed, but zone 2 and zone 3 rocks occur a short distance apart in adjacent outcrops. At this locality, flow structures in zone 3 trend parallel to the contact and dip 80 deg to the north.

Characteristics of zone 3 that serve to distinguish it in the field are variations in texture and structure. As a whole the zone is inhomogeneous. It contains large crystals of white K-feldspar (up to 22 in. long) that are about half as abundant as the K-feldspar phenocrysts in zone 2. Structures that are common include biotite schlieren, coarse feldspar clots and segregations, discontinuous aplite stringers and dikes, pegmatitic pods and dikes, miarolitic cavities with euhedral

crystals of quartz and schorl, and some larger openings associated with pegmatites. Most of these are discussed in later sections.

The zone contains two textural facies: 3A is seriate and 3B is porphyritic with an aplitic groundmass. Rocks of facies 3A are irregularly intruded by those of 3B, and a large dike of facies 3B granite extends several hundred feet into zone 2 rocks at one locality. Most of the zone 3 discordance is due to emplacement of rocks typical of facies 3B. Outcrops, and the structures listed above, are more characteristic of facies 3A rocks than those of facies 3B.

Facies 3A--Seriate Granite

Rocks typical of facies 3A have an excellent seriate texture, shown in a representative example in figure 13. All the essential minerals are seriate, and the idiomorphic character of these becomes better developed with increasing grain size. Larger quartz crystals, for example, are doubly terminated, nonaggregated, and have a good basal parting. K-feldspar varies from small anhedral intergranular grains to large euhedral crystals with boundaries that generally are ragged on a small scale. Plagioclase appears to be subhedral in even the smallest grain sizes.

Some important textural and compositional characteristics of the feldspars correspond to the variations in crystal grain size and morphology. The larger plagioclase crystals (An_{18-27}) display zoning that is grossly similar to that in rocks of facies 2, but it is better defined, and both marginal bands with oscillatory zoning and more evenly normal-zoned rims are wider than in facies 2 plagioclase crystals. The finer grained plagioclase crystals lack such well-developed zoning

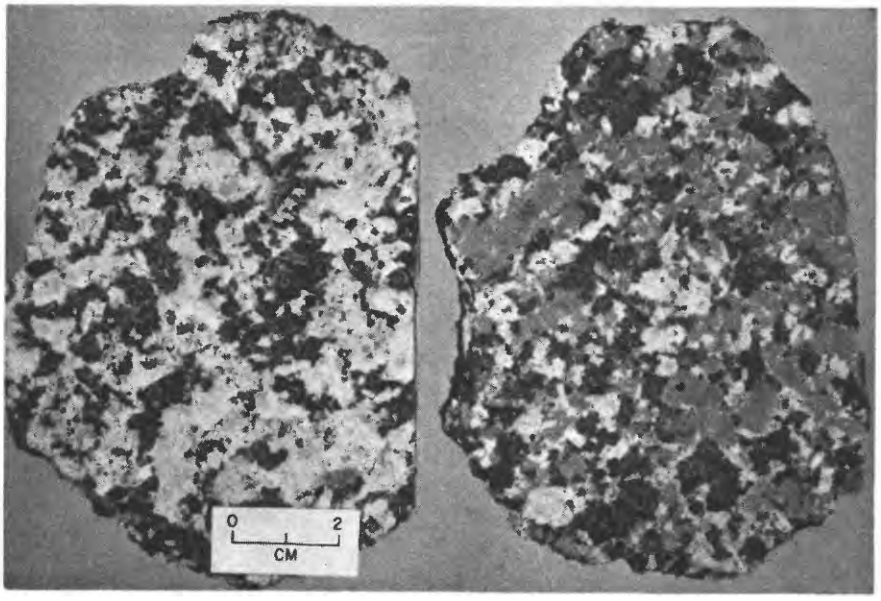

Figure 13. Representative specimens of textural facies 3A.

and contain distinctly less anorthite (An_{11-15}). The perthitic character and grid twinning of the K-feldspar increase with grain size. Larger crystals are good vein perthites similar to the phenocrysts of zone 2 except that some are a little larger and they are not pinkish in color. The smaller K-feldspar crystals are not strongly perthitic and have obscure grid twinning. X-ray studies of both the large perthites and the smaller K-feldspar crystals that do not contain microscopic albite segregations show that they are both maximum microclines but that there is a slight difference in their present albite contents. Two of the perthites have compositions of Or_{95} and Or_{92}, and two of the smaller crystals have compositions of Or_{97} and Or_{100}. As the compositions of perthites must have originally been much more albitic, these data show that the facies 3A rocks actually contain four feldspars: (1) larger well-zoned calcic oligoclase, (2) smaller unzoned sodic oligoclase, (3) larger sodic K-feldspar, and (4) smaller nonsodic K-feldspar.

Biotite is anhedral to euhedral and pleochroic in shades of amber brown, root-beer brown, and reddish brown in contrast to the general dark brown coloring of facies 2 biotite. The facies 3A biotite has variably abundant pleochroic halos and commonly includes apatite. Allanite, sphene, zircon, and magnetite are all present, dominantly as intergranular grains, but their abundance is variable.

Facies 3B--Composite-textured Granite

Rocks of this facies are found along the northeastern contact of the pluton and in small intrusive bodies with facies 3A rocks. A dike of this facies extends several hundred feet into the rocks of facies 2 from a point on the north-central contact of zone 3. The

facies 3A rocks generally do not form outcrops, and their distribution has mostly been determined mainly from their occurrence in frost-riven surface rubble. Even so, their contacts with adjacent rocks all appear to be sharp and discordant (fig. 15). The bulge along the northeastern side of the pluton is composed chiefly of rocks of this facies.

Representative examples of facies 3B are shown in figure 14. This facies is characterized by the presence of K-feldspar, plagioclase, quartz, and biotite phenocrysts in a very fine-grained, aplitic groundmass of the same minerals. Because of the marked bimodal nature of this texture, it is referred to as composite. The feldspar phenocrysts are subhedral to euhedral. Quartz phenocrysts are equant and in part idiomorphic, but generally appear rounded in cross section. They are fractured, and some of the fractures appear to be filled by groundmass K-feldspar fingers. The groundmass varies from as much as 80 percent to about 10 percent. Flow structures and feldspar segregations within the groundmass are locally present. There seems to be a complete textural gradation in hand specimens between composite and seriate, although the two are clearly the dominant textures within zone 3. The transitional textures are those in which most of the minerals are seriate to coarser grain sizes, but with a small proportion as distinctly finer and even-grained aggregates interstitial to larger crystals.

The phenocryst and groundmass mineral populations have distinctly different petrographic characteristics. The plagioclase phenocrysts display variable zoning relations and have maximum anorthite content of about An_{18}. Where the zoning relations are most obvious, they closely resemble facies 3A plagioclase, but the most distinctive characteristic of plagioclase crystals in this facies is that many phenocrysts do not

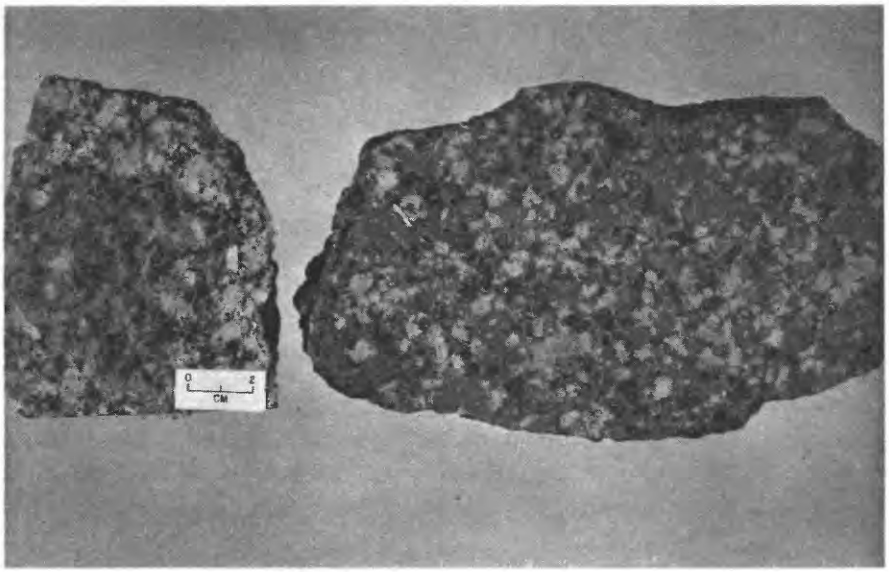

Figure 14. Representative specimens of textural facies 3B.

Figure 15. Exposed contact between facies 3A (above) and facies 3B (below) rocks located 1.5 mi northeast of Serpentine Hot Springs. Facies 3B rocks at the contact are composed of discontinuous very fine-grained light and dark bands. Dark bands contain more biotite, magnetite, and fluorite.

Feldspar-quartz pegmatite is localized at this contact immediately to left of photo. Pocket containing replacement selvage in facies 3A rocks (fig. 24) is exposed along a separated joint plane about 30 ft to the left of the photo.

show marked internal compositional variations. This is true for large crystals that clearly have well-developed oscillatory zoning as well as more typical phenocrysts that only appear to be markedly zoned because of twinning discontinuities or selective secondary mineral replacements such as sericitic bands or cores replaced by sericite, clay minerals, or iron hydroxides. The textural contrasts within the phenocrysts, including the apparent or real zoning but also well-developed albitic overgrowths, suggest a degree of compositional variability that actually is not present. The textural inhomogeneities appear to be ghost features inherited from original crystals that later were compositionally homogenized.

The K-feldspar phenocrysts can be as large as any in the complex but they are relatively less perthitic and contain fewer inclusions. Individual crystals are string microperthites and vein perthites, have grid twinning, and contain small plagioclase and ovoid quartz inclusions in subequal amounts. Overgrowths of nonperthitic K-feldspar are common. Biotite phenocrysts are subhedral to euhedral, dark brown to greenish brown, contain a moderate abundance of pleochroic halos, and in addition to apatite, commonly include magnetite and some relatively large euhedral zircon. Overall, accessory minerals are not abundant; magnetite is most prevalent, being both intergranular and included in biotite, and some well-formed sphene, allanite, and zircon crystals are present.

The groundmass is allotriomorphic to hypidiomorphic and equigranular, containing poorly twinned homogeneous plagioclase (An_{10}), nontwinned interstitial and partially connected K-feldspar, subequant quartz, and generally shreddy biotite crystals that are commonly replaced by chlorite and lesser muscovite.

Rocks of Zone 4

Rocks of zone 4 are exposed over an area of less than 0.5 sq mi in the central part of the complex. Outcrops are not present in this area, and all rock exposures are limited to surface accumulations of frost-riven rubble. The zone is roughly tear shaped in plan and is topographically expressed along its southern end as a small domal hill. It was originally recognized as a separate unit because of the presence of fine-grained equigranular and leucocratic granite which is not found elsewhere in the complex. Other distinguishing aspects are the dominance of fine-grained allotriomorphic to hypidiomorphic equigranular rocks, and the occurrence of abundant small open miarolitic cavities about 1 mm across, quartz stringers and veins, and some disseminated sulfide mineral(s). The rocks are transected by several faults along which zones of argillic and related alteration are present.

As outcrops are lacking, this zone was studied by examination of thin sections and hand specimens of rocks collected, for the most part, from float along a traverse across its maximum dimension. In this traverse, all lithologic variations were sampled. The specimens show that two textural facies predominate and that rocks texturally and compositionally similar to those typical of facies 3A also are present. The latter are seriate and subordinate in abundance to those of facies 4A and 4B, which are both fine to medium grained, allotriomorphic to hypidiomorphic, and equigranular, but facies 4A is biotite granite and facies 4B is leucogranite (fig. 16). Rocks of facies 4A are widespread through the zone, but facies 4B rocks are restricted to areas near hydrothermally altered fault zones. The presence of facies 3A type rocks, largely surrounding this zone as well as scattered through it,

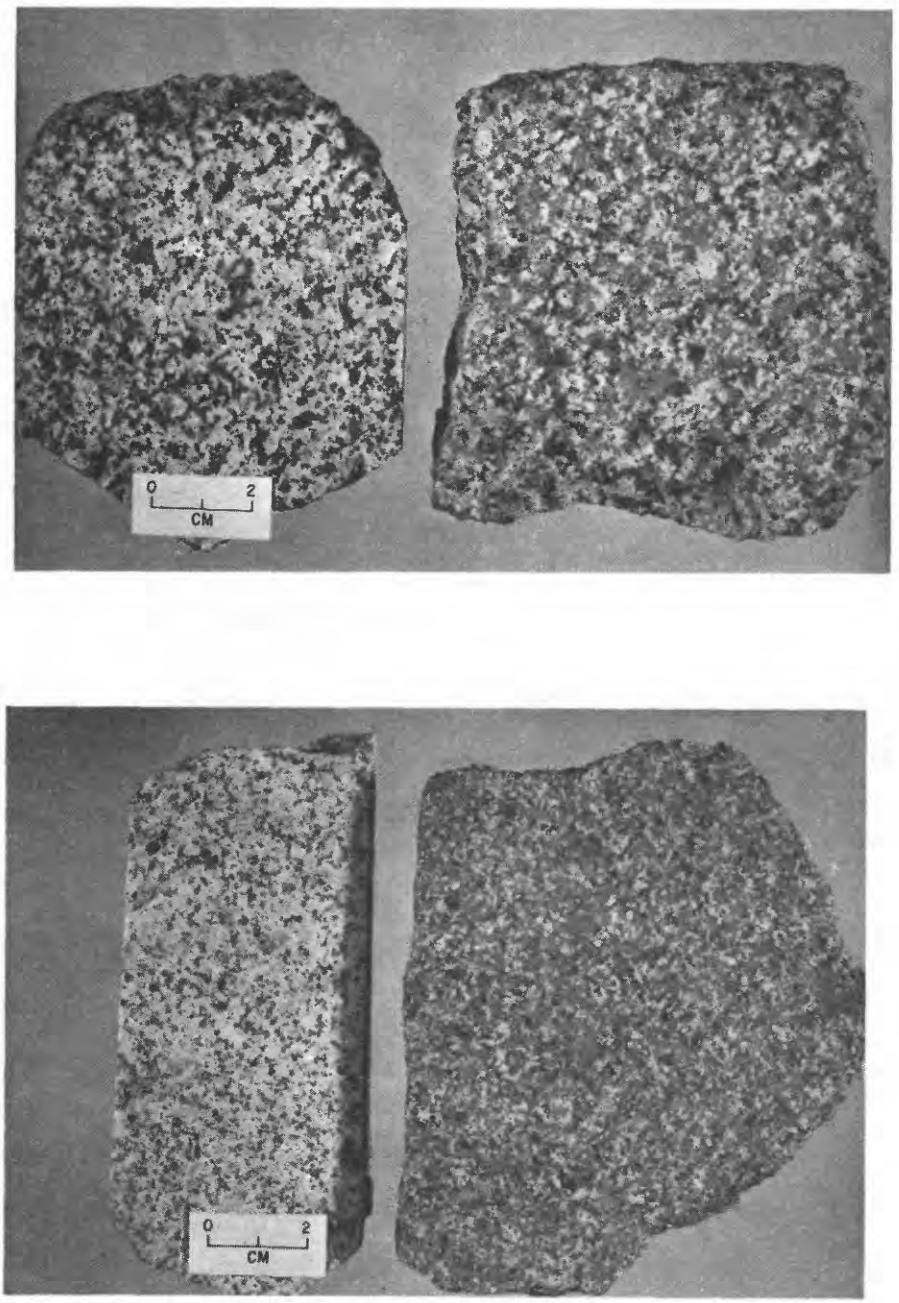

Figure 16. Representative specimens of textural facies 4A (top) and 4B (bottom).

suggests that zone 4 may be intrusive into facies 3A, but the field relations are inadequate to clearly reveal the nature of the contacts of this zone.

Facies 4A--Fine- to medium-grained equigranular granite. Rocks of this facies are fine to medium grained, allotriomorphic to hypidiomorphic, and equigranular with a few scattered megacrysts of feldspar and quartz. The quartz is light gray to medium light gray, and together with biotite (2 to 3 percent) imparts a light gray color to the rocks. Spotty oxidation of biotite, sericitization of plagioclase, and oxidation of disseminated sulfide(?) results in minor buff or cream discolorations. Miarolitic cavities are open, about 1 to 2 mm across, and appear to make up 1 to 2 percent of individual specimens.

Most plagioclase crystals in facies 4A are not obviously zoned, but a few are. The zoning characteristically consists of distinct cores, defined by selective secondary mineral replacements and differential extinction, that are surrounded by a slightly normal zoned rim. Oscillations are locally present, but generally are not common. The optical and compositional characteristics of the facies 4A plagioclase are similar to those of facies 4B except for the presence of the scattered zoned crystals in facies 4A.

The K-feldspar is dominantly anhedral, has undulose extinction, is microperthitic in part, and has variably developed grid twinning. In some specimens it is clouded by development of very fine-grained clay(?) minerals. Quartz is anhedral and interstitial to subequant. Graphic intergrowths are locally well developed. Biotite is reddish brown, subhedral to euhedral, has moderately abundant pleochroic halos, and contains small inclusions of sphene, zircon, and apatite. Generally

it is spottily interleaved with chlorite, but extensive replacement occurs in those specimens in which the K-feldspar is clouded. Accessory minerals are sparse and restricted to the sphene, zircon, and apatite included in biotite.

Facies 4B--Leucocratic granite. The rocks of this facies are the most conspicuous in zone 4, and they appear to be spatially associated with the hydrothermally altered fault zones. They are characteristically fine grained, allotriomorphic (except for plagioclase), equigranular, and leucocratic. Fresh surfaces are very light gray because biotite is sparse and the quartz is light gray. Buff discolorations are common, due to spotty iron hydroxide stainings that are in part associated with miarolitic cavities. The cavities are about 1 mm across, contain small amounts of earthy rust-stained material, and appear to be as abundant as those in facies 4A. Thin quartz veinlets are common and are discontinuously sheeted and interfingering in places. A few scattered medium-grained megacrysts of quartz and biotite are locally present.

The feldspars are partially clouded by clay minerals and contain scattered small grains of muscovite. Plagioclase (An_{6-15}) forms short subhedral grains that characteristically have even extinction and are unzoned. K-feldspar is faintly microperthitic, has undulose extinction, and the grain boundaries range from orthogonal to very irregular and interstitial. Graphic intergrowths are locally present. Quartz forms intergranular anhedral grains and small aggregates. Biotite occurs as remnant grains that have been partially replaced by muscovite. Muscovite also occurs as well-formed intergranular crystals of average grain size. Accessories are conspicuously absent except for very small unidentifiable remnant inclusions in altered biotite and relatively

coarse fluorite. Opaque material is sparse, and most is partially oxidized to bright orange-red iron hydroxides.

Microscopic Textures

Microscopic textures of special interest include those related to subsolidus albite, myrmekite, graphic intergrowths, and fringed biotite. Subsolidus albite, associated myrmekite, and fringed biotite are present in most parts of the complex, but graphic intergrowths are found only in those rocks that can be inferred to have crystallized rapidly and in the presence of a vapor phase.

Subsolidus Albite

Albite ($An_{\leq 5}$) is characteristically associated with coarser grains of K-feldspar throughout the complex. In addition to lamellae, patches, and veins in perthite, it commonly forms mantles on plagioclase inclusions, marginal rims on intergranular plagioclase, and small, discrete, interstitial grains that are generally associated with K-feldspar boundaries. Some examples are illustrated in figure 17.

Rims on plagioclase crystals are by far the most common occurrence and are present at most K-feldspar-plagioclase contacts. The albite is optically continuous with substrate plagioclase but the contact between them is sharp and is usually defined by differences in extinction and in many places by variations in twinning. Where the contacts with K-feldspar are semiparallel to (001) of the substrate plagioclase, the albite forms wide rims that are irregularly convex into the K-feldspar crystals. Where the albite has formed at boundaries semiparallel to (010) of the substrate plagioclase, the rims are thinner and straight along both contacts. Albite localized along other K-feldspar boundaries

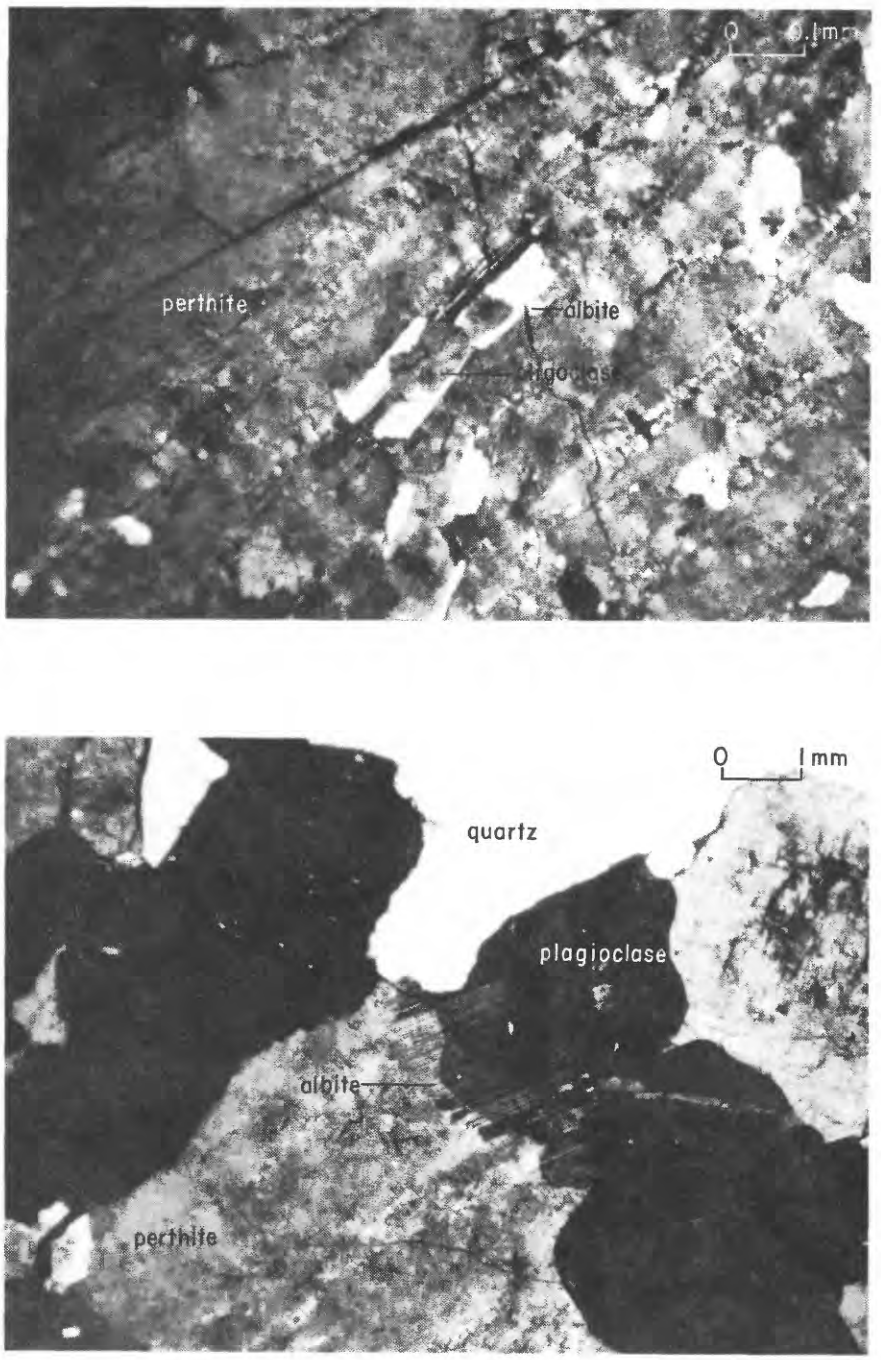

Figure 17. Photomicrographs (UXN) of subsolidus albite; overgrowth on included plagioclase crystal in perthite (top) and sharply defined rim on plagioclase at contact with perthite (bottom).

is much less common, and where found is present as small discrete grains. Inclusions of plagioclase in K-feldspar are mantled with albite. The plagioclase nuclei range from homogeneous subhedral cores with sharp differences in extinction and/or twinning from the albite to irregular, hazy, and anhedral centers within strongly normal-zoned grains that are generally smaller than the first type. Compositions of inclusions were determined in many specimens (mostly from zones 1 and 2), and grains with sharply defined homogeneous cores are characterized by a bimodal anorthite content in that the albite rims surround cores that are An_{20} regardless of the composition of intergranular plagioclase elsewhere in the specimen. Some larger inclusions do not show this relationship, but it is nonetheless common.

The albite is similar in many ways to that described by Ramberg (1962) in granulite-facies metamorphic rocks. That it is due to subsolidus crystallization is evidenced by the pronounced association with perthitic K-feldspar crystals and especially by the localization of the albite at K-feldspar-plagioclase boundaries. The rims on intergranular plagioclase appear to have grown in part by the replacement of K-feldspar, and essentially they form overgrowths on the substrate plagioclase (Ramberg, 1962, p. 21). However, that the crystallization of albite adjacent to plagioclase is not strictly an exchange process within the K-feldspar structure is evidenced by the composition of the plagioclase inclusions in the K-feldspar, as well as by the fact that the contact with substrate plagioclase is not strictly conformable with the primary crystal outline. The bimodal compositions of many included crystals indicate that sodium transfer, in or out depending

on the composition of the originally included plagioclase, has homogenized the nucleus plagioclase to a composition of about An_{20}. This intimate coexistence of two plagioclases is probably another example of the lack of solid solution in the low-temperature plagioclase series (Laves, 1954; Barth, 1969, p. 38-39). Inclusions that do not show the bimodal compositional relationship are probably of two kinds: (1) those that are the result of albite precipitation on an originally small nucleus in an environment within the host K-feldspar crystal where it could be albitized almost completely, leading to products that range from homogeneous grains of albite to the small, strongly normal-zoned grains with inhomogeneous irregular cores, and (2) those that are the result of albite precipitation on plagioclase inclusions too large to have been extensively homogenized by the subsolidus processes, yielding grains with unchanged original cores. The availability of albite in the vicinity of included plagioclase, the size of the included plagioclase grain, and the character of the K-feldspar structure in the vicinity of the inclusion all probably influenced the subsolidus development of the products now seen in the specimens. Detailed study of the included plagioclase crystals would yield much information about the low-temperature relations in the low-An plagioclase series and the mechanism of exchange responsible for subsolidus adjustments in these minerals.

Myrmekite

Myrmekite (fig. 18) is characteristically associated with subsolidus albite throughout the granite complex. It consists of very fine-grained intergrowths of quartz and recrystallized plagioclase on margins of primary plagioclase crystals, in mantles surrounding plagioclase

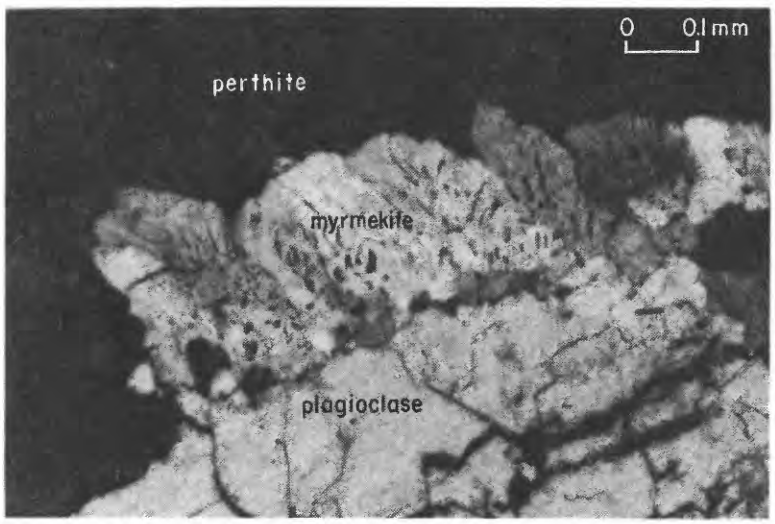

Figure 18. Photomicrograph (UXN) of interstitial myrmekite.

inclusions in K-feldspar crystals, and in discrete interstitial grains of albite.

In rims on primary plagioclase the quartz in the intergrowths occurs as thin plates that generally radiate outward from very near the substrate plagioclase boundary almost to the edge of the albite rim, but in many places the quartz becomes less abundant and terminates at some intermediate distance inward from the rim margin. The outer contact of myrmekite conforms to the original plagioclase boundary or it is smoothly convex and bulbous into adjacent K-feldspar crystals, thus producing the typical wartlike forms (Barker, 1970, p. 3343). As described by Phillips (1964, p. 53) the marginal band containing myrmekite can be subtly zoned outward to albite compositions, and this is the case in some of the rims that were examined. In some others, the zoning is not so subtle and the quartz occurs in a distinct band that has a composition intermediate between albite and the substrate plagioclase.

Interstitial myrmekitic albite contains quartz blebs, plates, and rods that are variously oriented and generally evenly distributed throughout individual grains. These occur as discrete grains localized at the contacts between K-feldspar and the other framework silicates, as well as in fine-grained aggregates. Grains within aggregates are generally anhedral and somewhat rounded looking, but discrete grains along boundaries are generally subhedral.

Myrmekite mantles on plagioclase inclusions in K-feldspar are commonly similar to the myrmekitic rims on intergranular plagioclase. However, the smaller and strongly normal-zoned inclusions that have

been more extensively albitized have irregularly oriented quartz blebs only in central areas where the anorthite content is higher.

Fringed Biotite

Throughout the complex, biotite crystals commonly have fringed borders (fig. 19). These fringes are very fine, interfingering extensions of the biotite that form a patchy interconnected network. The spaces within the fringe network appear to be occupied by material of the crystals immediately adjacent to the fringe or by very fine-grained aggregates of feldspar and quartz. Some skeletal-like biotite crystals occur as small discrete grains not associated with larger biotite plates. The fringes are most obvious at the borders of biotite sections semi-parallel to (001). They are developed along segments of the host biotite border and do not completely surround it. The spotty occurrence and localization at borders of larger crystals suggest that the fringes are the product of late crystallization processes.

Graphic Intergrowths

Graphic intergrowths (fig. 20) occur in plagioclase but are better developed and more common in K-feldspar. They are found only in rocks which can be inferred to have crystallized relatively rapidly and in the presence of a vapor phase, facies 1A (contact-zone rocks), facies 3B (composite-textured rocks with aplitic groundmass), and the fine- to medium-grained equigranular rocks of Zone 4 (facies 4A and 4B). In addition, large single host crystals with intergrowths (graphic granites) are up to 8 in. long in the interior parts of pegmatitic dikes. These dikes, and the graphic granite within them are discussed separately in a later section.

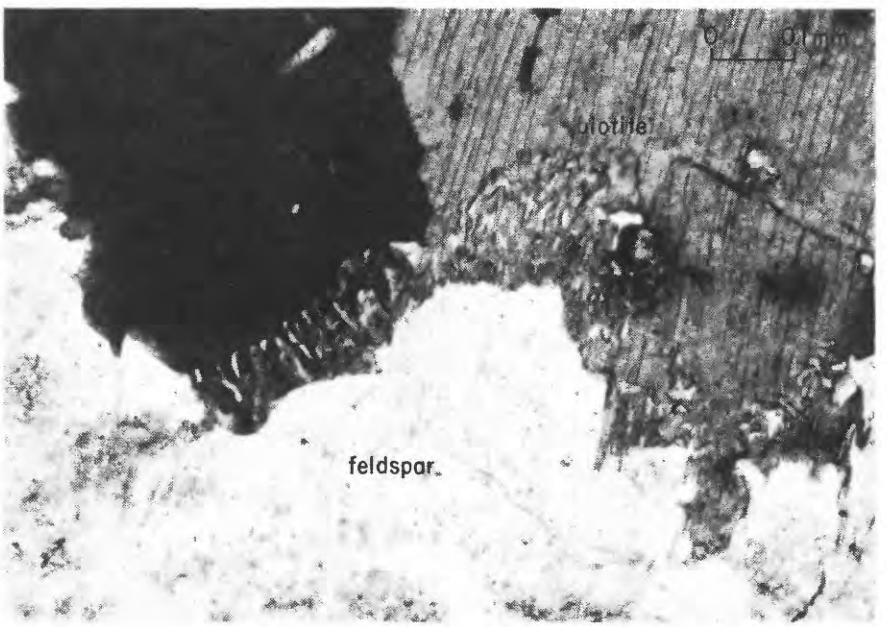

Figure 19. Photomicrograph of a fringed biotite crystal (plane polarized light).

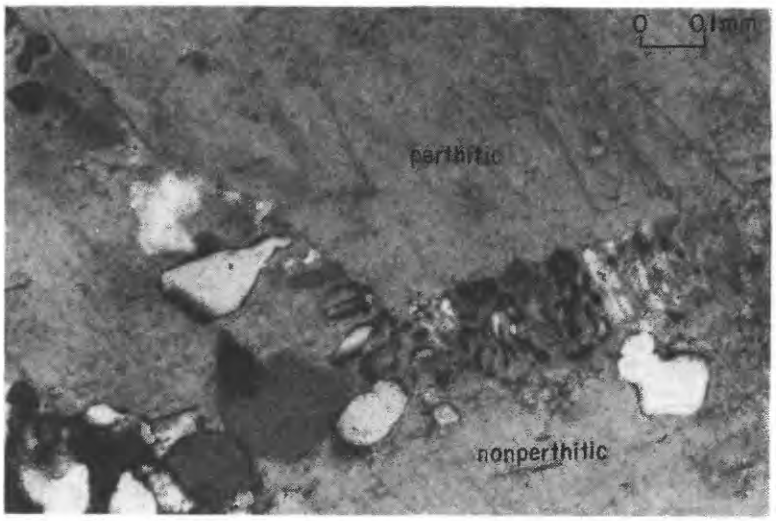

Figure 20. Photomicrograph (UXN) of a graphic intergrowth of quartz in potassium-feldspar that defines a distinct marginal band in a large perthite crystal.

The graphic intergrowths that form complete grains in parts of the granite are anhedral and have irregular boundaries. The quartz in these grains forms equant to elongate blebs that show no preferred orientation but are optically continuous. The blebs in K-feldspar hosts are smaller and more abundant than those in plagioclase.

Marginal bands with graphic intergrowths mantle many feldspar phenocrysts in rocks of facies 1A and 3B. K-feldspar phenocrysts have marginal bands with a few scattered, angular quartz inclusions, but the bands are characterized by thin zones with abundant small quartz blebs that sharply define what may be the original phenocryst outline. Where the quartz inclusions are elongate, they are generally semiperpendicular to the interface between the marginal band and the interior K-feldspar. As many as two such parallel zones of small inclusions have been observed in a single margin, and the principal difference between the K-feldspar of the interior and that of the margin is that the margin lacks microscopic albite lamellae and has a more uniform extinction. The quartz blebs in the thin zones consist of several different optically continuous subsets, and the inclusions belonging to a particular subset do not all occur together. In plagioclase phenocrysts, marginal bands with graphic intergrowths are not common. Where present, they consist of scattered, equant, and relatively large quartz inclusions in a band characterized by having homogeneous plagioclase extinction. This band is external to a distinct plagioclase core that differs from the margin in both extinction and zoning characteristics. Individual quartz blebs in the plagioclase are optically continuous with only a few others scattered through intergrowths.

Megascopic Structures

Megascopic structures are abundant, varied in nature, and inhomogeneously distributed in the complex. They include those related to foliations, diking, inclusions, jointing, and cavities. These structures, especially the planar fabrics, are locally very well developed, but efforts toward defining three-dimensional aspects of the complex are handicapped by the lack of outcrops and their variability of distribution. Many of the structural features are interrelated, but for convenience they are discussed separately below.

Foliations

Foliations are defined primarily by mineral segregations, phenocryst or inclusion orientation, and tabular swarms of inclusions. Mineral segregations are by far the most important; good examples are shown in figure 21. The segregations include biotite-rich bands, thin, discontinuous fine-grained leucocratic zones, and clots and bands of coarse K-feldspar crystals. These commonly occur together, and the biotite-rich bands generally border the fine-grained zones and coarse K-feldspar segregations. Individual segregations range in thickness from about 1 in. to almost a foot. Large K-feldspar crystals are tabular and show a weak to strongly developed preferred orientation in several parts of the complex. Their orientation generally defines a steep foliation, and in areas where segregations exist they are semiparallel to the foliation that is defined by the mineral segregations. Inclusions generally take the form of flattened ellipsoids, and their orientation as well as the orientation of tabular swarms also defines planar structure in several localities. The dark inclusions in figure 21

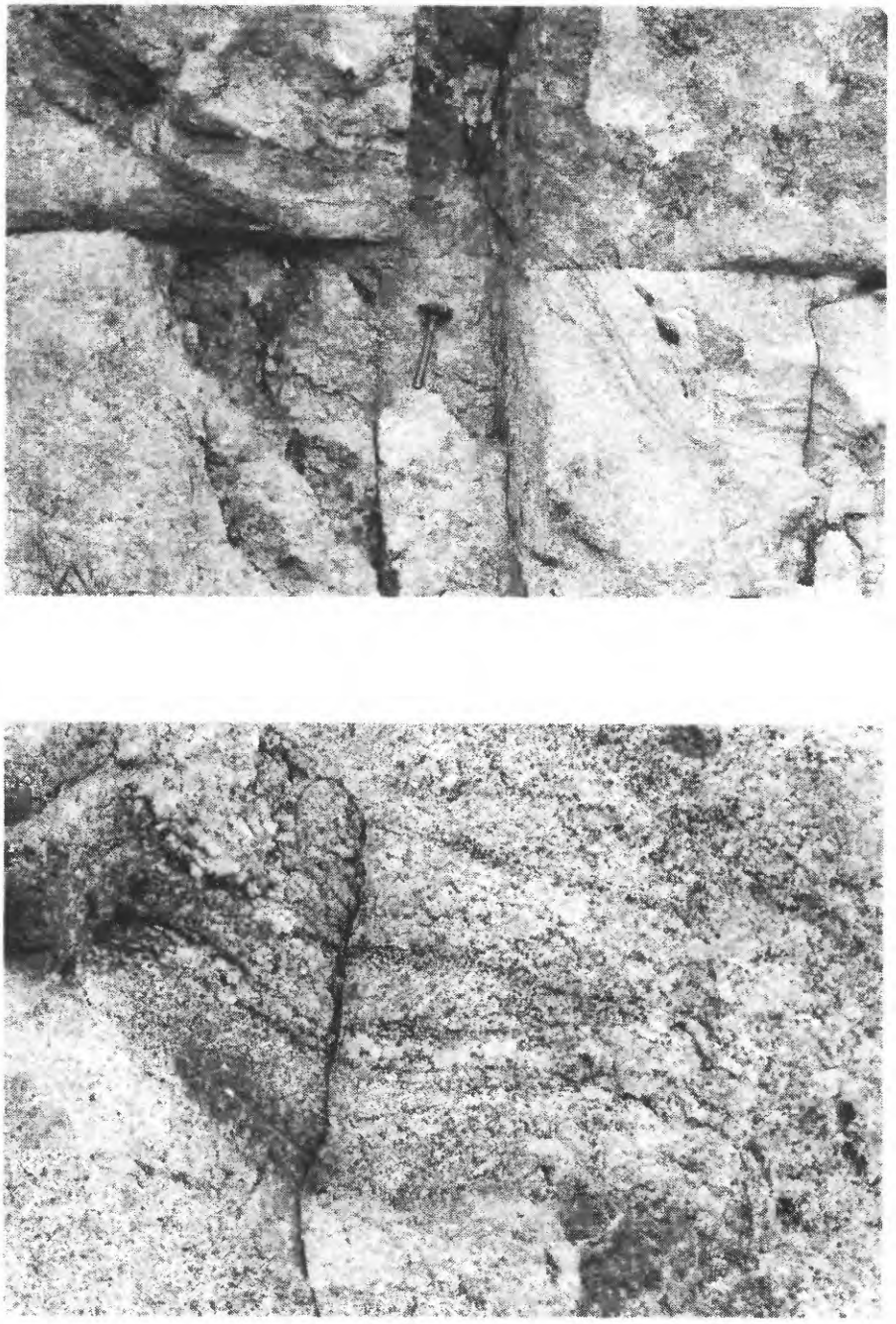

Figure 21. Mineral segregations in facies 3A rocks. Dark biotite-rich bands are separated by lighter colored bands of fine-grained granite and clusters of oriented, large potassium-feldspar crystals. Lensoid, dark xenoliths (right center, top photo) are oriented parallel to the segregation bands.

illustrate the preferred orientation of individuals and, as shown, such orientations are commonly parallel to other planar fabric in the immediate vicinity.

The planar fabrics are developed in zones 2 and 3 of the complex. In zone 2, K-feldspar phenocrysts are locally aligned and the best developed inclusion swarms are present. In zone 3, the seriate-textured facies (3A) contains the schlierenlike mineral segregations, and in the composite-textured facies (3B) alignment of K-feldspar phenocrysts is obvious in many hand specimens as are some flow structures within the aplitic groundmass. Unfortunately, rocks of facies 3B crop out at very few localities and further information about the planar fabrics is unavailable.

Dikes

Porphyritic, aplitic, and aplite-pegmatite dikes are present in the complex. They are all of granite composition and represent segregations of residual materials within mostly crystallized parts of the pluton or distinct intrusions of such materials into previously crystallized zones. Most are less than 2 ft in width.

The porphyritic dikes contain phenocrysts of biotite, quartz, K-feldspar, and plagioclase in an aplitic groundmass. Only two such dikes have been located. One is a foliated dike 2 to 5 in. thick, at an elevation of 800 ft in zone 2, 1 mi south of Serpentine Hot Springs. The other is a direct offshoot, about 1000 ft long, of the main intrusive body of facies 3B into zone 2 rocks at a point on its northern contact with zone 3 (shown on pl. 1). These represent distinct intrusions of partially crystallized materials into previously crystallized parts of zone 2.

Aplite dikes, commonly less than 3 in. thick, are by far the most widespread and abundant and are present in both zones 2 and 3. In zone 2, they are the most common dikes and occur in groups of 2 or 3 separate dikes that are oriented approximately parallel to one another. They are more abundant in zone 3 but in this zone they are discontinuous and interconnected (fig. 22).

Composite aplite-pegmatite dikes are restricted to facies 3A rocks except for a few in zone 2. They are texturally and compositionally zoned. Aplite typically forms the major portion of each dike and it borders the more centrally located pegmatite. The pegmatite contains coarse K-feldspar, plagioclase, quartz, and in places tourmaline and muscovite. Compositional inhomogeneity is defined by variations in feldspar distribution and, to a certain extent, in quartz distribution. Coarse K-feldspar has preferentially crystallized at the stratigraphic roof of the pegmatite zone, and in some thicker dikes it actually forms graphic crystals, several inches long, that extend downward into central parts of the zone. The K-feldspar concentration is accompanied by quartz, and plagioclase in turn has crystallized at the bottom of the zone and is commonly finer grained than the K-feldspar.

Some of the thicker dikes, for the most part aplite-pegmatite dikes, have many alternating mineral segregation bands parallel to, but not symmetrically distributed about them. Figure 23 illustrates this relationship and shows how fine-grained and aplitic granite within a zone of mineral segregation becomes more clearly defined up dip where it eventually has a pegmatite pod segregated in the central part of an aplite dike. Development of the aplite-pegmatite dikes in facies

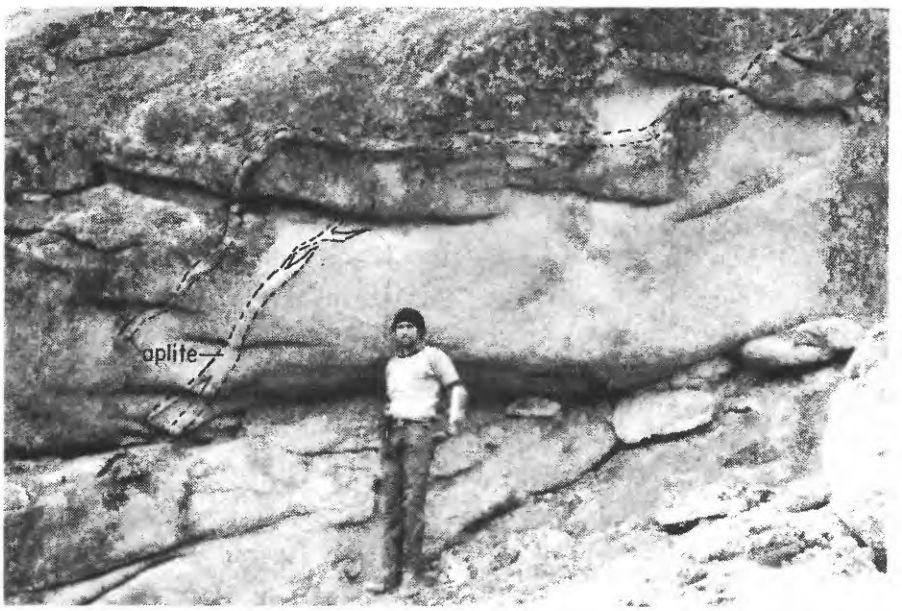

Figure 22. Discontinuous and interconnected aplite dikes in facies 3A rocks. Thicker parts of the dikes form ridges on the weathered and partially lichen-covered outcrop surface.

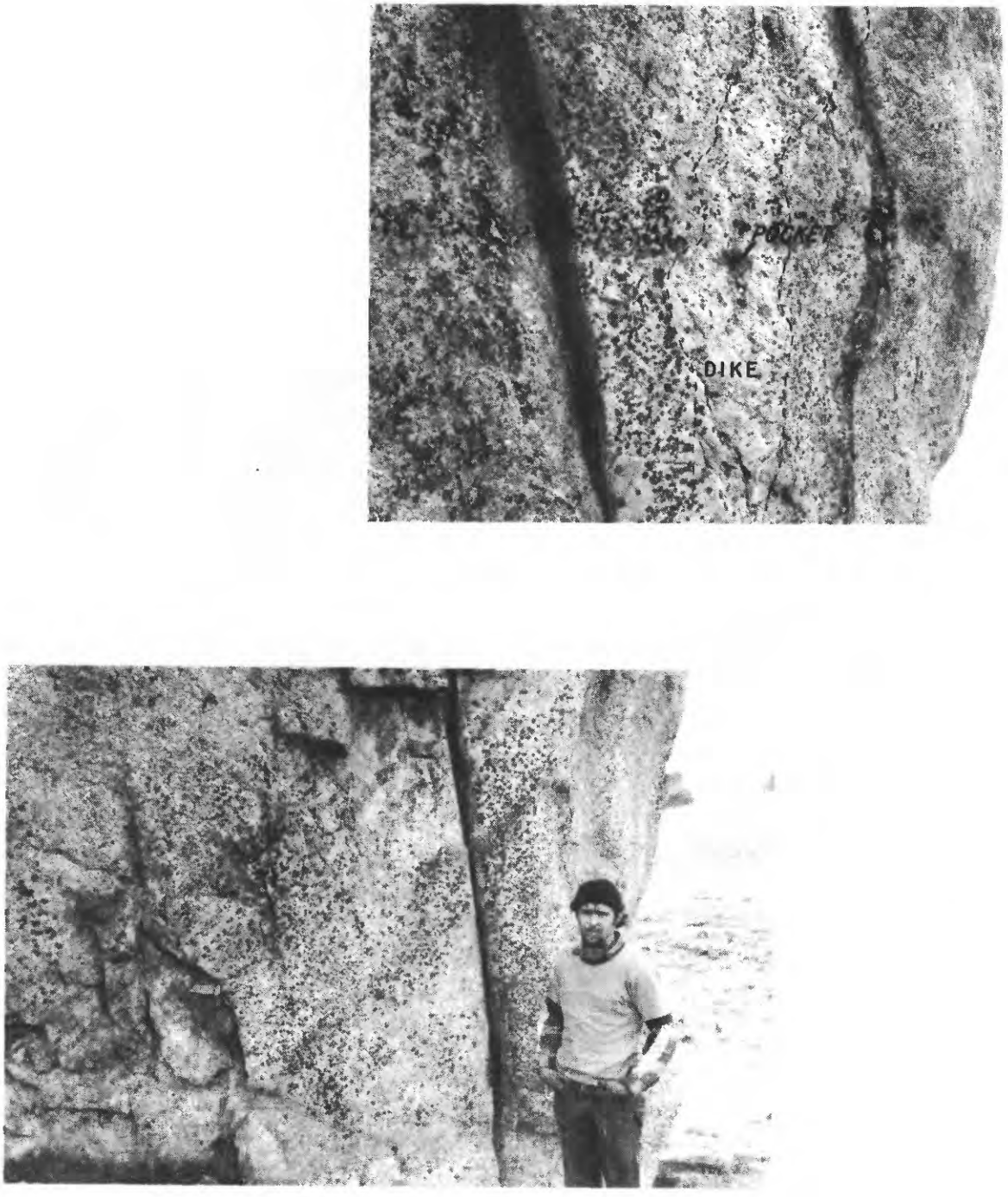

Figure 23. Composite, 3 ft wide, aplite-pegmatite dike (top) that grades down dip into banded, fine-grained granite zone (bottom).

3A rocks is believed to be the result of segregation processes in which residual melts and volatiles were concentrated into discontinuous dikelike bodies within the almost completely crystallized parent rocks. It is probable that all variations from the hazy and thin mineral segregations, such as illustrated in figure 21, to the well-defined, three-foot-thick aplite-pegmatite dike of figure 23 are present in facies 3A rocks.

There is one known example of a pegmatite pod within seriate-textured, facies 3A rocks. Figure 24 shows this body, which is zoned into a lower aplite and an upper coarse quartz-feldspar intergrowth with some vugs containing euhedral tourmaline and quartz. The aplite is in sharp contact with the host rocks, but the coarse intergrowth is separated from the seriate granite by a thin zone of equigranular material.

Cavities

Three principal types of cavities occur within the granite complex: (1) miarolitic cavities that contain late crystallizing minerals, (2) larger openings (pockets) that occur in or near pegmatitic bodies, and (3) small miarolitic cavities that are open voids without late crystallizing minerals.

The miarolitic cavities that contain late crystallizing minerals are found in the seriate-textured rocks (facies 3A) of zone 3. The cavities are irregular openings up to 2 cm across and contain euhedral crystals of dark-colored quartz, clevelandite, muscovite, tourmaline, and fluorite (in order of decreasing abundance). The cavities are associated with coarser K-feldspar crystals and clots of such crystals. Characteristically smaller cavities are located immediately adjacent

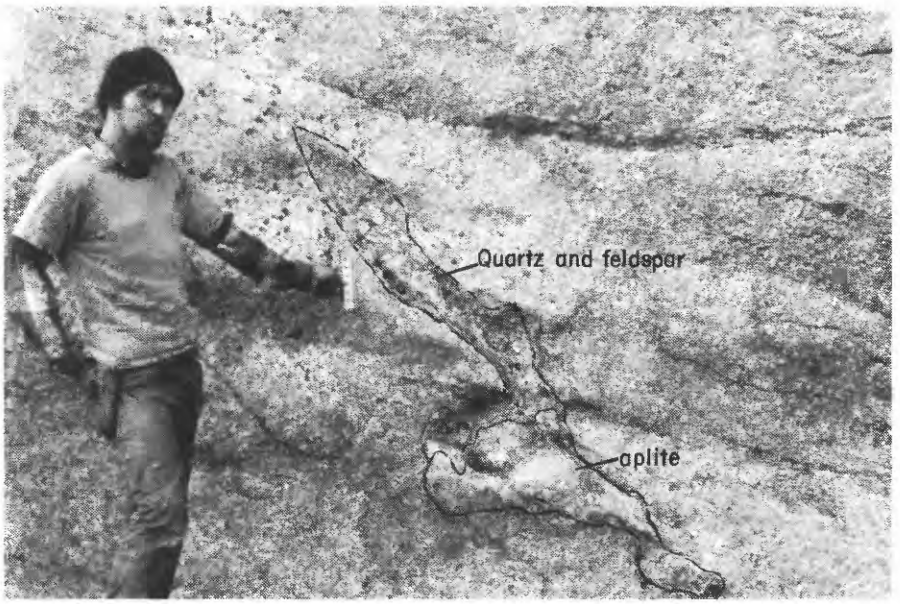

Figure 24. Quartz-feldspar pegmatitic pod in facies 3A rocks. Aplite segregation forms lower part of the pod.

to the big crystals. They are rust stained and an earthy buff-brown material commonly coats the euhedral minerals that project into the voids.

The pockets are also associated with seriate-textured rocks of facies 3A and mostly form openings as much as several inches across in pegmatitic dikes and pods, but one is an open void 2 ft across wholly within seriate-textured rocks. The pockets in pegmatitic rocks contain euhedral minerals as in the case of the miarolitic cavities described above, the principal difference between them being primarily one of scale. The walls of the 2 ft wide pocket (noted on pl. 1) contain a vuggy equigranular encrustation of euhedral clevelandite, muscovite, quartz, tourmaline, fluorite, and a trace of ilmenite that replaces the seriate-textured granite, in a selvage that is about 3 in. wide. Pseudomorphs of muscovite and albite after K-feldspar phenocrysts can be discerned within it (fig. 25). This pocket is found near a massive quartz-feldspar pegmatite that is localized at the contact between facies 3B rocks and the facies 3A rocks they intrude (fig. 14). Continuity between the pegmatite and the 20 ft distant (as now exposed) pocket is suspected but cannot be demonstrated because of the lack of exposure.

The third type of cavity is small miarolitic cavitites, to 2 mm across, that are abundant in the equigranular rocks of zone 4. They are characteristically open and do not contain late crystallizing minerals. However, some are rust stained and as interstitial fluorite and muscovite are observed in thin sections of these rocks, these minerals may in part occur in the small cavities. The cavities are estimated to compose 1 to 2 percent by volume of the host rocks. This abundance

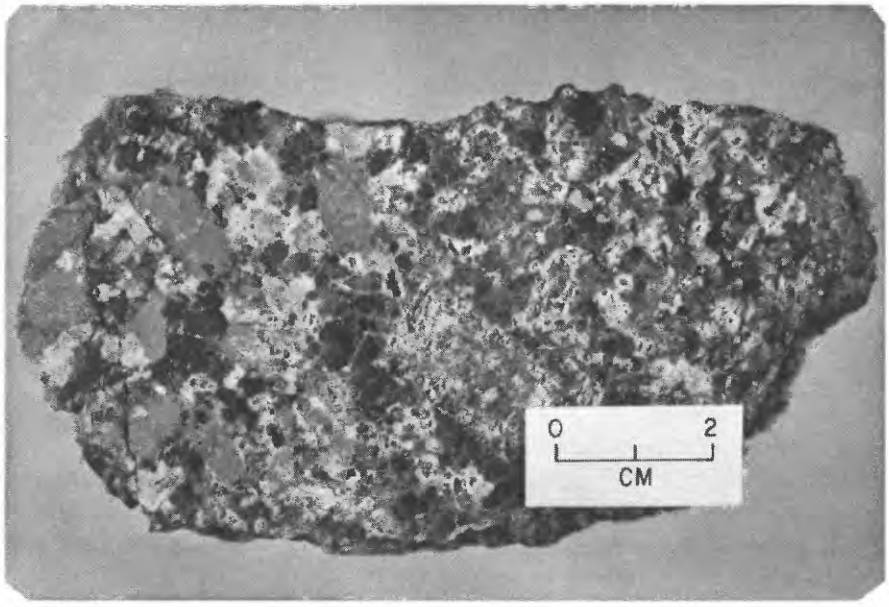

Figure 25. Vuggy replacement selvage along walls of 2 ft wide pocket in facies 3A rocks. Selvage is composed of subequal amounts of euhedral muscovite and albite with lesser amounts of fluorite, tourmaline, and rutile.

indicates that more interstitial aqueous fluid was present in zone 4 than anywhere alse in the pluton.

As discussed above, openings are most closely associated with rocks of zone 3 and zone 4. However, some miarolitic cavities containing euhedral minerals are found in dikes in country rocks and in rocks of zone 1 (facies 1A) very near the granite-country rock contact. There is a conspicuous absence of voids within the composite-textured rocks of facies 3B.

Inclusions

Two principal types of inclusions are present in the granite complex. One type is fine to medium grained, dark gray colored, and contains a few megacrysts of quartz, plagioclase, and pink K-feldspar. The other is brownish gray and has a "porphyritic" texture with coarse megacrysts of quartz, plagioclase, and pink K-feldspar in a fine-grained aggregate of the same minerals together with biotite. Those of the first type may be true xenoliths but the others are autoliths.

Common to both types of inclusions are finer grained anhedral microcline and equant quartz, plain brown biotite, and fine-grained plagioclase with characteristically smoothed crystal edges. The darker, finer grained inclusions contain more abundant biotite, disseminated acicular apatite, and green hornblende ($\leq$5 percent). In these, the microscopic textures include interlocking aggregates of small anhedral grains, networks of skeletal, inclusion-riddled quartz grains, and radiating clusters of plagioclase laths. In the inclusions with "porphyritic" texture the finer grained material forms an interlocking aggregate of semi-anhedral grains similar to that in many darker,

fine-grained inclusions, but it contains relatively more abundant microcline, and sphene and allanite as accessory minerals. The megacrysts are generally well formed but somewhat rounded. Reaction rims are present on plagioclase crystals, and some K-feldspar is mantled by thin bands of plagioclase. Large plagioclase crystals have faint oscillatory zoning, large distinct interiors with homogeneous extinction and well developed albite twinning, and thin reaction rims that locally contain minute inclusions and differ slightly in extinction and twinning from interior areas. K-feldspar megacrysts are perthitic, with irregular margins and partially albitized plagioclase inclusions. Coarser biotite grains form some megacrysts and contain magnetite and zircon inclusions. The finer grained biotite is generally inclusion free.

In form the inclusions are commonly irregular flattened ellipsoids 1 ft or less in maximum dimension, a very few are angular, and some are tabular and up to 3 ft long. Where planar structures such as schlieren are present the inclusions are aligned with them (fig. 21). They can be isolated or occur in groups that range from a few irregularly scattered in a small area to dense pipelike or tabular swarms that can be several feet wide and several tens of feet long (fig. 26). In the groups, both principal types are found together though one can predominate over the other.

The inclusions are exposed in outcrops of both zones 2 and 3 but they are most abundant in zone 2. Zone 2 contains the dense swarms as well as the numerous small clots, less than 2 cm in their maximum dimension, of fine-grained plagioclase, biotite, and lesser green hornblende that are present in more than half of the hand specimens examined.

Figure 26. Pipelike swarm of inclusions in facies 2 rocks on ridgeline west of Serpentine Hot Springs. Inclusions are as much as 1 ft across in their maximum dimension. Photograph by R. Ewing, 1970.

Joints

Joints are present in all large outcrops, and the outcrop forms are determined by the orientation and spacing of the joints because of preferential weathering along them. They are best developed in zone 2 but also are present in parts of zone 1 and zone 3. They are systematically oriented but are variably spaced, and three sets usually can be recognized in individual outcrops.

Two particularly prominent sets intersect at a high angle. One trends about N. 65^{o} E. and is steeply dipping, and the other trends N. 37^{o} W. and dips moderately to the northeast in central areas but is less systematically oriented and steeper in marginal areas. The third set strikes obliquely to one of the other sets and generally dips in the opposite direction.

Joints crosscut late intrusive units such as aplite and pegmatite dikes and small porphyritic plugs. They also have been observed to transect dark inclusions. In many places, dikes strike parallel to one of the joint sets but dip in an opposite direction. Locally (especially in zone 2), some fracture systems containing late muscovite, quartz, tourmaline, and fluorite are parallel to one of the clearly recognized joint sets, and the late minerals appear to have healed them. In eastern parts of the pluton where rocks of zone 1 are present, much differential movement has occurred along parallel sets of throughgoing joints(?) that in part appear to extend into country rocks. They are evidenced by linear topographic expressions, the presence of slickensided and polished granite fragments, and zones of increased hydroxide staining due to oxidation. Although oxidation appears to have been

localized along these fractures, they have not been mineralized and are mapped as fault zones on plate 1.

Deuteric Features

Products of deuteric crystallization are present in minor amounts in all the textural facies of the complex. They include materials related to the alteration of biotite and feldspar and to precipitation in interstitial voids. The character of the deuteric crystallization changes through the facies sequence.

In the facies of zone 1, the principal deuteric product is muscovite. It forms interstitial grains, scattered and relatively abundant inclusions in plagioclase, and small grains that are adjacent to or interleaved with biotite. The biotite is commonly preferentially replaced along the cleavages by a pale green chlorite with gray interference colors. Deuteric crystallization may merge with hydrothermal alteration in facies 1A where sericite is common in plagioclase, K-feldspar is very clouded by minute inclusions that are probably clay minerals, fluorite is associated with late-forming muscovite, and schorl is present in many cavities.

In zone 2, deuteric crystallization is characterized by the development of grass-green chlorite (with blue-gray interference colors) that replaces biotite along cleavages and in patches. Some of the biotite is a bright red brown near chloritized areas, but other late-stage products are restricted to scattered muscovite crystals in parts of some plagioclase grains.

In zone 3, the seriate-textured rocks (facies 3A) characteristically contain much deuteric muscovite that forms interstitial grains, as well

as patchy crystals in altered plagioclase, particularly in the interiors of zoned crystals. It is generally accompanied by small, anhedral, disseminated and interstitial grains of fluorite. Grass-green chlorite with blue-gray interference colors patchily replaces some biotite that is in part similar to altered biotite in zone 2. In composite-textured rocks (facies 3B), the groundmass crystals are characteristically more altered than the phenocrysts. Small shreddy grains of biotite are partially to completely replaced by pale to deep-green chlorite, and muscovite is relatively common as intergranular to interstitial grains and as crystals attached to the margins of larger biotite grains. Interstitial and anhedral fluorite is relatively common, and feldspars are variously clouded by minute inclusions.

In zone 4, the effects of deuteric crystallization merge with those of hydrothermal alteration. In facies 4A, equigranular rocks with biotite, the biotite is partially oxidized, is bright red brown, and is interleaved with muscovite. Muscovite also occurs intergranularly and as replacements in plagioclase. Interstitial fluorite is common and some interstitial tourmaline is present. Chlorite is lacking. In facies 4B, equigranular and leucocratic rocks, muscovite occurs as somewhat shreddy intergranular grains and interstitial fluorite is common. The shreddy muscovite has thin inclusions of opaques and sphene oriented along the cleavages, as well as discontinuous shreds that are pleochroic in shades of brown, thus indicating that it largely represents replaced biotite crystals. The altered nature of the feldspars in facies 4B varies considerably. In some specimens both plagioclase and K-feldspar are extensively clouded by minute inclusions, and in others plagioclase has been preferentially replaced. Yet there are facies 4B

specimens in which neither feldspar shows signs of late-stage alteration. Probably there is complete transition from rocks of facies 4B that contain unaltered feldspars, quartz veining, bleached quartz, and muscovite after biotite to the extensively argillized and silicified rocks present in the hydrothermally altered fault zones that cut Zone 4.

In summary, muscovite, chlorite, and clay minerals are the dominant late-stage products of deuteric crystallization. These minerals are accompanied by interstitial anhedral fluorite and locally by schorl. Both facies 1A and facies 4B rocks show evidence of extensive late-stage changes that appear to merge with those of hydrothermal alteration. These changes involve locally extensive replacements of feldspars by sericite-muscovite and clay minerals and muscovite replacements of biotite. In the facies 1B-1C-2 transition, the principal deuteric product is chlorite. The chlorite replaces biotite and becomes darker green and more anomalous in interference colors inward through this part of the facies sequence. Chlorite similar to that in facies 2 is present in facies 3A but the latter contains more muscovite and fluorite than facies 2. The groundmass of facies 3B contains very few nonchloritized biotite grains, and muscovite, fluorite, and clay(?) minerals are all relatively abundant. Deuteric crystallization in zone 4 is locally complex but overall it is characterized by the presence of muscovite and the absence of chlorite.

Plagioclase Composition

Plagioclase composition varies through the facies sequence, suggesting that there are several different plagioclase populations within the complex.

Composition of the plagioclase was determined optically using the a-normal method, and the results are shown diagrammatically in figure 27. Only one composition was measured for any particular grain, even though zoning commonly was present. This is because compositions within individual crystals commonly bracket An_{21}, the composition about which extinction angles vary only slightly from 0^{o}, and because, even in crystals with conspicuous zoning features, the compositional variation commonly is slight. The compositional variation within zoned crystals is comparable to the overall variation of plagioclase composition in facies 1B, 1C, 2, and 3A, but in facies 1A and 3B, the overall variation within the facies is greater than that observed in any single zoned crystal. Compositions determined on subsolidus albite crystals are shown in figure 27 for facies 3A rocks only. Similar subsolidus albite is present in the other facies. The data for facies 4A and 4B are not significantly different and have been plotted together in figure 27.

As shown in figure 27, plagioclase composition in facies 1A varies over a wide range. It is relatively uniform within facies 1B, 1C, and 2, and the anorthite content increases slightly inward through these facies. The range in composition is greatest in facies 3A, and the determinations fall into a group at about An_{25-27} and a group between An_{12} and An_{20}. The composition is somewhat evenly distributed about average values in facies 3B and Zone 4, and shows a slight shift toward albite in the last crystallizing facies. The general trend in the variation of plagioclase composition is one in which the average anorthite content increases from facies 1A through facies 2 (An_{17} to An_{25}), goes through some intermediate value in facies 3A, then drops

Figure 27. Plagioclase compositions in the textural facies of the granite complex as determined optically. Each dot represents a determination on a different plagioclase crystal.

toward albitic compositions ($<An_{11}$) in facies 3B through 4B. The details of the compositional variations, combined with petrographic variations, are important and are discussed more completely below.

The compositional data suggest that there are several different plagioclase populations within the complex: (1) heterogeneous crystals of facies 1A, (2) a transitional population that includes crystals of facies 1B, 1C, 2, and the calcic oligoclase of facies 3A, (3) albitic oligoclase in facies 3A, (4) the facies 3B crystals, and (5) the Zone 4 crystals. The facies 3B plagioclase compositional data apply to both phenocrysts and groundmass crystals and, although there is no distinct break in composition between them, the sharp break in grain size clearly defines two populations in this facies. The plagioclase compositional and petrographic data actually earmark several composite crystal populations in the complex. These crystal populations are identified and discussed more completely in a later section.

Modal Composition

Modal determinations were made on selected mineral populations in facies 3B, 4A, and 4B rocks. Modes on these facies were restricted to the finer grained mineral populations that surround a well-developed phenocryst population in the case of facies 3B rocks and a few scattered metacrysts in the case of facies 4A and 4B rocks. The modal composition of the groundmass in facies 3B rocks was determined by point counting thin sections stained for K-feldspar. The modal compositions of all other specimens were determined by point counting stained rock slabs.

Modal compositions were obtained for samples collected from all parts of the complex, and all the modal Pl:Q:Or ratios are plotted

together in figure 8. The ratios are evenly scattered and do not define any obvious variation trends. Because of the overall granite composition of the complex, the modal variations are necessarily small, but significant differences in modal composition do exist among the principal textural facies. Only the essential minerals and biotite were included in the modal determinations; accessory minerals are present in amounts less than 1 percent.

Variation of Modal Averages

The modal averages for each facies are plotted in figure 28. All involve whole-rock modes except that for facies 3B, which is the average mode of the aplitic groundmass. The plotted averages define several important variations: (1) biotite varies independently of the other essential minerals and shows a gradual increase to a maximum of 6 percent in facies 2, then decreases in more interior facies until it is only a minor constituent of the leucocratic facies 4B rocks, (2) the plagioclase and K-feldspar proportions diverge significantly from their more systematic trends in 1B, 1C, and 2, (3) the systematic variations among facies 1B, 1C, and 2 are defined by an increase in plagioclase, a slightly increasing or approximately constant K-feldspar percentage, and a corresponding depletion in quartz, (4) the groundmass of facies 3B is sharply depleted in plagioclase and correspondingly contains increased quartz and K-feldspar percentages, (5) facies 4A continues the plagioclase enrichment trend and is depleted in K-feldspar, and (6) facies 4B contains more plagioclase than any other facies, an increased K-feldspar content over that of facies 4A, and a low percentage of quartz. Quartz is believed to be the dependent modal variable in the fluctuations of

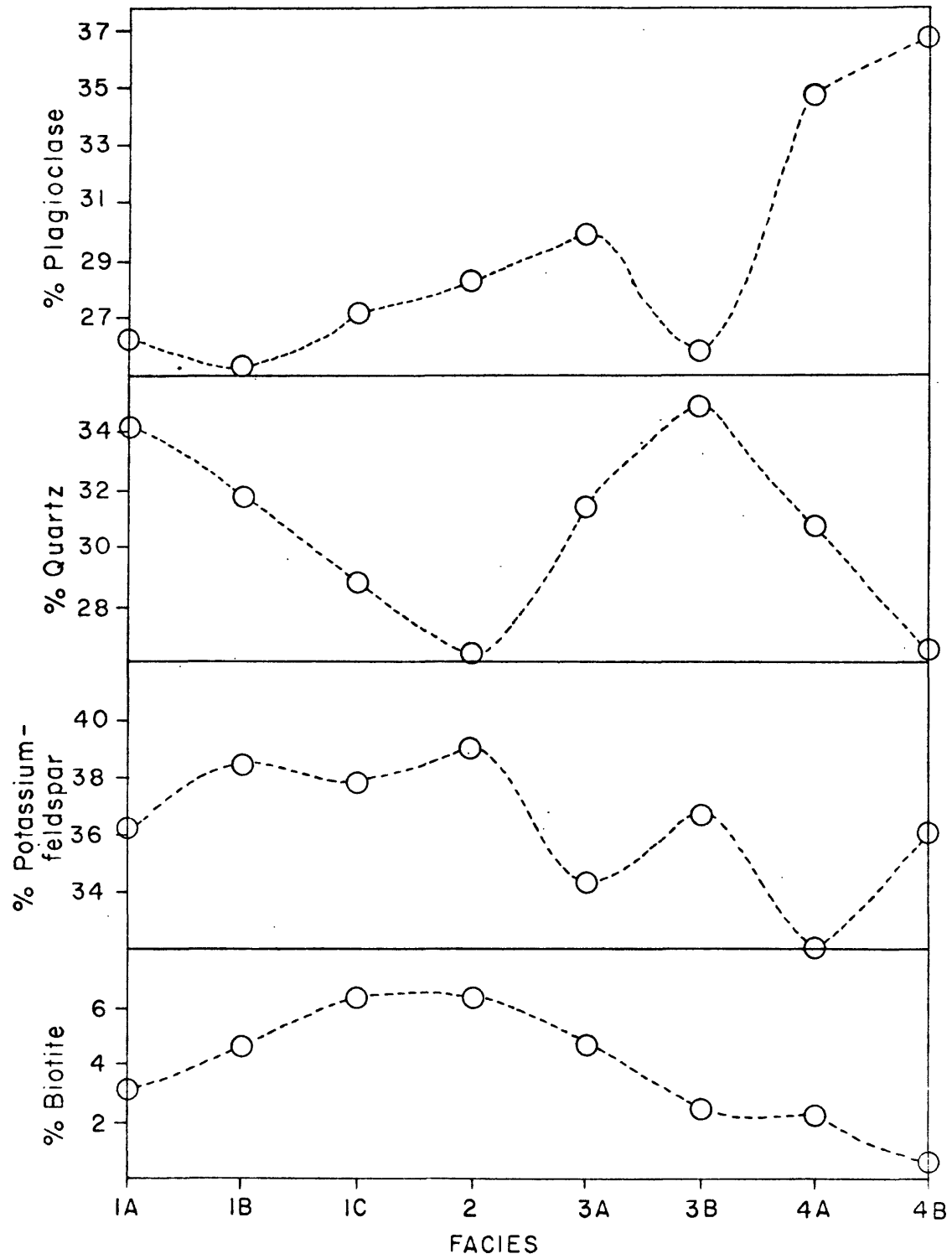

Figure 28. Variation of modal averages through the facies sequence. All data determined from whole-rock point counts except that for facies 3B which is for thin section point counts of the aplite groundmass only.

the framework silicate percentages in all the facies except 4B. Many of these variations are important to an understanding of the nature of the separate crystal populations in the complex that are identified and discussed farther on.

Chemical Composition

The major- and trace-element composition of 16 whole-rock samples and the trace-element composition of 18 mica separates from the complex have been determined by personnel of the Branch of Analytical Laboratories of the U. S. Geological Survey, and individual analysts are credited in the tables. The samples were collected from points throughout the complex and are typical of the facies they represent. The results for major oxides are listed in table 2, for whole-rock trace elements in tables 3 and 6, and for biotite trace elements in tables 4 and 5. The purpose of this section is to clarify the overall composition of the complex by comparison of its average whole-rock major- and trace-element and biotite trace-element compositions with some average granite and biotite compositions and to determine the nature of the principal chemical variations. Much of the major- and trace-element variation is systematic through the facies sequence and helps to clarify important aspects of the crystallization history.

Variation of Major Oxides

Most of the major-oxide compositions listed in table 2 are shown diagrammatically in figure 29. The variation diagrams of figure 29 bring out several important relationships: (1) there is a marked linear dependence of TiO_2, CaO, MgO, Fe_2O_3, and Al_2O_3 values with SiO_2 content, (2) K_2O values decrease slightly with increasing SiO_2,

Table 2.--*Whole-rock major oxide compositions of selected samples of the granite complex in weight percent.*

Field No.	Anal. Proc.	Facies	SiO_2	Al_2O_3	Fe_2O_3	FeO	MgO	CaO	Na_2O	K_2O	H_2O+	H_2O-	TiO_2	P_2O_5	MnO	CO_2	Sum
69AH289	*	1A	76.8	12.4	0.31	0.72	0.06	0.47	2.7	4.3	0.53	0.14	0.13	0.01	0.00	0.02	99
69AH295	*	1A	74.9	13.6	0.40	0.92	0.03	0.24	3.9	3.9	0.53	0.17	0.07	0.01	0.04	0.02	99
69AH277	*	1B	73.1	14.3	0.50	1.2	0.29	0.98	2.8	5.6	0.49	0.21	0.24	0.08	0.00	0.04	100
69AH278	*	1B	75.6	13.1	0.40	1.1	0.16	0.78	2.7	4.8	0.63	0.22	0.24	0.05	0.00	0.03	100
69AH228	x	1C	72.0	14.3	0.31	1.9	0.50	1.3	3.1	4.9	0.94	0.16	0.28	0.10	0.04	< 0.05	100
69AH427	*	1C	72.6	14.4	0.60	1.8	0.48	1.4	2.9	4.5	0.61	0.15	0.36	0.13	0.04	0.12	100
69AH272	*	2	71.2	14.6	0.70	1.7	0.51	1.6	2.9	5.1	0.51	0.11	0.44	0.17	0.04	0.02	100
69AH274	*	2	71.2	14.6	0.90	1.7	0.57	1.5	3.0	5.1	0.60	0.11	0.46	0.18	0.04	0.02	100
69AH283	x	2	70.8	14.8	0.73	1.7	0.58	1.6	3.4	5.1	0.63	0.11	0.38	0.14	0.05	<0.05	100
69AH286	*	2	71.6	14.6	0.70	1.7	0.54	1.5	2.8	4.7	1.1	0.22	0.42	0.17	0.04	0.02	100
69AH420	x	3A	71.1	14.5	0.39	2.1	0.53	1.5	3.0	5.2	0.75	0.09	0.40	0.13	0.05	<0.05	100
69AH242	*	3A	71.2	14.6	0.80	1.8	0.61	1.7	2.9	4.7	0.73	0.17	0.51	0.18	0.04	0.04	100
69AH227	x	3B	75.1	13.2	0.13	1.7	0.31	1.2	3.0	4.2	0.56	0.17	0.33	0.06	0.04	<0.05	100
69AH434	x	3B	76.3	12.9	0.38	0.56	0.08	0.74	4.0	4.2	0.39	0.08	0.04	0.00	0.03	<0.05	100
69AH460	*	4B	75.8	13.4	0.10	0.08	0.03	0.44	3.5	4.4	0.56	0.12	0.06	0.01	0.00	0.02	99
GS99-111	x	4B	76.9	13.2	0.00	0.28	0.04	0.54	3.9	4.4	0.34	0.11	0.02	0.00	0.00	<0.05	100
Average			73.5	13.9	0.46	1.31	0.33	1.09	3.2	4.7	0.67	0.15	0.27	0.09	0.03	0.04	100

Analytical procedure described in U.S. Geol. Survey Prof. Paper 575-B, p. 187-191 (*) and Bull. 1144-A supplemented by atomic absorption (x); Lowell Artis, P. Elmore, G. Chloe, H. Smith, J. Kelsey, J. Glenn, analysts.

Table 3.--*Whole-rock trace element composition of selected granite samples in ppm; Chris Heropoulos, analyst**.

Field No.	Facies	Mn (1)	B (7)	Ba (2)	Be (1)	Ce (70)	Co (2)	Cr (1)	Cu (1)	La (30)	Nb (7)	Nd (70)	Pb (7)	Sc (2)	Sn (7)	Sr (5)	V (3)	Y (10)	Zr (5)	Ga (2)	Li (200)	Yb (1)
68AH289	1A	150	N	50	7	N	N	N	7	-	15	-	30	N	5	10	N	10	70	20	200	1.5
69AH295	1A	300	100	7	20	N	N	N	2	-	100	-	70	5	30	N	N	15	100	30	700	3
69AH277	1B	200	N	700	5	200	N	2	7	150	15	70	50	3	N	200	7	30	100	20	<200	3
69AH278	1B	150	N	500	5	100	N	2	5	100	20	N	50	2	N	150	5	20	200	30	N	2
69AH228	1C	500	20	500	7	200	2	3	1	150	30	70	70	7	15	200	20	50	200	30	<200	5
69AH427	1C	300	N	700	5	200	3	3	1.5	100	30	70	30	3	10	300	15	50	150	20	N	5
69AH272	2	300	N	1,000	5	200	3	5	3	100	20	70	50	5	15	300	15	50	150	20	<200	5
69AH274	2	300	N	1,000	7	150	3	3	7	100	20	70	30	5	20	300	15	30	150	30	<200	3
69AH283	2	500	20	700	7	200	3	3	3	150	30	70	50	5	15	200	20	50	200	20	<200	5
69AH286	2	500	N	1,000	10	200	3	5	5	150	30	100	50	5	15	500	15	50	200	20	<200	5
69AH420	3A	500	10	700	5	200	3	3	1.5	150	20	70	70	5	10	200	20	50	200	50	<200	5
69AH242	3A	500	N	700	7	300	3	5	2	150	30	100	30	5	20	300	15	50	200	15	<200	5
69AH227	3B	500	20	150	10	150	2	1.5	1.5	70	30	N	70	5	20	70	10	50	150	20	200	5
69AH434	3B	300	15	20	10	N	N	N	5	N	50	-	150	N	50	10	N	100	150	30	300	10
69AH460	4C	10	10	30	10	N	N	1	5	N	50	-	150	3	10	10	N	150	100	50	N	15
GS99-111	4C	50	10	15	10	N	N	N	10	N	50	-	100	N	7	10	N	200	150	30	<200	20
Average		297	13	486	7	131	2	2	4	98	44	63	66	4	15	173	10	60	148	21	<200	6

*Semiquantitative spectrographic analyses; procedure described in U.S.G.S. Bulletin 1084-I.

Looked for but not detected (N); As, Au, Ni, Pd, Pt, Sb, Te, U, W, Zn Ge, Hf, In, Re, Ta, Th, Tl, Pr, Sm, Eu.

( ) Lower limit of detection in ppm.

Table 4.--*Results of semiquantitative spectrographic analysis of biotite separates from the granite complex, all results in ppm; R. E. Mays, analyst.*

Field No.	Facies	Ag (1)	B (7)	Ba (2)	Be (1)	Co (2)	Cr (1)	Cu (1)	Nb (7)	Ni (1)	Pb (7)	Sc (2)	Sn (7)	Sr (5)	V (3)	Y (10)	Zn (100)	Zr (5)	Li (200)
69AH289	1A	N	N	70	1.5	5	3	50	500	5	20	20	150	10	N	N	700	N	3,000
69AH277	1B	N	N	300	1.5	20	20	50	100	10	50	15	70	10	100	N	700	N	1,000
69AH278	1B	N	N	200	1.5	20	10	30	150	5	30	20	100	10	100	N	700	N	1,500
69AH228	1C	N	N	500	N	20	15	15	100	10	50	20	100	15	100	N	700	N	1,500
69AH64	2	N	N	300	N	30	15	30	50	15	20	10	70	10	70	N	700	N	1,500
69AH67	2	N	N	300	N	15	15	30	50	10	50	10	70	10	70	N	700	N	1,000
69AH272	2	N	N	300	1.5	30	15	50	70	15	15	15	70	10	100	N	700	N	2,000
69AH274	2	N	N	300	1.5	30	15	50	70	15	20	15	50	10	100	N	700	N	1,500
69AH283	2	N	N	300	1.5	30	15	70	70	15	20	15	70	10	100	N	700	N	2,000
69AH242	3A	N	N	300	1.5	30	20	10	70	15	20	10	70	10	100	N	700	30	1,500
69AH227	3B	N	N	300	3	20	15	15	100	7	70	20	200	10	70	20	1,000	N	2,000
69AH434	3B	N	7	100	2	5	7	30	300	N	50	20	1,000	10	15	30	700	N	G3,000
GS72-85	3B	N	N	300	1.5	20	15	70	100	10	30	20	300	10	50	20	700	N	3,000
69AH96	4B	7	N	300	2	15	20	10	100	5	70	20	100	10	50	20	700	30	2,000
GS98	4B	N	N	150	5	7	7	30	500	3	100	20	700	10	20	20	1,000	N	G3,000
GS99-111	4B	N	N	150	5	7	7	30	500	2	70	30	700	10	20	50	1,000	N	3,000
GS111	4B	N	N	150	5	7	7	30	300	2	200	20	500	10	30	30	1,000	N	3,000
69AH37D	*	N	150	200	10	5	10	15	20	5	N	15	700	10	15	10	150	N	3,000
Average (excluding 69AH37D and 69AH434)		0.5	0.0	285	1.8	20	14	36	175	9	52	17	175	10	71	9	920		1,967

*Muscovite from an albite-muscovite selvage along walls of a large pocket in rocks of facies 3A.
G Greater than value shown.
N Not detected at limit of detection.
Looked for but not detected; As, Au, Bi, Cd, La, Mo, Pd, Pt, Sb, Te, U, W, Ce, Ge, Hf, In, Re, Ta, Th, Tl, and Eu.
( ) Lower limits of detection, in ppm.

Table 5.--*Results of quantitative spectrographic analyses (1) for selected trace elements in biotite separates from the granite complex, all results in ppm; R. E. Mays, analyst.*

Field No.	Facies	B (7)	Be (1)	Cu (1)	Li (200)	Nb (7)	Sn (7)	Zn (100)
69AH289	1A	N20	2	33	2,300	300	160	800
69AH277	1B	N20	N2	48	680	160	90	1,100
69AH278	1B	N20	N2	33	1,100	90	120	900
69AH228	1C	N20	N2	18	1,000	130	120	950
69AH64	2	N20	N2	60	1,900	110	120	900
69AH67	2	N20	N2	32	1,200	65	90	750
69AH272	2	N20	N2	55	1,200	90	85	950
69AH274	2	N20	N2	55	1,100	65	75	850
69AH283	2	N20	N2	100	1,300	70	90	950
69AH242	3A	N20	N2	16	870	90	90	950
69AH227	3B	N20	3	14	4,800	65	280	1,300
69AH434	3B	N20	6	31	3,600	190	700	950
GS72-85	3B	N20	N2	65	3,100	140	300	1,100
69AH96	4B	N20	2	33	3,000	140	140	1,200
GS98	4B	N20	8	45	3,200	400	600	1,300
GS99-111	4B	N20	5	45	2,600	360	550	1,100
GS111	4B	N20	7	48	2,400	240	430	1,000
69AH37D	*	250	20	15	--	<20	550	90

(1) Accuracy is ±15 percent, except near the limits of detection, where only one digit is included.

* Muscovite from an albite-muscovite selvage along walls of a large pocket in rocks of facies 3A.

N Not detected at value shown.

( ) Lower limit of detection.

Table 6.--*Whole-rock trace element composition of five selected samples of the granite complex analyzed in 1975 by R. E. Mays.* All results in ppm.*

Field No.	Facies	Mn (.7)	B (2)	Ba (1)	Be (<.7)	Co (.7)	Cr (.7)	Cu (.7)	La (5)	Nb (7)	Ni (.7)	Pb (3)	Sc (.7)	Sn (2)	Sr (1)	V (1)	Y (5)	Zn (15)	Zr (3)	Ga (.7)	Li (100)	Yb (.7)
GS52	1A	300	10	70	7	N	5	1	N	30	N	50	5	7	15	N	20	N	50	20	500	5
69AH195	1B	500	10	500	7	1.5	10	3	100	10	1	50	5	7	200	7	20	30	50	20	300	3
69AH118	2	500	10	1,000	7	2	15	2	100	10	1	50	5	10	300	15	30	50	50	20	300	5
69AH452	3A	700	10	1,000	10	1.5	10	1	100	10	2	70	7	10	300	10	50	50	70	20	500	10
70AH756	4B	300	10	100	10	N	10	5	N	30	N	70	5	7	70	N	100	N	50	20	300	20

*Semiquantitative spectrographic analyses; procedure modified from that described in USGS Bulletin 1084-I.

N-Not detected at limit of detection.

Looked for but not detected; Ag, As, Au, Bi, Cd, Mo, Pd, Pt, Sb, Te, U, W, Ce, Ge, Hf, In, Re, Ta, Th, Tl, Eu.

( ) Lower limit of detection in ppm.

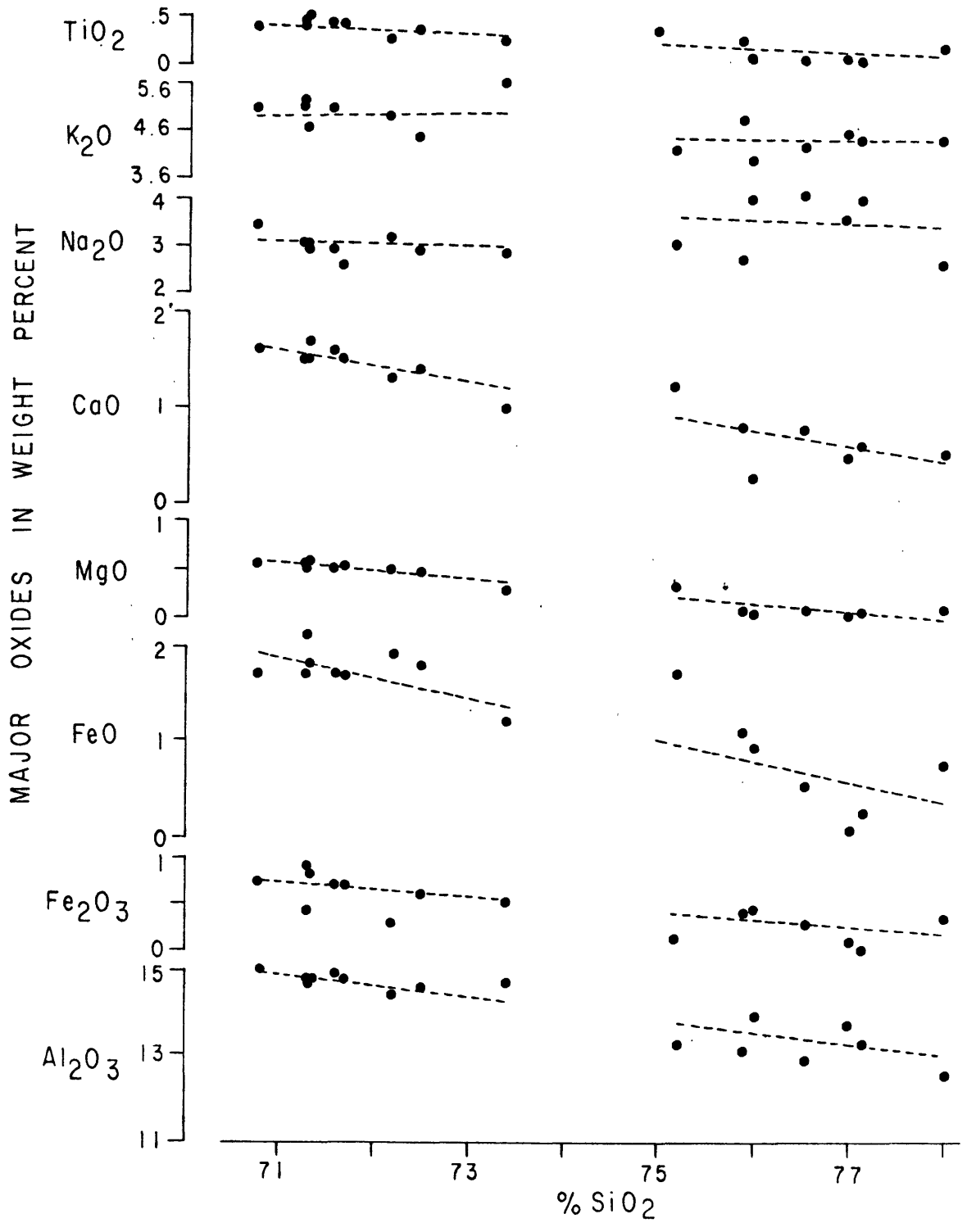

Figure 29. Variation of major oxides with percent SiO_2. Data from analyses listed in table 2 normalized to 100 percent. Dashed lines sketched by eye to illustrate general trends.

but Na_2O values generally are higher in samples high in SiO_2, and (3) there is a break in SiO_2 content between 74 and 75 percent, and this corresponds to shifts in the K_2O and Na_2O values. The regular and marked decrease of mafic oxides with increasing SiO_2 content suggests that the crystallization history of the complex is essentially one of magmatic differentiation. As the relative age relations of the different facies are known, the variation of major-oxide values with the facies sequence helps to clarify the nature of this differentiation.

The major-oxide values are plotted against the facies sequence in figure 30. Comparison of the variation in figure 29 with that in figure 30 quickly reveals major differences and shows that the facies sequence does not represent a simple trend toward more salic compositions. The variation within the facies sequence is of three types: (1) a decreasing SiO_2 trend that shifts to higher values in facies 3B and 4B, (2) increasing trends for TiO_2, CaO, MgO, FeO, Fe_2O_3, and Al_2O_3 with shifts to lower values in facies 3B and 4B, and (3) less regular trends for Na_2O and K_2O in which it appears that the Na_2O/K_2O ratio does not change significantly through facies 1B, 2, and 3A, but that it is distinctly high in facies 1A, 3B, and 4B.

The trends in figure 30 indicate that crystallization resulted sequentially in: (1) initial solidification of salic melts in the finer grained border facies, (2) an intermediate crystallization of relatively femic compositions in facies 1C through 3A, and (3) final crystallization of salic melts in facies 3B and 4B. Although they are not represented in the analyses, it is believed that samples of facies 4A would closely follow the trends in figure 30 and plot with samples from facies 3B and 4B. The negative slope of the SiO_2 variation

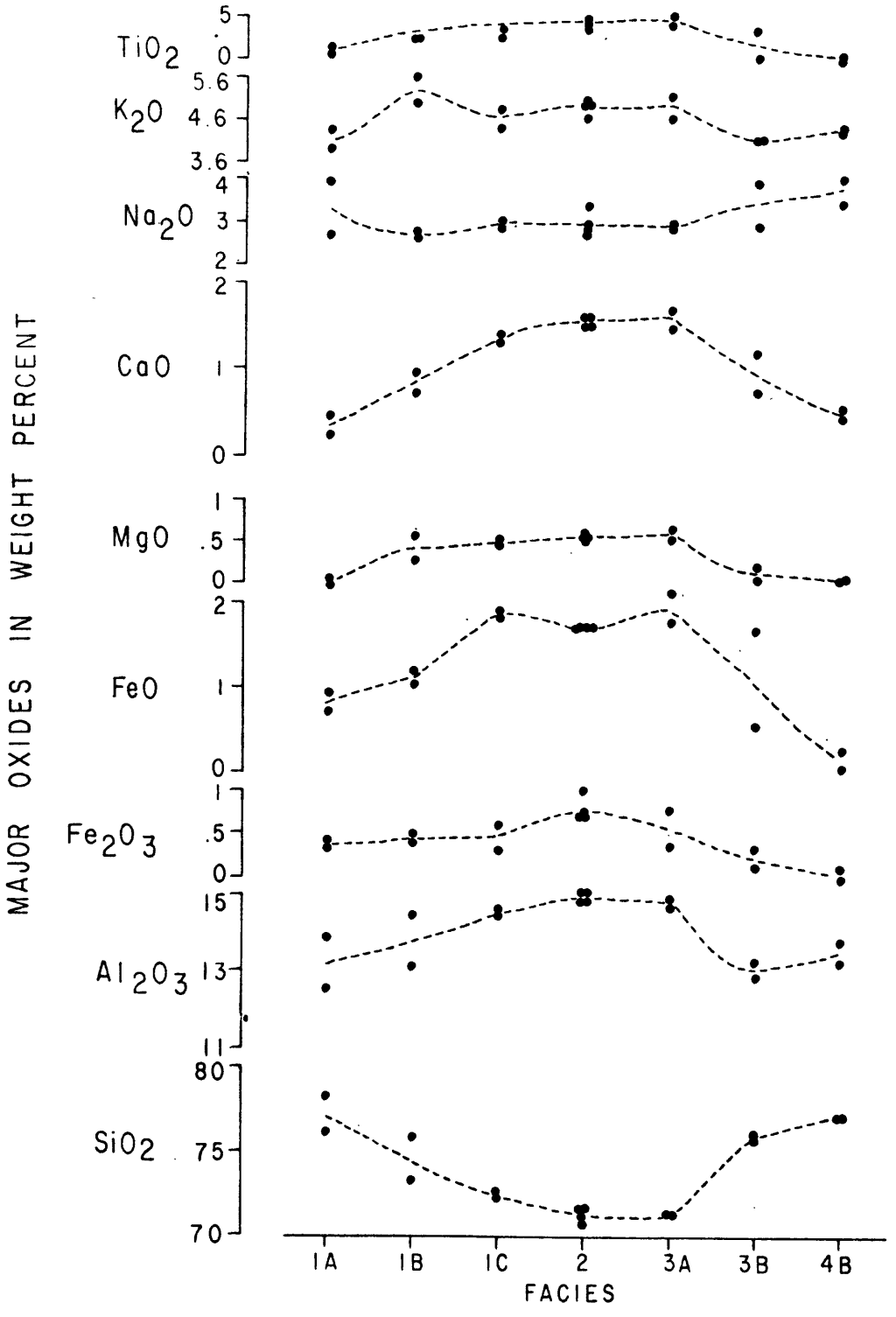

Figure 30. Variation of major oxides through the facies sequence. Data from analyses listed in table 2 normalized to 100 percent. Dashed lines sketched by eye to illustrate general trends.

indicates that the residual melt experienced enrichment in SiO_2; conversely, the positive slopes for TiO_2, CaO, MgO, FeO, Fe_2O_3, and Al_2O_3 indicate that the residual melt was depleted in these components by facies 1C through 3A crystallization. The marked shift in the direction and continuity of the trends upon crystallization of rocks of facies 3B and zone 4 indicate that these facies can represent residual melts that were developed by crystallization and separation from the melt-crystal system of facies 1C, 2, and 3A. The field data indicating that facies 3B and zone 4 were the parts of the complex to crystallize last, the cogenetic character of all the facies that is evidenced by the trends in figure 29, and the whole-rock and biotite trace-element data discussed below confirm this relationship.

The gap in SiO_2 values evident in figure 29 can be seen in figure 30 to be essentially a break between the values for the initial and final facies (1A, 3B, and 4B) and the values for the facies that crystallized at an intermediate stage (1C, 2, and 3A). The final facies clearly represent residual melts; the initial facies are composed of relatively rapidly crystallized rocks adjacent to or near the contact with the hornfels country rocks. Both the major- and trace-element irregularity are more pronounced in facies 1A rocks than in any other facies of the complex. This irregularity probably is the result of the complex interaction of several processes as discussed in the section dealing with the crystallization model for the pluton.

Variation of Trace Elements

The variations of some of the whole-rock trace-element abundances listed in table 3 through the facies sequence are shown diagrammatically

in figure 31. The concentrations in facies 1A are more irregular than in the other facies. In general, the concentrations increase from facies 1B to 3A and shift to divergent values in facies 3B and 4B. The trends are of two principal types: (1) markedly increasing values with maxima in rocks of facies 2 and shifts to low concentrations in facies 3B and 4B (Ba and Sr), and (2) gently increasing or nearly constant values with marked shifts to higher concentrations in facies 3B and 4B (Nb, Pb, and Be). Tin is an apparent exception to the general trends and is discussed separately below.

The trends of the first type, those for barium and strontium, are explained by preferential substitution of barium for potassium in K-feldspar and of strontium for calcium in plagioclase. The modal percentage of K-feldspar decreases then increases slightly from facies 1B through facies 2, then becomes slightly less in rocks of facies 3A. This modal trend closely follows the whole-rock barium trend through these facies. The modal facies trend for biotite is similar to that for K-feldspar, but the barium content of biotite is too low (table 4) to explain the observed whole-rock barium contents and variations. Strontium clearly follows calcium through the facies sequence, and as plagioclase is the only calcium-rich mineral of appreciable abundance, the distribution of strontium is mostly a function of the nature and distribution of this mineral. Both the modal-facies trend and composition of plagioclase correlate well with the observed strontium variation from facies 1B to facies 3A. The shift to low values for barium and strontium in facies 3B and 4C is in keeping with the more felsic nature of these later facies, but in addition it probably indicates that the barium and strontium concentrations that were present in the initial

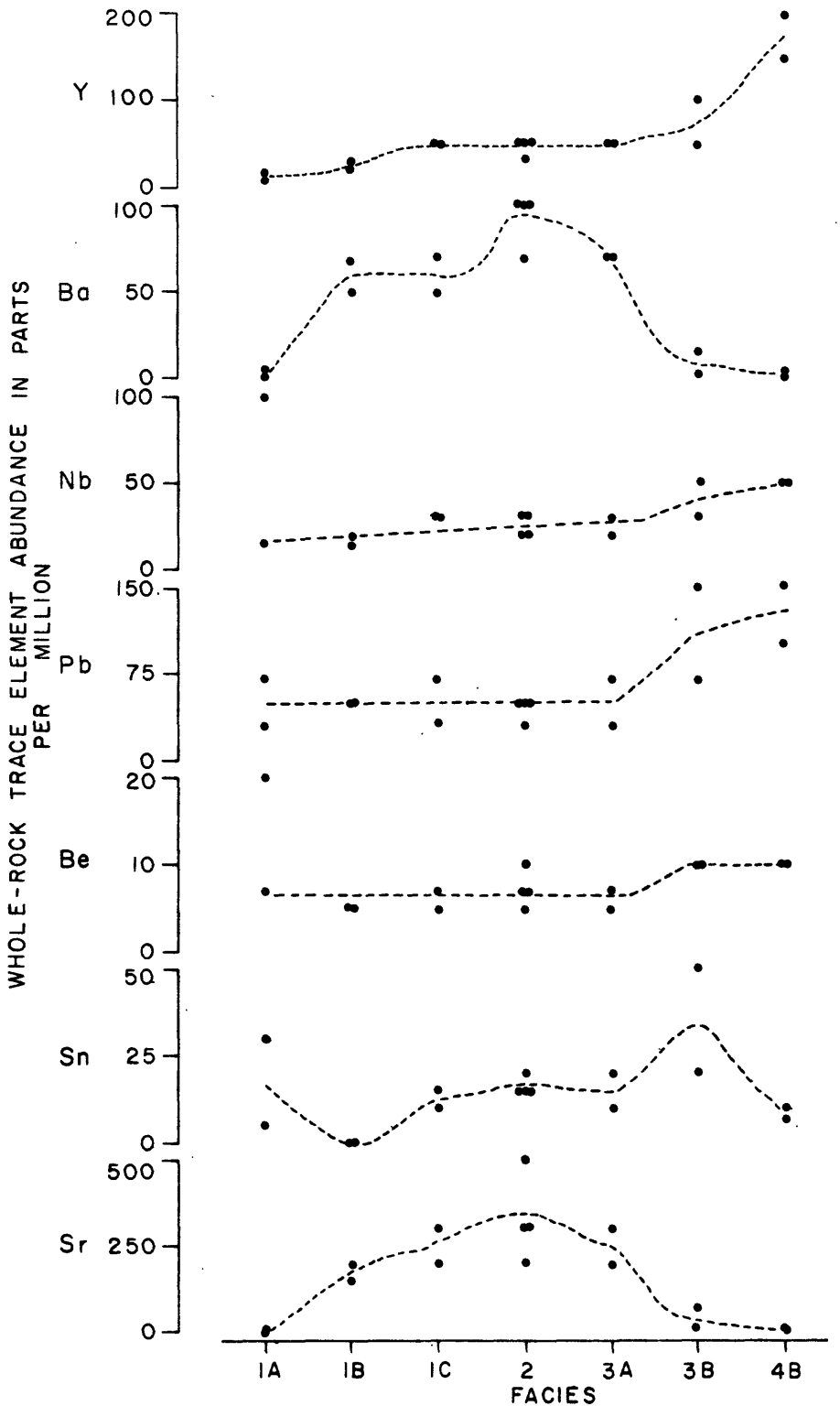

Figure 31. Variation of selected whole-rock trace elements through the facies sequence. Data listed in table 3. Dashed lines sketched by eye to illustrate general trends.

magma were essentially used up by incorporation in the K-feldspar and plagioclase of the more mafic intermediate facies. An interesting aspect of the barium and strontium distribution is that their higher concentrations in the intermediate facies probably were also enhanced by the slow crystallization rates that existed during crystallization of these facies.

The second type of trend, for niobium, lead, and beryllium, is explained by the inability of these elements to readily substitute for any of the major elements. These elements would be expected to concentrate throughout crystallization in the residual melt. Their concentration in facies 3B and 4B is commonly at least twice their concentration in earlier formed facies. The sharp shift to these higher concentrations in the last crystallized facies supports the conclusion that these facies represent mostly solidified residual melt.

The trend for tin through the facies sequence could be expected to be similar to that for the other trace elements that do not substitute readily for any of the major elements. There is some indication in the whole-rock trace-element data that tin follows the other fugitive elements in that the highest observed tin concentration is in one of the samples of facies 3B rocks, but the drop-off to lower values in facies 4B rocks must be explained. Rocks of facies 4B, unlike all other rocks in the complex, essentially lack biotite. They characteristically have many small miarolitic cavities, interstitial fluorite, and muscovite that in part has clearly replaced biotite. If high tin concentrations were present in these rocks when they first crystallized, it must have been removed by subsequent reactions. In the process, muscovite replaced pre-existing biotite.

Variation of Trace Elements in Biotite

Seventeen biotite separates from unaltered whole-rock samples and one muscovite separate from a muscovite-albite replacement selvage along the walls of a large pocket have been spectrographically analyzed for selected trace elements. These data are in two parts: (1) results of semiquantitative analyses for a large number of trace elements (table 4), and (2) results of quantitative analyses for the selected elements B, Be, Cu, Pb, Sn, and Zn (table 5). The semiquantitative data provide a scan of the trace-element composition and indicate the general abundance of those trace elements present in appreciable amounts in the micas. The quantitative data were obtained to more closely study the variation in trace-element abundance through the facies sequence. The elements determined quantitatively were chosen in part because Sainsbury and Hamilton (1968, p. F11) reported them to be present in readily detectable quantities in biotite from some other tin-granites of the Seward Peninsula. In addition, biotite is the preferred mineral host for most of these elements (Nb, Sn, Zn, and Li). The data in table 4 show that many elements are present in low but detectable amounts, and that barium, niobium, tin, zinc, and lithium are present in appreciable quantities. The semiquantitative data reveal that some of these elements, such as niobium and tin, show significant variation through the facies sequence, but for many, such as barium and zinc, the nature of the variation, if any, is not clear.

Most of the quantitative data in table 5 are shown diagrammatically in figure 32. The variation in copper content of the biotite through the facies sequence is irregular, and systematic differences from one facies to the next are not present. On the other hand, the variation

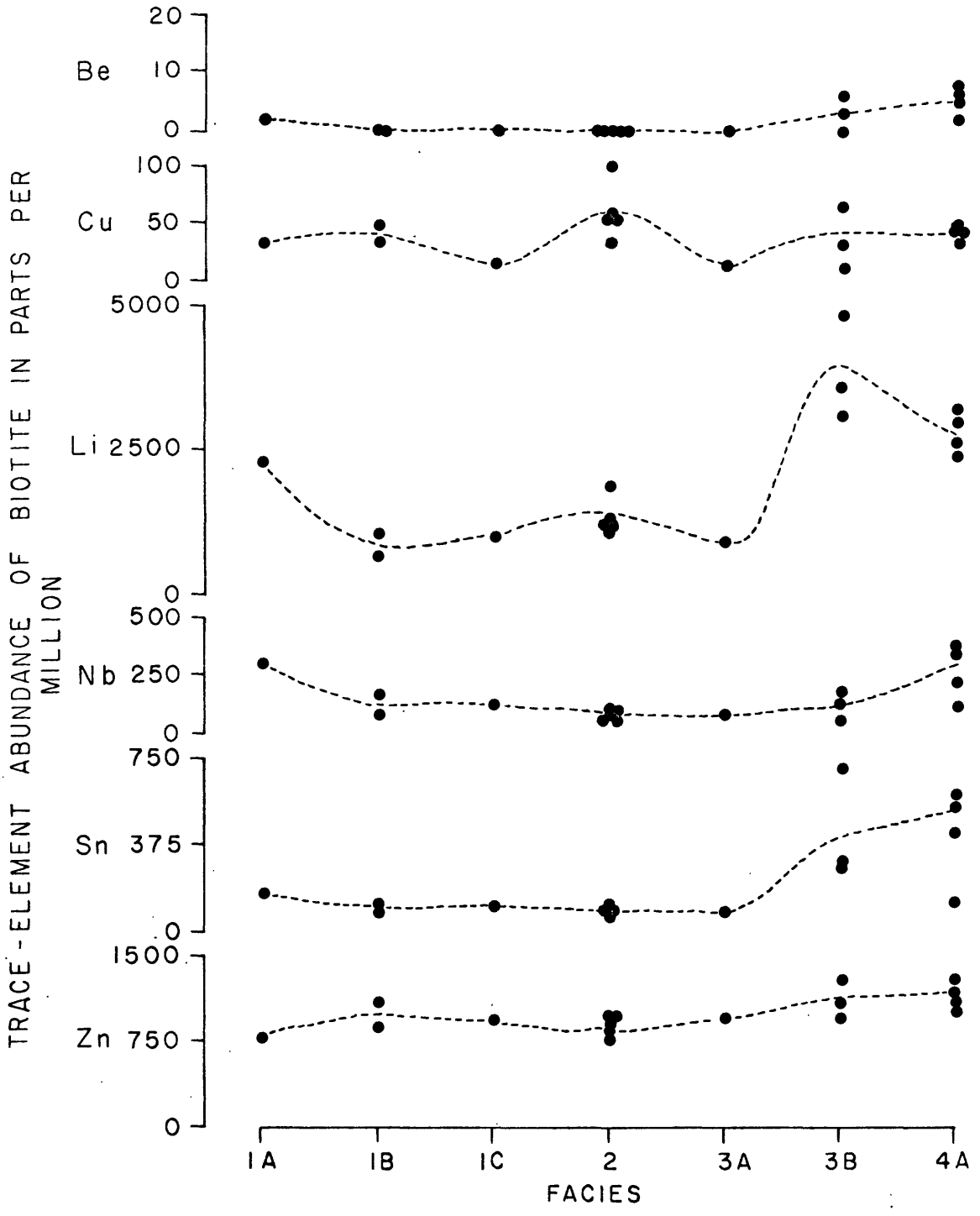

Figure 32. Variation of selected trace elements in biotite through the facies sequence. Data listed in table 5. Dashed lines sketched by eye to illustrate general trends.

for Be, Li, Nb, Sb, and Zn through the facies sequence is systematic, and the data for all these elements clearly show a slightly decreasing trend or almost constant value from facies 1A or 1B through facies 3A and then a shift to higher concentrations in facies 3B and 4A. In general, the highest values for these elements are in biotite from facies 4A. The highest observed lithium value is in facies 3B rocks.

The elements that show nearly constant or slightly decreasing concentrations through the intermediate facies and higher values in the final facies are those that substitute in limited amounts for major elements in the biotite structure. These variation trends indicate that, throughout intermediate-facies crystallization, these elements were being selectively partitioned to the residual melt.

The variation of tin concentration in the biotite provides some explanation of the observed whole-rock variation of this element. The nearly constant tin concentration in biotite through the intermediate facies indicates that the whole-rock variations through these facies shown in figure 31 must be due to variations in the amount of biotite present or the contributions of other minerals. Both factors probably contribute to the slight whole-rock tin increase; modal biotite increases to a maximum in facies 2 (fig. 28) and sphene, a likely concentrator of tin, is present in minor but above-average amounts in this facies. The whole-rock tin content apparently cannot be completely explained by the distribution and composition of biotite alone, in that the whole-rock tin concentration is commonly about twice the amount that could be contributed by biotite. Either the whole-rock concentration of tin reported in table 3 is too high, or significant amounts of tin are present in minerals other than biotite.

Some recent data suggest that the semiquantitative whole-rock determinations for tin listed in table 3 are too high. Five additional whole-rock samples, two from facies 2 and one each from facies 1A, 3A, and 4B, were analyzed in 1975 for the entire trace-element suite by semiquantitative techniques. The procedures used in 1975 are revised from earlier ones and are considered to be more accurate (R. E. Mays, 1975, pers. commun.). The 1975 results are listed in table 6 and show tin contents that are less than or equal to 10 ppm. The conclusion is that the whole-rock tin concentrations in table 3 are too high, and that the tin content and distribution of biotite readily explains the whole-rock tin variation shown in figure 31. The newer data in table 3 have not been used to study the trace element variation between facies because data from all the facies are not available. The newer data do not reveal any differences in the general trends exhibited by the older data in table 3, and, as the older data were obtained under the same laboratory and analytical conditions, they are entirely satisfactory for studying the trace element variation through the facies sequence. The new data differ from the old only in that: (1) nickel and zinc are present in detectable amounts, (2) values for chromium are consistently higher, but those for tin, and probably niobium, are consistently lower, and (3) the values for lithium are more consistently within detectable limits.

The mica trace-element data provide one more important link to the whole-rock data. The lack of whole-rock analyses for facies 4A is a serious gap in the analytical data, more so for the trace elements than for the major oxides. The mica data partly fill the trace element void for this facies, and show that tin was concentrated to high values

in the residual facies of the complex. As discussed more completely later, facies 4B rocks are leached facies 4A rocks and the tin they once contained has been removed, resulting in the low whole-rock values as illustrated in figure 31.

Trace-Elements in Pocket Muscovite

Muscovite was separated from the replacement selvage (fig. 25) that is present along the walls of a large pocket in facies 3A rocks. The semiquantitative and quantitative trace-element data for this mineral are included in tables 4 and 5 along with those for the other micas from the complex. The muscovite has high concentrations of beryllium, lithium, and tin, but low concentrations of copper, niobium, and zinc. The high boron content shown in table 5 for this sample is probably due to contamination by small grains of schorl, which is a minor but important constituent of the selvage material.

The selvage material probably represents the products of reaction between a separated and trapped aqueous phase and the enclosing seriate-textured rocks of facies 3A. The most obvious chemical change has been the addition of Na_2O, and the selvage is essentially albitized granite. Water, boron, and fluorine also have been added. As the muscovite is part of the reaction products, its trace-element composition should reflect, at least in part, the trace-element composition of the coexisting aqueous phase. The high concentrations of beryllium, lithium, and tin in the muscovite support the conclusion that the coexisting aqueous phase was enriched in these elements. As muscovite forms about 50 percent of the selvage material, the whole-rock tin concentration for this material is about 300 ppm. This is 30 times the average tin

concentration of the granite samples and clearly shows not only that tin was concentrated toward the residual melt throughout magmatic fractionation, but also that once a separate vapor phase was evolved, the tin was strongly partitioned to it. This relationship is also supported for beryllium and lithium. The muscovite trace-element data do not reveal what has happened to the other elements that were concentrated through magmatic fractionation, but it seems likely that they were also partitioned to the evolved vapor phase. Once in this phase, their distribution apparently became governed by the complex relations of a high-temperature hydrothermal system (only part of which is exposed in the pocket), and they were effectively not available for direct precipitation or substitution in the muscovite structure under the conditions that must have prevailed in the pocket environment.

Comparison with Average Compositions of Granite and Biotite

The overall chemistry of the complex is defined by comparisons with compiled major-oxide, whole-rock trace-element, and biotite trace-element averages. For the major oxides, the average and calculated bulk compositions of the complex are shown in table 7 along with the average for most of the analyzed tin-granites of the world (Štemprok and Škvor, 1974), some biotite granites (Nockolds, 1954), and general calc-alkalic granites (Nockolds, 1954). The calculated bulk composition of the complex is slightly more mafic than the arithmetic average. Comparison of the bulk composition with the other granite averages shows that the complex is similar to the average for tin-granites but that there is one significant difference with respect to the other

Table 7.--*Average and calculated bulk major-oxide composition of the granite complex and other granite averages in weight percent.*

Oxide	Average (from table 2)	Calculated bulk composition	World tin-granite average (1)	Biotite-granite average (2)	Calc-alkali granite average (2)
SiO_2	73.5	72.92	73.02	73.28	72.08
Al_2O_3	13.9	14.20	13.9	13.33	13.86
Fe_2O_3	.46	.52	.78	.87	.86
FeO	1.31	1.59	1.34	1.38	1.67
MgO	.33	.42	.52	.50	.52
CaO	1.09	1.26	1.24	1.17	1.33
Na_2O	3.2	3.03	3.28	2.96	3.08
K_2O	4.7	4.84	4.57	5.52	5.46
H_2O+	.67	.48	.73	.50	.53
H_2O-	.15	--	.17	--	--
TiO_2	.27	.33	.21	.30	.37
P_2O_5	.09	.11	.15	.14	.18
MnO	.03	.03	.05	.05	.06
Co_2	.04	.05	--	--	--

(1) Štemprok and Škvor, 1974, p. 71.

(2) Nockolds, 1954, p. 1012.

granite averages. The Serpentine Hot Springs complex and evidently other tin-granites have a distinctly lower K_2O/Na_2O ratio.

The average values for selected trace elements in the complex are shown in table 8 along with the average for trace elements in low-calcium granites as compiled by Turekian and Wedepohl (1961). The complex contains distinctly less Mn, Cr, Cu, and V and distinctly more Be, La, Nb, Pb, Sn, and Li than the compiled low-calcium granite average. Of those elements that are more abundant in the complex, the values for Be, Nb, Pb, and Sn are two times or more above the average values for low-calcium granites.

Biotite is the preferred mineral host in the complex for many of the elements listed in table 8, and its trace-element composition more clearly indicates the nature of the overall trace-element composition of the complex. The average trace-element composition of biotite in the complex (table 9) has been calculated from the results of 16 of the analyses listed in table 4. Data for sample 69AH434 were not included in the calculation because its composition is somewhat anomalous. Also shown in table 9 is the average trace-element composition of 28 biotites from 7 different intrusive bodies in the western United States. The average for the western United States biotites was calculated from data reported by Lovering (1972).

Compared to the data reported by Lovering (1972), the biotites from the granite complex in the Serpentine Hot Springs area have a distinct trace-element composition that is characterized by two different element suites. The first suite includes those elements with high concentrations (Be, Nb, Pb, Sn, Zn, and Li) and the second includes those with low concentrations (Ba, Co, Cr, Ni, Sc, V, and Y). Zirconium

Table 8.--*Average trace element composition of the granite complex and of low Ca granites(1) in ppm.*

Element	Average (from table 3)	Low Ca granite average
Mn	297	390
B	13	10
Ba	486	840
Be	7	3
Co	2	1.0
Cr	2	4.1
Cu	4	10
La	98	55
Nb	44	21
Pb	66	19
Sc	4	7
Sn	8*	3
Sr	173	100
V	10	44
Y	60	40
Zr	148	175
Ce	131	92
Ga	21	17
Li	380*	40
Yb	6	4
Nd	63	37

(1) Turekian and Wedepohl, 1961

*from table 6

Table 9.--*Average and range of trace element abundances in biotites from some felsic intrusive rocks in the western United States and from the Serpentine Hot Springs area. All data in ppm.*

Element	Western United States[1/]		Serpentine Hot Springs area		Concentration factor[2/]
	Average	Range	Average	Range	
Ba	1,925	300-5,000	285	70-300	0.15
Be	0.5	0-2	2	0-10	4
Co	50	20-100	20	5-30	0.4
Cr	120	7-300	14	3-20	0.12
Cu	39	5-200	36	10-70	0.92
Nb	46	0-150	175	70-500	3.8
Ni	91	15-500	9	0-15	0.1
Pb	10	0-70	52	15-200	5.2
Sc	170	0-150	17	15-30	0.10
Sn	10	0-50	175	50-500	18
Sr	64	10-300	10	10-15	0.16
V	313	150-700	71	0-100	0.27
Y	41	0-300	9	0-50	0.2
Zn	75	0-500	920	700-1,000	12
Zr	190	15-500	2	0-30	0.01
Li	34	0-300	2,000	1,000-3,000	60

[1/] Calculated from data reported by Lovering (1972) for 28 biotites separated from seven intrusive complexes of quartz monzonite and granite composition.

[2/] Average Serpentine Hot Springs area/average western United States.

appears to be part of the depleted suite, but since zircon inclusions play a major role in the distribution of this element the data in table 9 are inconclusive without additional petrographic information. The copper averages are about the same for the two different biotite groups, but the range of values for the biotites from the Serpentine Hot Springs area is narrower. The degree of enrichment for some of the elements is spectacular; the lowest values for tin, zinc, and lithium in biotites from the Serpentine Hot Springs area are equal to, or greater than, the highest values for these elements in biotites studied by Lovering.

Much work has been done to clarify the trace-element geochemistry of tin-granites and their constituent minerals, and the data in table 9 confirm many general relationships identified by others (for example, Bradshaw, 1967; Odikadze, 1967; Sainsbury and others, 1968; Štemprok, 1971; Groves, 1972). But because the calculated averages in table 9 characterize the trace-element composition of the granite complex as a whole and the data are for a relatively large suite of elements, they also provide the basis for making some interpretations concerning the origin of the tin-granite magma, as discussed later.

The comparison of averages has shown that the complex is similar in major-oxide composition to other tin-granites and that it has a distinctly lower K_2O/Na_2O ratio than average biotite granite as compiled by Nockolds (1954). The whole-rock trace-element composition is also similar to that in other tin-granites (Štemprok, 1970, p. 116; Sainsbury and Hamilton, 1968), but it differs significantly from the averages compiled for low-calcium granites by Turekian and Wedepohl (1961). Compared to the averages in low-calcium granites, the granite complex

is more fractionated and contains enriched concentrations of several fugitive elements including tin. The trace-element composition of biotite clearly identifies the overall fractionated nature of the complex; the biotites are exceptionally enriched in the fugitive elements. The important differences all point to the fact that the complex, as a whole, is more fractionated than average granites.

Crystal Populations

The textural, petrographic, and compositional data together help to identify and characterize eight major crystal populations within the complex. As referred to here a crystal population includes those crystals, regardless of mineralogy, that grew together and were simultaneously affected by any later changes in the crystallizing environment. The different crystal populations include: (1) equigranular crystals of facies 1A, (2) the texturally and compositionally transitional crystals of facies 1B, 1C, and 2, (3) the larger well-formed crystals of facies 3A, (4) the finer grained poorly formed crystals of facies 3A, (5) the phenocrysts of facies 3B, (6) the fine-grained crystals in the aplitic groundmass in facies 3B, (7) the crystals of facies 4A, and (8) the crystals of facies 4B. These crystal populations are discussed separately below. Their characteristics together define the framework within which a complete crystallization model for the complex can be set up.

The equigranular crystals of facies 1A form a population that has many anomalous textural and compositional characteristics. This population has high SiO_2, Na_2O, Sn, Pb, Be, and Nb values and low K_2O, CaO, MgO, MnO, FeO, Y, Ba, and Sr values. The variation diagrams of

figure 30 show that the values for all the major oxides except Na_2O and K_2O are not markedly divergent from the variation trends in the facies transitional inward from facies 1A; the Na_2O values are enriched and the K_2O values are depleted in this facies. Also anomalous are the highly variable compositions of the dominantly unzoned plagioclase (fig. 27), the shift in modal population of feldspars (fig. 28), the clouded nature of the feldspars, and the local but extensive replacements by muscovite. Together, these data suggest that processes affecting the alkali content of these rocks are in large part responsible for their anomalous nature.

The texturally and compositionally transitional plagioclase, K-feldspar, and biotite crystals of facies 1B, 1C, and 2 constitute another distinct crystal population within the complex. Nowhere in the facies 1B to 2 transition does quartz display any evidence of having coexisted as a liquidus phase with plagioclase, K-feldspar, and biotite. It invariably forms anhedral grains or aggregates of grains that are interstitial to the other essential minerals, and it is therefore not considered to be part of the facies 1B, 1C, and 2 crystal population. The transitional compositions between facies 1B and 2 are evident in the chemical data (figs. 30, 31, 32), in the modal data (fig. 28), and in the inward increase in anorthite content of the plagioclase (fig. 27). The inward change in biotite color and in the perthitic nature of K-feldspar suggests that these minerals also gradually shift in composition inward.

The nature of the transitions with the facies 1B, 1C, and 2 crystal populations is especially well illustrated by megascopic textural shifts inward, such as the increasing aggregation, size,

and morphological development of K-feldspar, and also by the progressive changes in plagioclase zoning relations. In general, the zoning divides the individual plagioclase crystals into three parts: (1) homogeneous calcic cores that commonly show even extinction, but can have patchy extinction, twinning discontinuities, and selective development of secondary minerals, (2) normal-zoned marginal bands that surround the cores and have thin and somewhat faint oscillations, and (3) sodic rims that lack oscillations and have even or normal-zoned extinction. The compositional variation within the zoned crystals is commonly not great, but it is consistently normal in that the cores are calcic oligoclase (An_{22-27}), the marginal bands are normal-zoned toward sodic oligoclase, and the rims are sodic oligoclase (An_{10-18}). The progressive changes in the zoning relations from facies 1B to facies 2 include changes in the composition and physical characteristics of cores, the degree of oscillation development within the marginal bands, the sharpness of normal zoning within the rims, and distinct changes in the relative proportions of marginal bands and rims. Through this part of the facies sequence, the cores change inward from being the dominant part to being one-third of individual crystals, and from being poorly defined and having even extinction to being sharply defined by twinning discontinuities and inclusions. The marginal bands gradually change from being thin, poorly defined, and containing only a few faint oscillations in facies 1B to having many faint oscillations and being half or more of individual crystals in facies 2. The rims are well developed in facies 1B, where they are one-fourth to one-third of individual crystals and are moderately normal zoned, but they become narrower and commonly inconspicuous to absent in rocks of facies 2.

The larger, morphologically well-developed calcic oligoclase, perthitic K-feldspar, quartz, and biotite crystals of facies 3A constitute a separate crystal population. This is the first facies interior from the facies 1A rocks in which quartz appears to have coexisted as a stable liquidus phase with the other essential minerals. Some aspects of the feldspars in this crystal population are similar to those in facies 2. The larger plagioclase crystals in facies 3A correspond to the inward pattern of change in that their well-defined cores are slightly higher in anorthite content than facies 2 plagioclase. The principal difference between the larger plagioclase crystals in facies 3A and the plagioclase of facies 1B through 2 is that the marginal band is condensed and the rim better developed in the former.

The large K-feldspar crystals are similar to the perthite phenocrysts in facies 2 except that they are not pinkish and are slightly larger. The finer grained crystals of facies 3A are distinctly different in several respects from the larger crystals of this facies and together constitute another crystal population. This population contains dominantly unzoned albitic oligoclase, nonperthitic Or-rich K-feldspar, quartz, and probably some biotite that for the most part form subhedral or anhedral intergranular grains. The most important aspect of this population is the clearly different composition of the feldspars from that of the coarser crystal population. The difference between the two crystal populations in facies 3A explains why facies 3A is very similar to facies 2 in composition (figs. 30, 31, 32) but modally contains less K-feldspar (fig. 28). This diminished modal K-feldspar percentage is in keeping with the less albitic nature of the second-

generation K-feldspar, which is more abundant than the earlier formed large perthite crystals of the first population.

Facies 3B is another facies that contains two different crystal populations, in this case clearly identified by the grain size contrast between phenocrysts and groundmass. The phenocrysts include albitic oligoclase, perthitic K-feldspar, quartz, and biotite. The plagioclase has albite overgrowths, and the coarse perthite has overgrowths of nonperthitic K-feldspar. Another important characteristic of this population is the nature of the plagioclase zoning and composition. The plagioclase phenocrysts display some gross zoning relations that are similar to the larger plagioclase crystals in facies 3A, but they are different in two important ways. First, the overall compositional variation is within the sodic oligoclase range, about An_{18} to An_{10}, and second, many phenocrysts have features suggestive of well-developed primary zoning and corresponding compositional heterogeneity but they are actually fairly homogeneous in composition. The allotriomorphic mosaic of crystals in the aplitic groundmass is the second and clearly later crystal population in facies 3B. It includes unzoned albite-oligoclase, nonperthitic K-feldspar, quartz, and biotite. The feldspars are commonly clouded and the modal data (fig. 28) show that the mosaic has a low percentage of plagioclase.

Each of the two facies in zone 4 represents a crystal population. The equigranular hypidiomorphic crystals of facies 4A include albite-oligoclase, slightly perthitic K-feldspar, relatively dark-colored quartz, and biotite. This population is clearly more felsic than those that formed earlier (escepting facies 1A), if only on the basis of the petrographic (fig. 27) and modal data (fig. 28). The biotite

trace-element data (fig. 32) show that some of the highest abundances of the fugitive elements are present in micas from the facies 4A crystal population. Muscovite replacement of biotite, light-colored quartz, and a decreased modal percentage of quartz distinguish the last crystal population, that of facies 4B. The feldspars tend to be clouded in this facies and plagioclase superficially resembles that of facies 4A, but the latter contains some crystals that are zoned, whereas plagioclase in facies 4B is characteristically unzoned and has even extinction. The trace-element data (fig. 31) show that tin is very low in this crystal population.

Geometry of the Complex

Some exposed spatial relationships provide a basis for modeling the size and shape of the complex. The spatial relationships permit estimation of the overall pluton volume and of the volume relationships of the internal zones. The volume relationships provide the data needed to determine bulk composition of the pluton and to estimate the degree of crystallization that accompanied formation of the successive internal zones.

External Form

The general external form of the complex appears to be that of an elongate tadpole or cylinder-shaped body that plunges shallowly to the southeast. This form and attitude is suggested by the present exposed outline and facies distribution as well as certain contact zone relations. The exposed surface approximates a horizontal section through the body. The most conspicuous feature shown by this section is the oval outline of the external contact and the concentric zoning parallel to it in the

central and western parts of the pluton. This outline is distorted along the northeast contact by an eastward projecting bulge. The mapped facies distribution clearly shows that this bulge was formed by intrusion of facies 3A and 3B rocks. At the present level of exposure the concentric and oval form of the body apparently existed intact throughout crystallization of the marginal zones, but the northeast contact was a zone of structural weakness that localized upward displacements of magma during the later stages of crystallization. The exposed outline and facies distribution thus emphasize the initial oval nature of the pluton, and these relationships are believed to dominate the overall horizontal shape of the body at depth.

The general attitude of the pluton can be inferred from several relationships in the contact zone. The most important of these are observed dips of the pluton-country rock contact, variations in the width of the thermal aureole, and the spatial relationship of mineralized areas to the exposed pluton. The pluton-country rock contact has a shallow dip, locally only about 10^{o}, at several places along the southeast margin. The thermal aureole is widest along this part of the contact and, together with the restriction of mineralization to country rock areas southeast of the exposed granite, this further suggests that the upper surface of the pluton dips shallowly to the southeast. The attitude of the contact along other parts of the pluton margin is not clearly shown by any of the mapped field relations. The only indication that the northern contact may dip in the same direction as the southeastern contact is the distribution of sample localities from which rocks of facies 1A were collected. Rocks of this facies are present only along or near the pluton-country rock contact, and are

found over a wider area long the northern contact than along any other part of the margin. The wider band of facies 1A rocks here is on a southeast-facing slope. This may indicate that the northern contact dips semi-parallel to the ground surface, thereby increasing the exposed width of facies 1A rocks. This can only be a tentative conclusion, however, because the samples were all collected from surface rubble and downslope movement may have helped increase the width over which facies 1A rocks are present.

Because of the relationships noted above, the modeling of the internal geometry of the complex that follows below assumes that the initially emplaced pluton was distinctly elongate, oval in cross section, and had a shallow plunge to the southeast.

In outlining the inferred crystallization history for the complex, a series of diagrams is useful for realistically depicting the internal geometry of the pluton as it evolved during cooling and consolidation. The diagrams are based on a model that can be used to calculate the relative volume relationships within the complex. The model is a concentrically zoned cylindrical mass that is oval in cross section. The radius relationships of the concentric cylindrical shells were estimated from the distance between outer zone margins as exposed along a line trending N. 20^{o} W. through the center of zone 4, and the lengths of the shells were estimated from the projections shown in the cross section of plate 1. These dimensions, together with the calculated volumes and their relative proportions, are listed in table 10.

As considerable variation in composition exists among the facies of zone 1 and zone 3, the relative proportions of these different

TABLE 10.--Dimensions and calculated volumes of the granite complex based on a cylindrical shell model for Zones 1 through 4. Volume proportions of facies within Zone 1 and 3 are assumed.

Zone	Radius (km)	Length (km)	Volume* $(km)^3$	Facies	Facies volume / Zone volume	Volume % of pluton
1	4.0	16	473	1A	0.1	6
				1B	0.3	18
				1C	0.6	35
2	2.7	14.5	181	2	1	23
3	1.9	13.5	144	3A	0.7	12
				3B	0.3	5
4	0.4	11.3	6	4A+4B	1	1
Total			804			

*Volume of indicated zone cylinder minus volume of zone cylinders internal to it.

facies have been estimated in order to calculate a bulk composition for the pluton. The estimated facies proportions also are listed in table 10. The calculated volume relationships were used to determine the bulk major oxide composition that is shown in table 7. In addition, the volume relationships show that the major proportion of the pluton crystallized to form the various facies of zones 1 and 2. The internal displacements that were followed or accompanied by crystallization of the facies of zone 3 and 4 affected relatively small volumes of internal parts of the pluton, and they took place only after the entire complex was more than three-quarters crystallized.

Crystallization of the Granite Complex

The field relationships, the petrographic, textural, and modal variations, and the major-element and trace-element chemistry of the granitic rocks provide a framework within which a crystallization model for the complex can be defined. This model, as here proposed, integrates all the available data toward a conceptual understanding of the magmatic processes that were operative. The following discussion is based upon two principal assumptions: (1) following initial emplacement of magma, most of the crystallization occurred in an essentially closed system without further addition of magma from below, and (2) the initial magma was compositionally homogeneous.

The most important single aspect of the granite complex is the wide spectrum of textural variations among rocks that everywhere are of granite composition. Study of the complex has been aided tremendously by the recognition and mapping of the texturally contrasting facies. Discontinuities between such facies provide the primary basis for

subdividing the crystallization history of the complex into five different stages, as follows:

1. Crystallization of fine-grained equigranular rocks (facies 1A) at and near the margin of the pluton,

2. Crystallization of the outermost parts of the pluton to yield the completely transitional textures and compositional trends observed among rocks of facies 1B, 1C, and 2,

3. Emplacement and crystallization of seriate rocks of facies 3A,

4. Emplacement and crystallization of a crystal-rich system to form composite-textured rocks of facies 3B,

5. Final crystallization of facies 4A rocks under vapor-saturated residual-melt conditions, and localized formation of rocks of facies 4B.

These crystallization stages are discussed separately below, and the principal magmatic processes that were important during the successive stages are identified. The discussions utilize a series of diagrams that depict the evolution of the granite complex. Though necessarily schematic, they have been prepared approximately to scale.

Stage 1--Crystallization of Facies 1A

Stage 1 crystallization developed the fine- to medium-grained equigranular rocks of facies 1A. The granite magma was emplaced into relatively cool country rocks, and at and near the contact the heat loss to surrounding rocks quickly lowered the magma temperature below its solidus. Relatively rapid and complete solidification produced the fine- and even-grained texture. The presence of miarolitic cavities in facies 1A rocks shows that solidification was accompanied by vapor saturation. At this time the relations in the pluton were probably

as shown in figure 33. The facies 1A rocks, composed of crystals and coexisting vapor, graded inward into higher temperature domains where crystals + melt + vapor existed. Farther inward, however, only crystals + melt existed.

The relatively rapid drop of temperature to subsolidus levels at and near the contact, accompanied by rapid crystallization, might be expected to yield rocks with quenchlike characteristics. But there are complexities, most obvious in the chemistry of these rocks, which suggest that they are not totally the result of simple quenchlike crystallization of the initially emplaced magma. The most apparent problem is that the facies 1A rocks do not have a bulk major-element or trace-element composition that is intermediate between the compositions of the most felsic and most mafic rocks of the complex. Indeed, these rocks are similar in many aspects of their chemistry to the most felsic parts of the pluton except that their Na_2O/K_2O ratio is anomalously high. As discussed in the section dealing with crystal populations, the generally anomalous nature of facies 1A rocks is probably due to processes that in part have significantly affected their alkali content. The petrographic, textural, and compositional relationships all suggest that the facies 1A rocks, and especially their feldspar populations, have been altered by hydrothermal processes. These processes must have affected the rocks immediately following their complete solidification in the presence of a coexisting vapor phase and at subsolidus but elevated temperatures. What is the nature of the hydrothermal processes that should be expected in the contact-zone environment? Some experimental data are directly pertinent to this question.

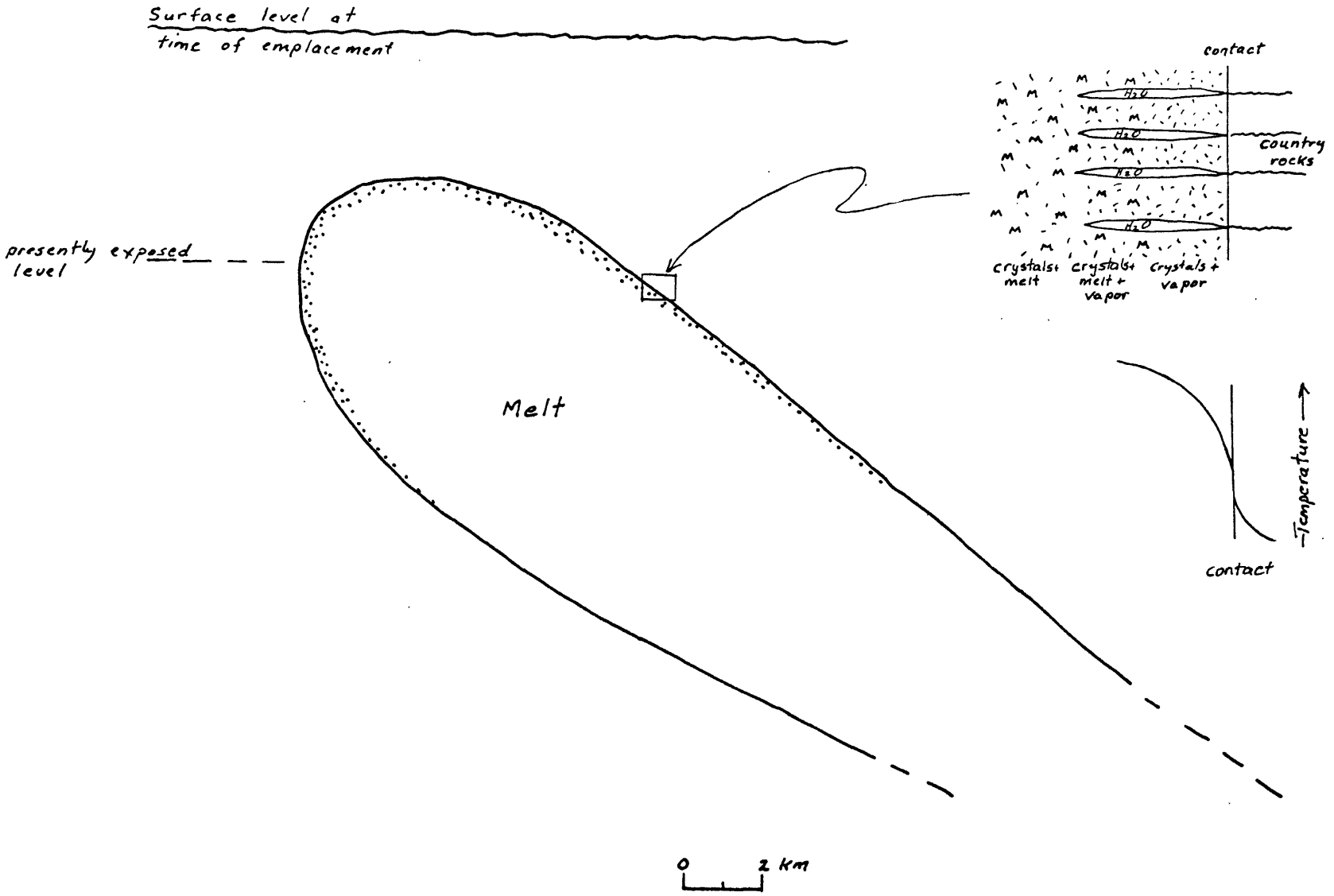

Figure 33. Schematic illustration showing possible relations within the granite stock soon after emplacement. Sharp cooling at the contact solidified facies 1A rocks, and vapor saturation occurred upon complete crystallization. Vapor-saturated rocks graded inward into unsaturated, partly crystallized magma.

Tuttle and Bowen (1958, p. 89-91), Orville (1963), and Martin and Jahns (1976, pers. commun.) have demonstrated experimentally that, for vapor-saturated rock systems in the presence of a temperature gradient, significant and differential transfer of major rock constituents is to be expected. In general, felsic constituents, and especially K_2O, migrate through aqueous vapor and precipitate at regions of lower temperature without mass transfer of vapor itself. That a sharp temperature gradient existed in the vicinity of the facies 1A rocks during and after their crystallization is indicated by the transitional increase of grain size inward from the contact and by the presence of hornfels in adjacent country rocks. The compositional relationships in facies 1A rocks therefore can be explained in terms of simultaneous (1) down-temperature migration of K_2O from facies 1A rocks into country rocks, and (2) possible down-temperature migration of Na_2O from adjacent inner parts of the pluton (areas where crystals + melt + vapor existed, fig. 33) into facies 1A rocks.

Analytical data on the country rocks needed to test this hypothesis are not available, but local replacement by muscovite, combined with the distinctly altered nature of K-feldspar in many facies 1A rocks, support the conclusion that potash metasomatism was active in the contact zone and that the K_2O involved was derived by interaction of a coexisting vapor phase with initially crystallized K-feldspar crystals. The addition of Na_2O into facies 1A rocks seems to be required because their total alkali content is not as drastically different from that in other parts of the pluton, as would be expected if selective K_2O leaching had occurred. The effect of Na_2O addition has been to incompletely albitize existing

plagioclase crystals, as is evidenced by the wide range in plagioclase composition from An_8 to An_{27}.

In summary, stage 1 crystallization was not a simple process. It included rapid crystallization of the initially emplaced granite magma and subsequent subsolidus reactions that resulted in significant alkali transfer, both into and out of facies 1A rocks. The alkali transfer took place via a coexisting vapor phase in response to a sharp temperature gradient that existed from points within to points just outside the pluton. The resulting rocks, facies 1A rocks, therefore have complex characteristics developed by two very different processes. Thus they are highly irregular in details of petrography and composition, and they represent a distinct subsystem of the granite complex.

Stage 2--Crystallization of Facies 1B, 1C, and 2

Stage 2 crystallization formed the rocks of facies 1B, 1C, and 2, which are transitional inward from the contact-zone rocks of facies 1A. During this stage about 75 percent of the complex was crystallized to yield rocks that are characterized by completely transitional relationships in virtually every aspect of their petrology and chemistry. The conditions inferred to have existed within the complex near the end of this stage are shown in figure 34. The materials of facies 1B, 1C, and 2 had been added to the walls of the pluton, and the remaining melt-rich zone in the interior contained scattered suspended crystals. There is no evidence that anything but crystal-melt equilibria were involved in stage 2 crystallization, except perhaps locally in its terminal parts.

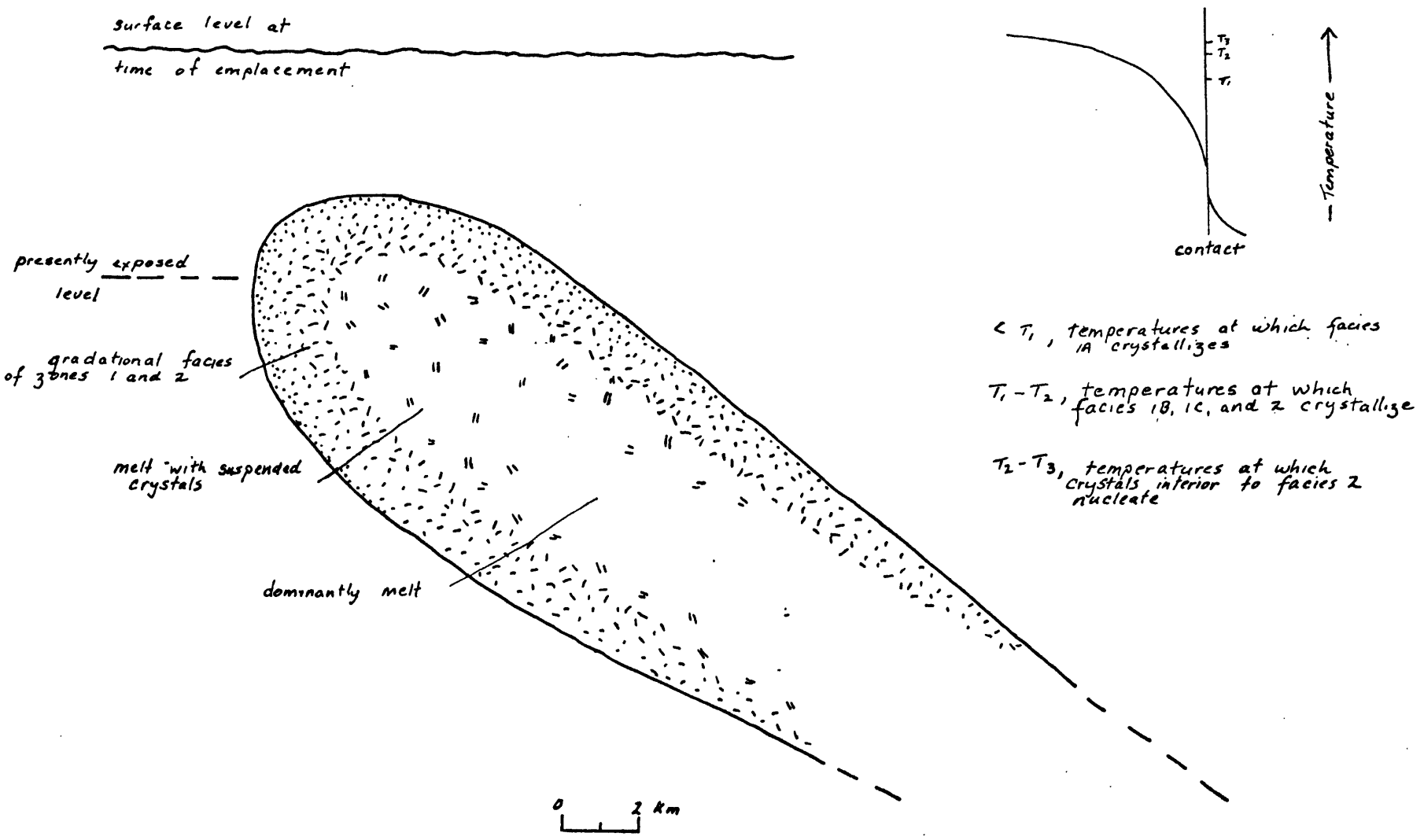

Figure 34. Schematic illustration showing possible relations within the granite stock near the end of stage 2 crystallization. Gradational facies of zones 1 and 2 had crystallized along the margins of the stock. The interior magma contained suspended crystals that were apparently concentrated at higher levels in the magma chamber and adjacent to the solidified walls.

The continuity of the inward textural gradation indicates that the facies 1B-2 transition was formed by one process. Because of the compositional variations developed within this transition and the large part of the complex it represents, the crystallization process that formed facies 1B, 1C, and 2 is critical to understanding the crystallization of the complex as a whole. The nature of every systematically varying parameter between facies 1B and 2 directly reflects the proximity of the immediate crystallizing environment to the external contact of the pluton. As temperature is the only physical parameter of the crystallizing environment that can be expected to have changed systematically inward from the contact, the present petrologic and chemical relationships could well reflect the influence of a temperature gradient inward from the contact. This gradient would have been positive inward, as schematically illustrated in figure 34. It must have had two major influences on the crystallizing environment: (1) it led to significantly different crystallization rates inward, and (2) it determined the liquidus phases and their compositions.

That the successively higher temperature regimes inward from facies 1A rocks crystallized more slowly is evidenced directly by the major textural variations through the facies 1B to 2 sequence: (1) increasing grain size, (2) increasing aggregation of anhedral quartz, and (3) (3) increasing aggregation and morphological development of K-feldspar. An interesting aspect of the textural transition is that it may preserve a record of the textural adjustments that occurred within facies 2. Because this part of the pluton presumably was able to crystallize more slowly, *in-situ* textural evolution was not stopped at intermediate stages

(facies 1B and 1C) but progressed to the very homogeneous porphyritic texture of facies 2.

Throughout stage 2 crystallization the principal minerals that can be readily assumed to have been liquidus phases are relatively anorthite-rich plagioclase, sodic K-feldspar, and biotite. There is no clear indication that quartz was a liquidus phase. Among the liquidus phases, it has been shown that the anorthite content of plagioclase increases inward within the complex, and it is probable that the albite content of K-feldspar does also. The systematic shifts in biotite color may mean that it also changes composition inward. All of these shifts in mineral composition could reflect an inward increase of temperature within the pluton.

The relations discussed above imply that rocks of facies 1B, 1C, and 2 crystallized essentially in place. If the initial magma was compositionally homogeneous, then some important changes in bulk composition through the facies 1B to 2 sequence remain to be explained. All the important compositional parameters show that this sequence represents a continuous systematic shift toward more mafic compositions. Such a shift requires that salic constituents of the magma be removed from facies 1C and 2 rocks. A mechanism for producing the selective removal of salic components during *in-situ* crystallization has been proposed by Vance (1961). He suggests that a migrating front of vapor saturation accompanies an inwardly advancing zone of total solidification. This vapor contains residual alkali and silica components and could redissolve in the interior melt-rich parts of the pluton adjacent to the totally solidified zone. The end result, if the process operates effectively, is a salic, water-rich magma in the central parts of the crystallizing

complex. This mechanism is consistent with the available data for the Serpentine Hot Springs granite complex, and it could very well explain the development of the relatively mafic rocks in facies 1C and 2 as well as the more water-rich and more felsic facies in interior parts of the pluton.

In summary, the facies 1B-1C-2 transition probably formed as the result of relatively slow and essentially *in-situ* crystallization. Oligoclase, sodic K-feldspar, and biotite probably nucleated simultaneously throughout the marginal facies, but these minerals grew at successively higher temperatures and therefore at slower rates inward. Residual alkali and silica constituents were selectively transferred from facies 1B and 2 to interior parts of the pluton by redissolving of an interstitial vapor phase in melt-rich parts of the pluton adjacent to an inwardly advancing zone of total solidification. By the end of stage 2 crystallization about 80 percent (facies 1A + 1B + 1C + 2) of the initially emplaced magma was solidified. This stage of crystallization therefore represents the major fractionating event in the history of the complex, during which the major segregation of felsic materials to the interior of the pluton must have taken place.

Stage 3--Emplacement and Crystallization of Facies 3A

Stage 3 crystallization was a distinctly separate event in development of the complex. It followed marginal crystallization of facies 1B, 1C, and 2 (stage 2 crystallization) and produced the seriate-textured rocks of facies 3A. At the beginning of this stage the pluton was more than 80 percent crystallized, and the spatial relationships within the complex probably were as shown in figure 34. At the end of this stage

the spatial relationships presumably had changed to those shown in figure 35; a part of the magma internal to crystallized facies 2 rocks was displaced slightly upward throughout the complex but was preferentially intruded along a structurally weak zone at the northeast contact. This magma displacement probably was caused by an inward movement of the pluton walls in response to the volume decrease that accompanied major crystallization of the initially emplaced magma.

The facies 3A rocks have some unique characteristics, but they also are similar in some respects to facies 2 rocks. The similarities, which are important to an understanding of the nature of stage 3 crystallization, are in the bulk major-oxide and trace-element compositions (figs. 30 and 31) and in the nature of the large feldspars Large crystals of plagioclase in facies 3A rocks conform to the trend of inward increasing anorthite content seen in the marginal facies, and they are similar in gross zoning characteristics to the plagioclase in facies 2. The large crystals of K-feldspar are well-developed perthites, slightly larger and nonpink in color but otherwise apparently similar to perthite phenocrysts of facies 2. The similarities between rocks of facies 2 and 3A indicate that the magma that was displaced and crystallized to facies 3A rocks was close to being a parent of facies 2 rocks. Its bulk composition was similar to that of facies 2 rocks, and the scattered large feldspars it contained were much like those accreted to the walls during facies 2 crystallization. This suggests that the facies 3A magma was a crystal + melt selvage adjacent the solidified walls of the pluton, and that its principal compositional characteristics were developed during the major fractionation that accompanied stage 2 crystallization.

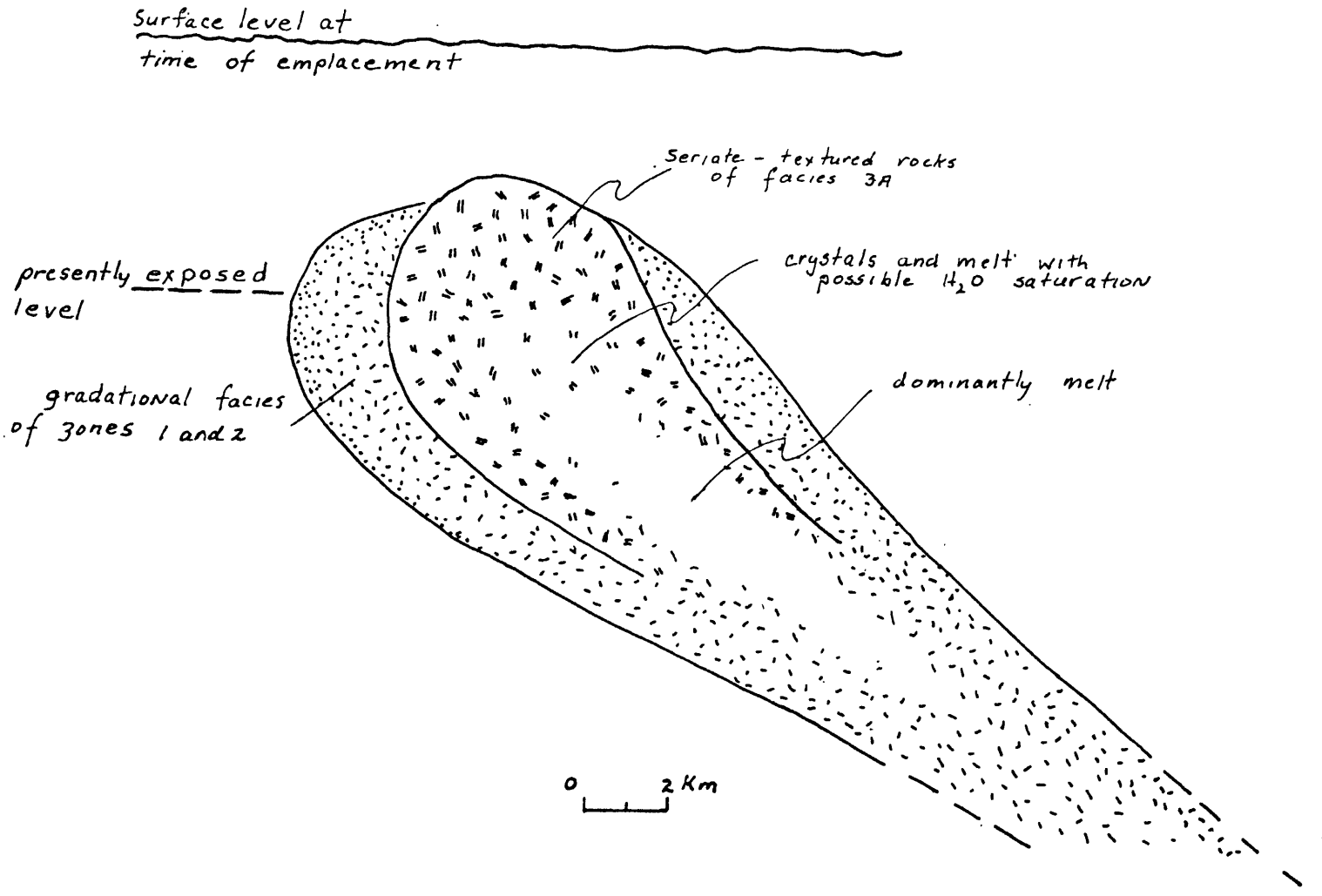

Figure 35. Schematic illustration showing possible relations within the granite stock after stage 3 crystallization. Slight upward displacement of a magma selvage adjacent to the solidified walls was accompanied by disequilibrium crystallization of seriate-textured rocks of facies 3A.

But stage 2 crystallization was terminated by inward movement of the pluton walls that forced magma adjacent to the crystallized facies 2 rocks to move differentially upward (fig. 35). Crystallization accompanied this displacement and produced the unique characteristics of facies 3A rocks, including the development of a second crystal population and seriate texture. When the magma was initially forced to move it contained crystals of calcic oligoclase, sodic K-feldspar, biotite, and quartz. Upon displacement of the magma a second crystal population comprising sodic oligoclase, nonsodic K-feldspar, biotite, and quartz was nucleated. These minerals plated onto appropriate existing crystals and also formed many new crystals. The crystallization rate was fast enough to prevent reaction between the early-formed suspended crystals and the melt, but slow enough to prohibit the development of a distinct granularity contrast between the early- and late-formed populations. The final results of this disequilibrium crystallization were the seriate-textured, fine- to coarse-grained rocks of facies 3A that contain four different feldspars.

In summary, major fractionation during stage 2 crystallization produced not only the solidified walls of the pluton but also an inhomogeneous magma interior to the crystallized zones. Near the walls this magma was similar in bulk composition to the adjacent crystallized zone, and it contained early-formed higher temperature feldspars. The temperature in the interior of the pluton evidently had lowered enough so that quartz was also a liquidus phase. Inward adjustment of the walls of the pluton forced the crystal + melt selvage that had developed adjacent to facies 2 rocks to be displaced. Stage 3 disequilibrium crystallization was initiated by the displacement of the

magma, and it produced the seriate-textured rocks of facies 3A. Part of the residual materials that had been concentrated toward the interior of the pluton throughout most of stage 2 crystallization was present in the crystal + melt selvage. Local vapor saturation was common upon near-complete solidification, and it produced pegmatitic pods and miaroles containing euhedral albite, tourmaline, and quartz. Residual magma in solidified facies 3A rocks produced discontinuous dikes of aplite and aplite-pegmatite.

Stage 4--Emplacement and Crystallization of Facies 3B

The emplacement and crystallization of facies 3A rocks could be likened to a slight rupture of a toothpaste tube. The magma selvage adjacent to facies 2 rocks was able to move a relatively short distance before it totally crystallized and sealed up the ruptured part of the pluton. At this time the spatial relations may well have been as shown in figure 35. The seriate-textured rocks passed gradually downward and inward into an inhomogeneous core of partially crystallized residual melt. Stage 4 crystallization occurred both prior to and during the intrusion of magma to form the composite-textured rocks of facies 3B. At the close of stage 4 crystallization, the spatial relationships within the complex could have been as shown in figure 36. The intrusions that formed facies 3B rocks produced small apophyses within seriate-textured rocks, and a larger mass along the structurally weak northeast contact of the pluton.

The formation of facies 3B rocks marked the first step in the crystallization of the residual magma system that had been developed in the interior of the pluton, largely during stage 2 crystallization.

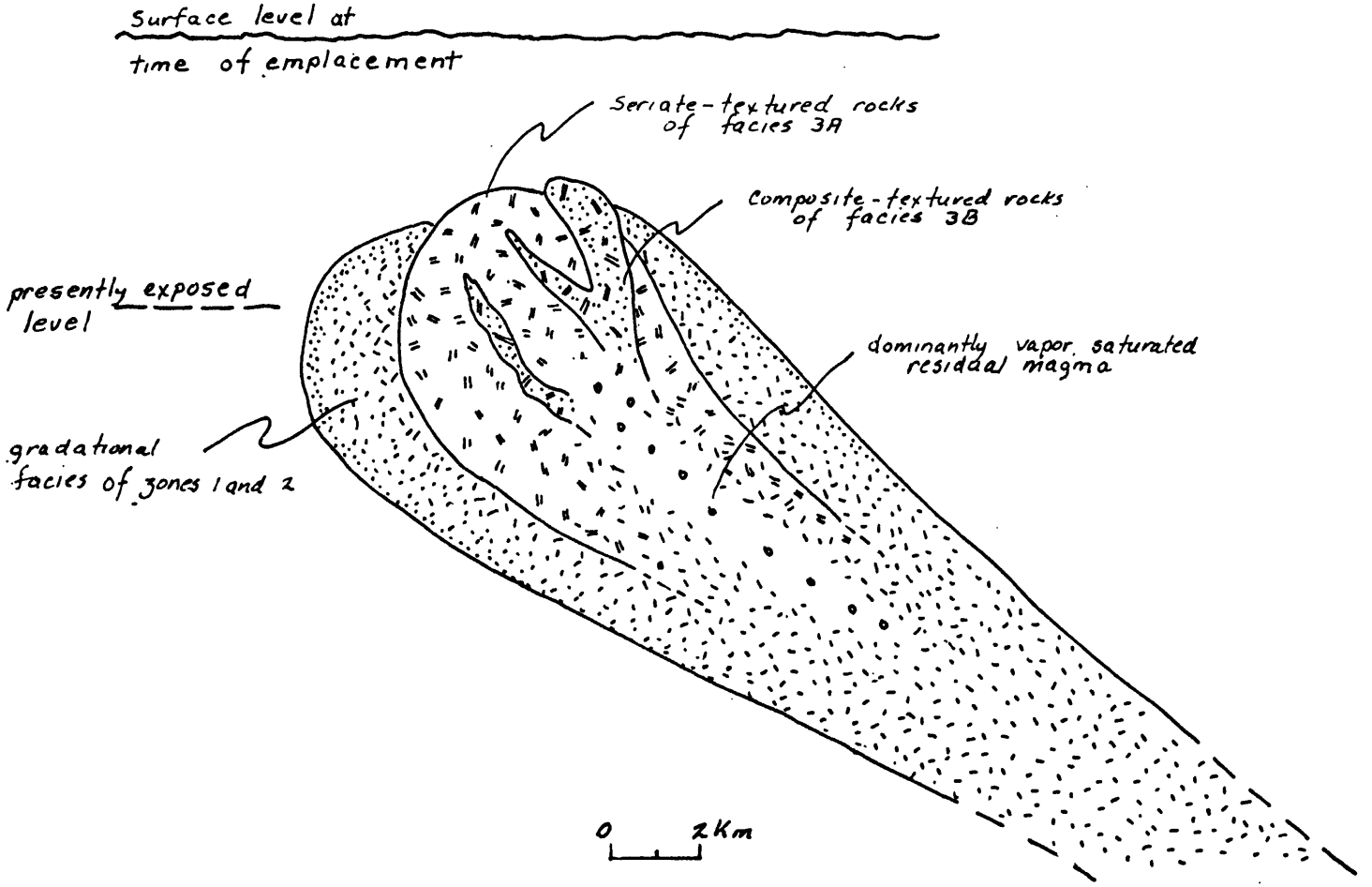

Figure 36. Schematic illustration showing possible relations within the granite stock after stage 4 crystallization. Upward displacement of the crystal-rich roots of facies 3A rocks was accompanied by rapid loss of a coexisting aqueous vapor phase along joints in earlier crystallized rocks. This resulted in quenching of the interstitial melt to produce the composite-textured rocks of facies 3B.

Both chemically and petrologically these rocks represent a mixture of residual magma materials and earlier crystallized materials. The major-oxide and trace-element data (figs. 30 and 31) all show values in the facies 3B rocks that are distinctly felsic but intermediate between that of the final crystallized facies of zone 4 and that of earlier formed more mafic facies. Petrologically the facies 3B rocks clearly contain two distinct crystal populations: the early-formed phenocrysts that probably represent crystal roots of the surrounding seriate-textured rocks (oligoclase, sodic K-feldspar, biotite, and quartz), and the minerals of the aplitic groundmass (albite, K-feldspar, quartz, and biotite). But the phenocrysts show some features that indicate reaction with surrounding material before the magma was intruded and completely crystallized. These features are the tendency of the plagioclase phenocrysts to show compositions trending toward sodic oligoclase even though they characteristically have distinct remnant cores, and the presence of overgrowths on both plagioclase and alkali K-feldspar phenocrysts. Wide albitic rims occur on plagioclase and nonperthitic K-feldspar margins occur on large perthite crystals.

The development of albitic plagioclase phenocrysts probably explains the low modal plagioclase in the aplitic groundmass that crystallized from the melt surrounding the phenocrysts. The presence of aplitic groundmass clearly indicates that final crystallization was very rapid and distinctly nonequilibrium, hence the reaction between phenocrysts and surrounding melt must have preceded intrusion and complete solidification. Prior to intrusion, therefore, the situation in the pluton (as shown in fig. 36) must have involved a carapace of crystals and melt surrounding an internal core that was essentially free of crystals.

The pluton was almost wholly crystallized, and it appears likely that vapor saturation was reached in the interior at this time. The presence of a vapor phase would have aided the reaction of the phenocrysts with the surrounding melt. Intrusion of this crystal-melt-vapor system may have been initiated in part by the increase in internal pressure that could well have accompanied vapor saturation. In any case, upward displacement of the crystal-rich carapace did occur, and a relief of confining pressure evidently accompanied this magma movement. The vapor phase escaped rapidly and produced quartz veins, greisen selvages, and porphyry dikes along joints in surrounding crystallized rocks. Some of the vapor may have escaped into the country rocks, but pertinent evidence is not available. Release of the vapor quenched the melt in the facies 3B magma, thereby producing the distinct aplitic groundmass. As this magma was frozen, the rupture accompanying intrusion was healed and stage 4 crystallization was terminated.

Stage 5--Crystallization of Facies 4A and 4B

Stage 5 crystallization completed solidification of the granite complex by forming the fine- and even-grained felsic rocks of zone 4 from the residual melt in the core of the pluton. This stage is considered to be a separate one mostly for convenience, but the important processes involved in this part of the crystallization history are closely related to those of stage 4. Several different physical changes in the crystallizing environment occurred during the transition from stage 4 crystallization to complete solidification of the complex, and they resulted in important differences in the final products, but the changes are all interrelated and for the most part were either simultaneous or closely spaced in time. The spatial relationships in and adjacent to the

complex after final crystallization probably were as shown in figure 37. Final crystallization was a combination of two different processes, *in-situ* crystallization at or slightly below solidus temperatures for all the mineral constituents, and localized lower temperature interaction of coexisting vapor and crystalline core after the pluton margin was displaced by normal faults.

Crystallization at or slightly below the solidus for all the mineral constituents occurred during or soon after emplacement of the magma that formed facies 3B rocks. The lowering of confining pressure marked by this intrusive event probably also had the effect of moving the internal residual melt below its solidus through exsolution of aqueous vapor. At this time the interior of the pluton was everywhere vapor saturated, and the textural and mineralogic homogeneity of the facies 4A rocks is the result of complete crystallization of the residual melt under these conditions.

The last important event in the crystallization history was the fracturing of the pluton by normal faults that displaced the marginal zones but terminated as a series of splays in the interior of the pluton. This faulting occurred very soon after complete solidification of the residual melt, and these throughgoing structures must have tapped and localized the tin-rich vapor phase that coexisted with the totally crystallized, slightly subsolidus facies 4A rocks. This faulting is very likely to have been just one aspect of the dynamic adjustments within and near the pluton as its volume decreased near the end of crystallization. When viewed in this context, it becomes apparent that the intrusion of magma to form facies 3B rocks, the complete *in-situ* crystallization of facies 4A rocks under vapor-saturated

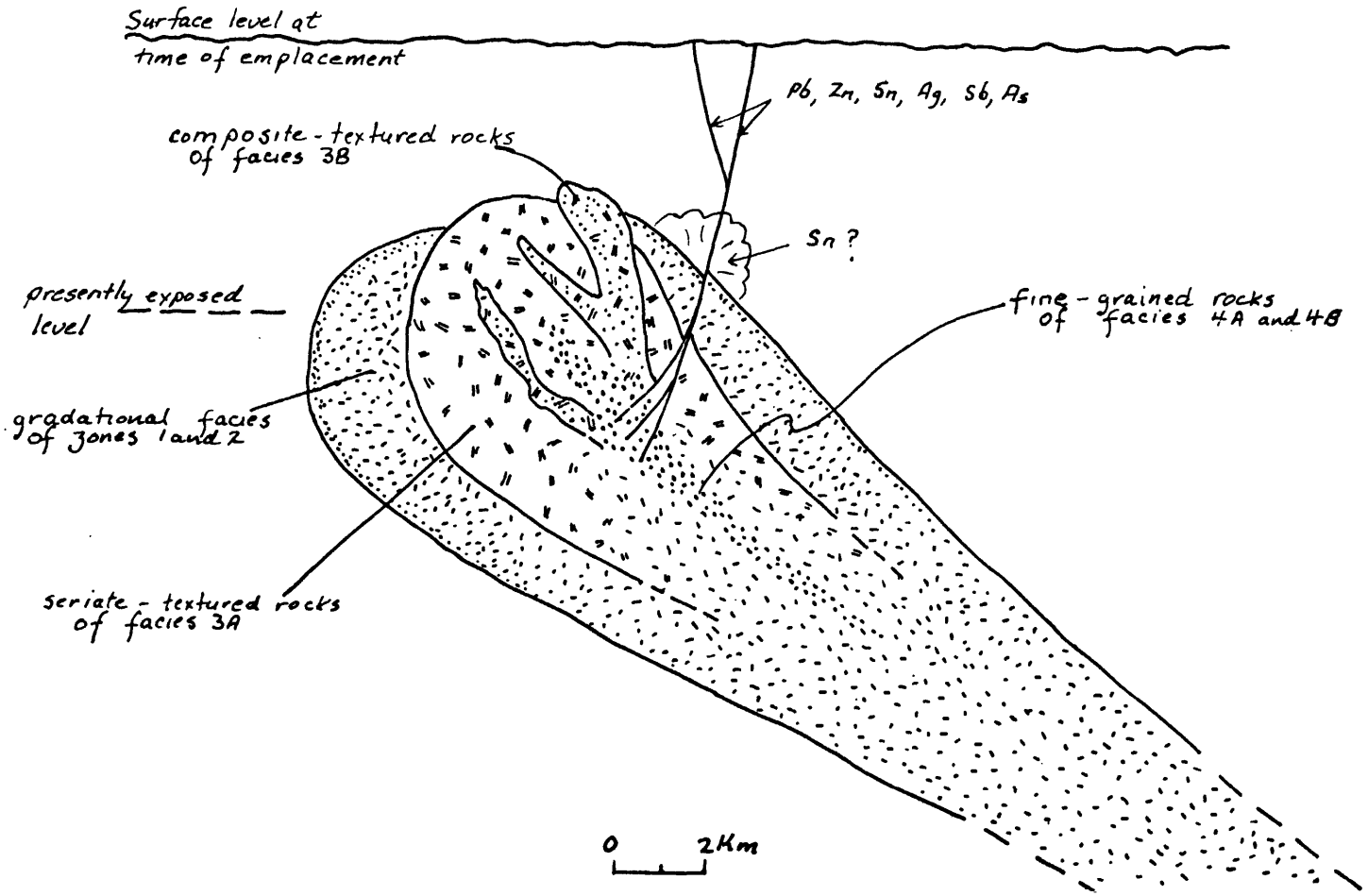

Figure 37. Schematic illustration showing possible relations within the granite stock after complete crystallization. Normal faulting displaced the margins of the pluton and allowed escape of a vapor phase and some residual magma. The vapor phase produced mineralized zones at higher levels of the fault system. Remnants of the vapor phase remained in the roots of the fault system and reacted with solidified facies 4A rocks to produce leucocratic rocks of facies 4B.

conditions, and the faulting to release the confined vapor phase are all related events, closely sequential in time, that almost terminated crystallization of the complex.

These events did not end the crystallization history because facies 4B rocks still remained to be formed. It has been shown that facies 4B rocks are essentially equivalent to facies 4A rocks in texture and composition except that they show distinct effects of reaction with a vapor phase at temperatures below those of facies 4A crystallization. The facies 4B rocks are spatially related to the crosscutting fault splays, which are clearly defined by even lower temperature argillic alteration and replacement by silica. It appears that the formation of facies 4B rocks was the last crystallization event, and that it was accomplished under totally subsolidus conditions by reaction of a coexisting vapor, at this time only present in the vicinity of the cross-cutting fault structures, with rocks that, before reaction, probably were typical facies 4A rocks. The principal chemical changes that accompanied these reactions were caused by leaching of silica and certain trace elements, particularly tin, from the parent facies 4A rocks.

In summary, the principal events of stage 5 crystallization were those that closely followed intrusion of facies 3B rocks (stage 4 crystallization), including (1) crystallization of facies 4A rocks under vapor-saturated conditions and at temperatures near the solidus, and (2) localized reaction of a vapor phase with previously crystallized facies 4A rocks to produce the leached rocks of facies 4B. This was the last event in crystallization of the complex.

Alternative Interpretations

The crystallization model presented above is consistent with the available data and seems required if the principal assumptions are valid. These assumptions are that the initially emplaced magma was compositionally homogeneous and that no further addition of magma (from depths where the magma was generated) occurred during crystallization. Should one or both of these assumptions be invalid, alternative interpretations of the crystallization history are possible. The formation of the transitional marginal facies remains as the critical part of the crystallization history in any alternative explanation.

The gradual shift toward more mafic compositions inward through the marginal facies of zones 1 and 2 could be explained by an initially inhomogeneous magma. This inhomogeneity could have been produced by progressive tapping of a vertically inhomogeneous magma source (batholith) or by flow differentiation as the magma rose to its level of emplacement. The magma source could have been segregated so that it became progressively more salic at higher levels. This vertical segregation could have been preserved in the separated and rising magma column so that the first-emplaced magma (at the contact) was salic and graded inward to more femic compositions. However, this does not seem likely because the processes that might produce a vertically segregated magma source do not appear to be applicable here. Vapor saturation and subsequent migration, along with dissolved alkali and silica constituents, to higher levels of the parent batholith is unlikely because the pressures at the depths of the parent batholith would prohibit vapor saturation unless the magma were extraordinarily rich in volatiles. Crystal settling is discounted because the granite complex of the Serpentine Hot Springs

area does not contain minerals, such as amphibole, that might have segregated vertically in a parent batholith.

Flow differentiation during rise of the granite magma may have occurred even though the magma appears to have been dominantly molten upon emplacement. This is possible because the mafic inclusions in the complex may not be homogeneously distributed. The distribution of these xenoliths was not studied in detail, but the larger ones appear to be concentrated in facies 2 rocks where they locally form screens and pipe-like swarms. If the percentage of mafic xenoliths does increase inward through the marginal facies it could have been caused by segregation of the xenoliths toward the interior parts of the magma during its rise to the level of emplacement. These xenoliths appear to be refractory remnants, and materials partially assimilated from them could have been responsible, at least in part, for the progressive shift to more mafic compositions through the marginal facies.

Another possible interpretation does not require an initially inhomogeneous magma to explain development of the marginal facies. It could be argued that conditions within the initially emplaced magma chamber were conducive to large-scale transfer of residual constituents from interior parts of the marginal facies (facies 1C and 2) in outward directions. This interpretation requires that the process considered responsible for stage 1 crystallization was operative throughout zones 1 and 2. If conditions of vapor saturation existed simultaneously throughout zones 1 and 2 and if the postulated positive temperature gradient inward did exist, then some residual constituents could have been selectively transferred from facies 1C and 2 rocks toward the

pluton margin, resulting in the increasingly more felsic compositions outward.

Regardless of the alternative interpretation(s) favored for development of the marginal facies, it appears that they formed by dominantly *in-situ* crystallization. Further evolution of the interior of the complex would have to be explained by crystallization processes at depth and subsequent intrusion of magma that was less directly related to the marginal facies than suggested in the detailed five-stage crystallization model presented earlier.

Economic Geology

The Serpentine Hot Springs area includes placer deposits of gold and cassiterite and several bedrock areas with anomalous concentrations of base metals, silver, and tin. The presence of cassiterite in placers was first reported by Collier (1904, p. 28) and later confirmed by Knopf (1908, p. 63). Moxham and West (1953) outlined the occurrence of mineralization, lode prospects, and placer deposits in the Serpentine-Kougarok area and summarized the results of investigations for radioactive minerals in this area. Sainsbury and others (1968) presented data on the nature of cassiterite in the gold placers of Humbolt Creek and suggested nearby areas favorable for lode deposits of tin. The presence of significant amounts of cassiterite in the Humbolt Creek drainage led to reconnaissance and detailed geochemical surveys that showed the distribution of many anomalous metal concentrations in both alluvial and bedrock materials (Sainsbury and others, 1970). The following discussion of the nature of the mineralized areas is based on the geologic mapping by the author and geochemical data presented

by Sainsbury and others (1970), supplemented by an additional detailed geochemical soil survey in one of the bedrock areas. The main purpose of this part of the report is to summarize the nature of the mineralized areas and to discuss their spatial and genetic relationships to the granite complex. These relationships are similar to those found in many other tin-mineralized areas of the world.

Geochemical Surveys

The geochemical surveys included spectrographic analyses of stream sediments, panned concentrates, some sluice concentrates, and bedrock and soil samples. The geochemical results identify many anomalous metal concentrations in bedrock and alluvial materials from a large area directly southeast of the granite contact. No element associations are obviously correlated with the tin anomalies in alluvial materials, but lead, zinc, silver, arsenic, and antimony are commonly associated with tin anomalies in bedrock materials.

Alluvial Materials

A reconnaissance stream sediment survey of the entire area identified a few weakly anomalous tin concentrations, mostly in areas within or directly adjacent to the granite complex. The failure of these sediment samples (-80 mesh) to identify the tin concentrations known to exist along Humbolt Creek (Sainsbury and others, 1968) led to a second more detailed examination of the alluvial materials in the streams draining the eastern part of the area. In this study (Sainsbury and others, 1970), panned concentrates were found to be particularly useful in detecting important metal concentrations in the stream

sediments and in tracing the metal concentrations to their possible source areas.

The detailed study showed that anomalous concentrations of tin are present in sediments of both Humbolt and Ferndale Creeks. The tin anomalies were identified locally along the entire lengths of these streams in the study area, and they are headed in the hilly areas just southeast of the granite complex. Other metals commonly present in anomalous concentrations are gold, zinc, molybdenum, and locally lead, but the panned concentrates did not reveal any strong correlations between these elements and the tin anomalies.

Bedrock Materials

A search for lode occurrences of cassiterite was undertaken in the bedrock areas between the granite complex and the headwaters of Ferndale and Humbolt Creeks. This search was seriously handicapped by the extensive accumulations of frost-riven rubble that mantles almost all of this area. The geochemical investigations were therefore restricted to the sampling of surface materials including rock fragments, vein materials, and soils from altered zones. The altered zones were usually identified by the surface accumulations of discolored, generally iron-hydroxide encrusted rock or gossan fragments, and especially localized concentrations of fine-grained soil materials in place of the usual rock fragments. Three mineralized bedrock areas with anomalous concentrations of tin were identified, although no definite lode occurrences of cassiterite were found.

The three mineralized bedrock areas are shown in plate 1. The two easternmost areas (localities A and B, pl. 1) are discussed by

Sainsbury and others (1970). The third (locality C, pl. 1) is nearer the eastern contact of the granite complex, and data supplemental to those of Sainsbury and others (1970) concerning this area are presented here. This zone is defined by discolored and rusty soil materials and iron-hydroxide encrusted fragments that occur adjacent to a very fine-grained granite dike that trends N. 80° E. This dike appears to have been emplaced along a fault, and slickensided fragments of altered rocks present in the surface materials suggest that movement along the fault has been recurrent and in part postdates mineralization. Soil samples, including selected altered rock fragments, were collected along the length of the altered zone, and the results of spectrographic analyses of these samples are listed in table 11. The samples contain highly anomalous amounts of silver, arsenic, lead, antimony, tin, and zinc. This association of elements is present in all the bedrock mineralized areas with anomalous concentrations of tin. Of these elements, the most abundant are lead and zinc.

Spatial and Structural Controls

The geochemical surveys clearly show that mineralization in the Serpentine Hot Springs area is localized in the hilly area southeast of the granite contact. This part of the area is unique in that it lies directly above the granite stock. The individual mineralized areas all occur along faults, as is evidenced by the presence of subtle to conspicuous topographic discontinuities, distinctly linear trains of altered rock or soil materials, and the common occurrence of brecciated or slickensided rock fragments in the surface rubble. The most important localizing faults are those that trend northwest, and the major one of

Table 11.--*Results of semiquantitative spectrographic analyses of composite grab samples of soil, altered rock, and gossan fragments collected along fault zone containing fine-grained granite dike (plate 1); K. J. Curry, analyst. All data in ppm.*

Field No.	Lab. No.	Mn	Ag	As	B	Ba	Be	Cd	Co	Cr	Cu	La	Mo	Nb	Ni	Pb	Sb	Sc	Sn	Sr	V	Zn
70AH714A	BAY001	G(5,000)	15	7,000	700	700	7	150	30	300	150	150	L	20	100	5,000	500	30	300	150	500	5,000
70AH714B	BAY002	1,500	1.5	L	300	700	5	N	20	300	100	100	5	20	70	700	200	30	20	150	500	2,000
70AH714C	BAY003	G(5,000)	50	7,000	500	700	5	150	20	300	500	100	5	20	70	G(20,000)	1,500	30	700	150	300	7,000
70AH714D	BAY004	1,500	3	700	700	700	7	N	30	300	200	150	7	20	70	1,000	100	30	70	150	500	500
70AH714E	BAY005	G(5,000)	20	10,000	300	700	2	200	30	200	200	70	L	20	70	15,000	1,500	30	500	200	300	10,000
70AH714F	BAY006	2,000	20	500	200	700	7	N	30	200	150	50	L	20	100	15,000	700	30	150	200	300	3,000
70AH714G	BAY007	G(5,000)	30	7,000	700	700	3	70	30	300	200	150	L	20	100	20,000	700	30	500	150	500	G(10,000)
70AH714H	BAY008	5,000	3	500	200	700	10	N	30	200	70	70	L	20	100	5,000	150	30	500	150	300	1,500
70AH714I	BAY009	G(5,000)	150	10,000	300	700	3	100	30	150	500	70	L	20	70	G(20,000)	2,000	30	500	150	300	7,000
70AH714J	BAY010	2,000	7	200	200	500	5	N	30	200	70	70	5	20	150	2,000	L	30	100	150	300	700
70AH714K	BAY011	3,000	3	L	300	1000	7	N	30	300	150	100	5	20	150	1,000	N	30	30	150	500	700
70AH714L	BAY012	1,500	10	L	200	700	5	N	30	300	150	100	L	20	150	2,000	N	30	20	150	300	300

G Greater than value shown

L Detected but below limit of determination

N Looked for but not detected (Au, Bi)

these appears to be the throughgoing structure that extends from the headwaters of Humbolt Creek to the central parts of the exposed granite complex. This fault terminates as a series of splays in hydrothermally altered zone 4 rocks. The splays localized the development of the leached, leucocratic rocks of facies 4B. It is probable that additional work would locate other mineralized structures, either parallel or subsidiary to the northwest-trending set of fault zones.

Similarities to Other Tin-Mineralized Areas

The tin and related mineralization present in the Serpentine Hot Springs area has certain characteristics indicating that the area is similar to other tin-mineralized areas even though commercial lode deposits of cassiterite have not yet been identified. The similarities are those that characterize the general geologic environment and the processes that have concentrated, mobilized, and localized tin. The processes controlling tin distribution in the Serpentine Hot Springs area are believed to be typical of those responsible for other tin deposits associated with granite plutons, i.e., most of the major tin deposits of the world.

The most important similarity is the close spatial association of cassiterite and other anomalous concentrations of tin with an epizonal, composite granite pluton that is geochemically specialized for tin and other fugitive elements (Sainsbury and others, 1968; Štemprok, 1971; Groves, 1972). The consistent spatial association of most of the world's major tin deposits with such granite plutons, mostly biotite granites but including some two-mica granites, has long been recognized and has led Sainsbury and Reed (1973, p. 647) to conclude that the consistency

of this association is comparable to that of chromite deposits and their host rocks.

The second important characteristic of the mineralized areas is their localization by faults, particularly faults that either transect the granite or localize granite dikes. This type of structure is important in localizing tin deposits in many areas (Hosking, 1967; Sainsbury and Reed, 1973). In the major tin districts where faults are known to play an important role in localizing the deposits, the timing of mineralization, faulting, and final crystallization of associated granites has been a perplexing and generally confusing problem. This is discussed later but, as in the Serpentine Hot Springs area, the main problem is that mineralization has followed movement on faults that transect the main granite pluton, yet they commonly localize fine-grained ("rhyolitic") dikes.

The third important aspect of the mineralized zones in the Serpentine Hot Springs area is that the element suite associated with the bedrock tin anomalies is characteristic of the lead-zinc zone developed in many tin-mineralized areas. Metal distributions in tin-mineralized areas commonly show a preferred spatial relationship to areas mineralized with cassiterite or the associated granite complexes (Dewey, 1925; Sainsbury and Hamilton, 1967). The metal suite present in anomalous concentrations in the bedrock areas southeast of the granite complex is characteristic of the lead-zinc zone of tin districts, a zone characteristic of the fringe or outer areas of mineralization in the district. The implication for the Serpentine Hot Springs area is that the major tin-mineralized areas have not been exposed. It is possible, if not probable, that the principal tin mineralization lies down-dip

on the mineralized structures, at depths that are near or within the granite complex.

Therefore, based on similarities in the general geologic environment and the nature of mineralized areas, it is concluded that metal-concentrating processes that have been operative in the Serpentine Hot Springs area are typical of major tin-mineralized areas elsewhere in the world. For this reason, the following discussion of the origin of the mineralization in the study area has several important implications concerning the origin of tin deposits in general.

Origin of Mineralization

The spatial association of tin mineralization with the granite complex is also believed to be a genetic association. This study has shown that the granite complex: (1) is geochemically specialized for tin and other fugitive elements, (2) underwent fractional crystallization and concentrated tin and related elements to an evolving residual melt, and (3) evolved a separate aqueous phase during the last stages of crystallization that concentrated the tin and associated elements.

The bedrock mineralized areas are localized along structures that were either developed or reactivated during the late stages of crystallization, and because these areas are mineralized with a suite of elements that includes those known to have been concentrated during crystallization of the granite complex, it is believed that the fluids responsible for development of the tin mineralization are those that evolved directly from the associated granite complex at the end stages of crystallization. Such an origin is generally accepted by most other workers on tin deposits, even though some opposition to this relationship exists (Štemprok,

1967). The development or reactivation of faulting at the end stages of crystallization and the subsequent localization of dikes and mineralization along them is common in tin deposits (e.g. Hosking, 1967). The variations in the pressure regime of the crystallizing granite complex are believed to have important implications concerning the timing of final crystallization, faulting, and mineralization. The close timing between these events is probably not coincidental, and is discussed further below.

It should be noted here that there is evidence for two tin-mineralizing processes. First, it has been shown that the vapor that coexisted at near-solidus temperatures with facies 4A rocks was probably enriched in tin. Escape of this vapor immediately upon faulting of the margins of the complex would lead to mineralization at higher, cooler levels in the crosscutting fault system. Second, the remnant vapor that occupied the roots of the fault system reacted with crystallized facies 4A rocks and, among other things, allowed removal of trace elements as the temperature lowered. The latter tin-mineralizing process, leaching of tin-rich biotite granite, is favored by some workers (Tischendorf and others, 1971, p. 19), but it is probable that the first, direct escape of higher temperature tin-rich vapor, is also a major tin-mineralizing process.

CHAPTER III

IMPLICATIONS OF THE STUDY

The granite complex is believed to be representative of a large number of epizonal granite plutons, particularly those associated with tin deposits. Because of this, the implications of this study touch on major problems of igneous petrology as well as the genesis of ore deposits. These are discussed separately below. The discussions present many ideas that are in the formulative stage and, therefore, actually outline major areas in which research is needed.

Crystallization of Zoned Granitic Complexes

The general crystallization pattern determined for the granite complex can now be compared to that of other granitic complexes to see whether the crystallization processes identified in this study are more generally operative in the formation of zoned plutons. The general crystallization pattern of importance here is: (1) the gradual inward change of texture and composition that testifies to slow marginal accretion of increasingly mafic materials, and (2) termination of marginal accretion and development of divergent crystallization patterns as a result of the displacements of interior more felsic residual magma. Of less importance to the general crystallization pattern are the metasomatic alterations of rock compositions and some petrographic relations that may occur at both the beginning and end stages of crystallization.

A preliminary survey of the literature on zoned granitic complexes clearly shows that the general crystallization pattern is of more than limited occurrence and that many plutons have crystallized in a manner similar to that of the granite complex of the Serpentine Hot Springs area. The most apparent are the other tin-granites of the Seward Peninsula (Knopf, 1908; Steidtmann and Cathcart, 1922), but many additional granite complexes associated with tin deposits are probably also similar. Similar plutons are the White Creek batholith of British Columbia (Ressor, 1958) and several batholiths in east-central Texas (Keppel, 1940). One of the Texas occurrences, the Enchanted Rock batholith, has been extensively studied (Hutchinson, 1956; Ragland and others, 1967, 1968). All of these batholiths are of intermediate and felsic composition and have well-developed thermal aureoles. They show, on the basis of field, mineralogic, or chemical data, evidence of marginal accretion that developed inwardly gradational textures and increasingly mafic compositions through the major part of their crystallization histories. The inward gradational relationships are terminated by the intrusion of centrally located, relatively felsic magmas. The Enchanted Rock batholith also has an anomalous contact facies with a composition that appears to have been affected by alkali metasomatism.

It appears then that the crystallization pattern of the granite complex of the Serpentine Hot Springs area is duplicated in several plutons other than those of northern Seward Peninsula and other tin-mineralized areas. This pattern has been developed on both stock and batholithic scales, and the crystallization processes responsible seem to result commonly when intermediate to felsic magmas are intruded

into somewhat stable epizonal environments. Such conditions enable the development of temperature gradients within the plutons and are conducive to protracted crystallization histories. The mode of crystallization documented for the granite complex of the Serpentine Hot Springs area is, therefore, believed to be of much more general occurrence than now recognized.

Origin of Tin-Bearing Granites

It is generally accepted that tin-granites are biotite or two-mica granites that form epizonal, composite plutons and have late-crystallizing facies. But there is considerable discussion in the literature concerning whether or not tin-granites are significantly different from other granites. Most of the discussion has focused on the geochemistry of the plutons and differing conclusions have been reached (Rattigan, 1963; Hosking, 1967; Štemprok and Škvor, 1974). Much of the confusion in understanding the geochemical data is believed to exist because the data have been generated by sampling programs without full knowledge of the field relations necessary to understanding the observed compositional variations. Even so, the overwhelming evidence is that tin-granites are geochemically specialized; they contain high concentrations of such elements as tin, lithium, fluorine, beryllium, and niobium (Rattigan, 1963; Sainsbury and others, 1968; Štemprok, 1971; Groves, 1972; Tischendorf, 1973).

The trace-element data from the granite complex of the Serpentine Hot Springs area show especially well the nature of this geochemical specialization. Because these data apply to a large suite of elements, it has been shown that the specialization is a systematic enrichment

in fugitive elements and a depletion in those elements expected to enter mafic mineral structures. This systematic enrichment-depletion relationship not only characterizes the geochemical specialization but also implies that the bulk trace-element composition is the product of crystal-melt processes.

How does such a geochemically specialized granite originate? Granite melts can be formed as a result of two very different processes: anatectic melting or fractional crystallization. In high-grade metamorphic environments that remain closed systems an initial granite melt might be expected to scavenge fugitive trace elements such as those associated in tin-granites. However, metamorphic environments are not characteristically closed systems and dispersal of fugitive elements during progressive metamorphism is to be expected. Therefore, it is believed that tin-granite melts are more likely to be the product of fractional crystallization of larger batholithic masses than of anatectic melting. Such an origin provides the necessary initial melt temperatures and imposes the constraints of crystal-liquid equilibria on the evolving trace-element composition, a composition that is strongly suggestive of such an origin. An interesting possibility is that, if the progenitor batholith were granodioritic in composition and therefore precipitating significant amounts of K-feldspar and possibly biotite, the resulting residual granite magma might be expected to have the low K_2O/Na_2O that tin-granites apparently have.

Regardless of the choice of origin as discussed above, it may be important here to mention that tin-granites appear to be the result of crustal processes. The nature of the initial geochemical specialization and the later distribution within the crystallizing granites clearly indicate that crystal-melt equilibria control the main trace-

element distribution. Such regular and systematic relationships would not be expected to be produced by the most assuredly complex interaction of streaming volatiles from subcrustal sources (Mitchell and Garson, 1972, p. B22).

The Concept of Metallogenetic Provinces

The inhomogeneous distribution of ore deposits in rocks of the earth's crust has fostered the concept of metallogenetic provinces. The basic premise of this concept is that the observed inhomogeneous distribution is due to one, or a combination of, the following two factors: (1) certain elements are inhomogeneously distributed in the earth's crust or mantle, and ore deposits are the result of general geologic processes acting in areas of higher metal concentrations, and (2) the processes chiefly responsible for determining certain element concentrations are of a specialized nature and of variable occurrence in space and time. If inhomogeneous metal distributions exist they probably developed early in the earth's history and may be in the mantle (Noble, 1970, p. 1619) or in the crust (Krauskopf, 1970, p. 657) or both.

Important regional variations in the distribution of tin deposits have long been recognized. Tin metallogenetic provinces, commonly called tin belts, have been mapped on global scales (Schuiling, 1967; Sainsbury and others, 1969). The important question concerning this distribution pattern of tin was asked by Goldschmidt (1958, p. 393): "Is this unquestionable difference in the abundance of tin. . .in various regions of the globe due to regional differences in the efficiency of the processes that concentrate tin in such rocks as granites?" This question is entirely valid today and strikes at the heart of the

metallogenetic concept: are the observed tin distributions due to the occurrence of special processes or do they reflect special primitive tin distributions? The probable origin of the Serpentine Hot Springs granite complex and the genesis of associated mineralization provide some important insights into this question.

If the granite melt that crystallized to form the granite complex was itself a residual melt developed by batholithic fractionation, then the origin of associated tin deposits can be visualized as the end result of a complex multistage process: (1)generation of a batholithic melt that (2) fractionally crystallized and (3) separated a residual granite melt that was (4) emplaced in an epizonal environment and (5) fractionated so that it (6) developed a residual melt-aqueous phase system that was enriched in fugitive trace elements, and the aqueous phase was then (7) localized along timely structures or in favorable parts of the granite complex. This multistage process indicates that maps showing the distribution of tin deposits directly reveal places in the earth's crust where a rather unique sequence of events must have occurred. The tin-granite--tin deposit environment does not directly shed light on general crustal or subcrustal characteristics but it may do so indirectly. This question is unresolved but potentially resolvable; the critical questions of special process versus special element distribution must be asked of the geologic environments in which batholithic melts are generated and crystallized. With respect to the progenitors of tin-granites some of the important questions are:

1. Are the batholithic melts generated in crustal or subcrustal environments?

2. What is the nature and influence of the tectonic environment that accompanied batholithic generation and crystallization?

3. Did the batholiths have a specialized crystallization history? Did such factors as mineral stabilities (hornblende vs. biotite) play a role in aiding the initial concentration of fugitive elements?

4. Were the prebatholithic rocks enriched in tin?

The evaluation of the data pertinent to these questions is beyond the scope of this report but, on the basis of tin occurrences on the Seward Peninsula, it appears that progenitor batholiths are biotite granodiorites generated in crustal environments (for the most part in old, Precambrian crust) not directly relatable to active continental margins. The major point of this discussion is that the origin of tin deposits is very likely a result of crustal processes, and that therefore the fundamental questions concerning the metallogenetic concepts of special process or special element distribution (or both) are probably answerable by direct observation of the pertinent geologic environments.

This origin of tin deposits conforms well with the ideas of Krauskopf (1970), which strongly support a multistage origin for the world's principal ore deposits. The geochemical data yet to be gained may also confirm his tentative conclusion that early geochemical specialization of crustal materials plays an important role in determining the potential of these materials for fostering mineral deposits. In either case, it seems clear that tin deposits are the result of crustal processes; there is no need to resort to subcrustal processes to explain their origin even though physical interaction of crustal-

subcrustal materials may play a role in creating environments where crustal batholithic melts can be generated (Barker and others, 1975).

Timing of Fracturing, Final Crystallization, and Mineralization

A common feature of many of the world's tin-mineralized areas is the close but sequential development in space and time of fracturing of the main consolidated granite mass, crystallization of the final residual magma, and mineralization. A few examples of this relationship are: (1) the elvan dikes of Cornwall which are coincidental with "emanative centers" in a zone of crustal weakness of deep-seated fissuring that first allowed release of the elvan magma and later the ore-bearing solutions (Dines, 1956, p. 7); (2) the localization of intrusions, extrusions, dislocations, and mineralization along deep faults in the Erzgebirge (Tischendorf and others, 1971, p. 18); and (3) the association of rhyolite dikes, lode deposits, and fault zones at Lost River, Alaska (Sainsbury, 1964). The mineralized areas of the Serpentine Hot Springs area seem to be similar in a general way to the above examples because the mineralizing fluids and at least one porphyry dike were localized along fractures, the most important of which transects the main mass of consolidated granite and dies out as a series of hydrothermally altered splays in the part of the complex occupied by the evolved residual magma. The timing of fracturing, final crystallization, and mineralization is an important problem because their obvious sequential development has led to some confusion in understanding the relationship between the magmatic processes and the ore-forming processes.

The problems are interpretive and come from trying to decide just how far apart the different steps are in time and whether or not they are the result of one continuous geologic process or of distinctly different processes that coincidentally occur in the same space at about the same time. For example, Boyle (1970, p. 4) considers the fact that mineralized veins commonly cut and offset granitic bodies and related rocks such as porphyries as very good evidence that hydrothermal ore deposits, in general, are unrelated to magmatic processes. Important "post-granite" localizing faults in tin-mineralized areas have been interpreted as parts of regional systems that are unrelated to the local epizonal plutonic environment. Mineralization along these structures is considered to be evidence that the mineralizing fluids originate at deep levels below that of the exposed granite bodies and, in part at least, are unrelated to them (Sainsbury and Hamilton, 1967). It is the purpose of this discussion to show that the sequence of fracturing, final crystallization, and mineralization represents the record of an essentially continuous process that is not coincidental in space or time and is to be expected in most of the epizonal magmatic environments that characterize tin-mineralized areas. The key to understanding these relationships lies in a conceptualization of the general physical environment that exists in the vicinity of a fractionating epizonal pluton that approaches, or reaches, vapor saturation during the final stages of crystallization.

The typical epizonal tin-granite pluton is post-tectonic and is emplaced into crustal levels where rocks are capable of brittle fracture. Consequently pre-emplacement faults are likely to exist, and the pluton may actually be localized in part by them. After emplacement,

crystallization proceeds and is accompanied by two important changes. The first is that the total volume occupied by granite material decreases throughout crystallization and the second is that the water (and other volatile) content of the developing residual magma increases. Both of these changes are important influences on the physical environment because they increase the instability of the local pressure regime. In the first case, the decrease in the total volume occupied by granite materials means that adjacent country rocks must adjust inward. If they have sufficient strength, inward adjustment may not be gradual nor may it happen until near the final stages of crystallization. In this situation, fractures that are essentially analogous to collapse structures can develop, and the dislocations may be along new faults or along reactivated pre-emplacement faults. Development of these structures would have the immediate effect of lowering the local pressure regime in the vicinity of the residual magma. In the second case, the build-up of water content is important because if saturation occurs, the local pressure regime can in some cases increase drastically because of the increased volume of the separated aqueous phase. Therefore, as final crystallization approaches, the combination of the above two major changes in the local physical environment creates a dynamically unstable space in the vicinity of the crystallizing pluton. Under these conditions it is to be expected that fracturing, probably by some combination of collapselike movements and displacements caused by forceful expulsion of the high-pressure aqueous phase and associated melt will occur. When the confining nature of the country rocks and of the consolidated granite margins is terminated by this fracturing, then the local pressure

regime in the residual melt system in drastically lowered and the final crystallization process begins.

The process of final crystallization is essentially one of continuous transformation from a dominantly melt system to a completely aqueous vapor system. When the pressure is lowered in the residual melt system, rapid separation and expansion of the aqueous phase occurs and portions of the residual melt are forced into the country rocks, typically as porphyry dikes, along with portions of the aqueous phase. Almost immediately the residual melt is quenched, both in the expelled dikes and in deeper parts of the magma chamber. Throughout freezing of the residual melt it is likely that aqueous-phase evolution continues both from internal parts of the residual melt system and from the externally expelled dikes. As the temperature lowers after quenching of the residual melt, reaction of the evolved aqueous phase with adjacent rocks, including those which have just been formed by quenching, creates the common altered and mineralized zones. Thus, during final crystallization of many tin-granites the most important physical changes are those that directly affect the local pressure regime. As final crystallization approaches, the physical environment is dynamically unstable and the commonly encountered sequence of fracturing, residual-melt freezing, and mineralization represents related aspects of a continuous and in part virtually simultaneous process that transforms a residual, water-rich melt system to a system dominated by an evolved aqueous phase.

The main point of this discussion is to emphasize the element of continuity between the magmatic and ore-forming processes in the tin-granite environment. The essential mechanisms involved have been

discussed in the literature and applied to understanding individual deposits for some time. For example, Emmons (1934) considered the importance of volume changes accompanying aqueous phase separation, Raymond and others (1971) applied this concept to an understanding of the structural controls of tin mineralization at Wheal Jane, Cornwall, and Phillips (1973) examined the possible structural effects of retrograde boiling in shallow crustal environments. The data on the molal volume properties of water reported by Burnham and Davis (1971) further emphasize the tremendous effects that an evolved aqueous phase can initiate in a magmatic environment under certain conditions. Inhomogeneous and rapidly, even violently, changing pressure regimes are to be expected in these environments.

Importance of Depth in Environments of Tin Mineralization

The search for similarities among tin deposits is useful but much can also be learned by examining their differences. The most obvious differences are those that are defined by the spatial and structural nature of the tin-bearing areas. In this regard, the depth of formation of tin deposits is believed to be directly responsible for more of the major differences than any other single factor. To help clarify this, tin deposits can be grouped into five general categories which, according to their increasing depth of formation, are: (1) deposits formed at the surface, (2) deposits formed in near-surface environments, (3) deposits formed mostly exterior to parent granite bodies, (4) deposits formed within parent granite bodies, and (5) certain pegmatites. The general characteristics of these groups are as follows:

1. Deposits formed at the surface occur in rhyolite flows and domes and consist of hematite-cassiterite veinlets, veins, encrustations, and disseminations that are localized along joints, fractures, flow bands, intraformational breccias, or in cavities. The host rocks are commonly devitrified and may be replaced by zeolites and silica. Production is mostly from placers that are derived from the commonly low-grade lodes. Numerous examples of this type of deposit are found in Mexico, New Mexico, and Nevada.

2. Deposits formed in near-surface environments are structurally and mineralogically complex polymetallic veins and stockworks. They are associated with intrusive dike complexes and plugs that commonly grade into coeval volcanic rocks. Breccia structures, at least in part diatremes, are common. Hydrothermal alteration of the host rocks can be extensive and includes chloritization, sericitization, and silicification. The exceptionally rich tin-silver deposits of Bolivia are commonly cited as examples of this group, but others exist and the group may also include deposits such as those associated with ring-dike complexes in Brazil and Africa.

3. Deposits formed mostly exterior to parent granite bodies are probably the most abundant and economically important tin deposits of the world. They are commonly tin-tungsten-sulfide deposits, and quartz is the most important gangue mineral. The veins tend to be localized along porphyry dikes and can have a preferred orientation within a particular mineralized area. Zoning of metal distribution within mineralized districts or within individual veins is common. Alteration clearly is spatially related to mineralized structures and includes such types as greisenization, sericitization, albitization, and

tourmalinization. Postmineralization argillization is a distinct characteristic of some of these deposits. Some of the best examples of deposits in this group are the veins of Cornwall.

4. Deposits formed within parent granite bodies are characteristically low-grade deposits in which cassiterite occurs in disseminations, veinlet stockworks, and local pegmatitic pods or lenses within a composite pluton. Contacts between early- and late-crystallizing facies may act as structural traps and control localization of greisen and ore. In this situation, the greisen and ore are preferentially developed in the later crystallizing, generally fine-grained facies. Wolframite may occur in the deposit as well as fluorite, lithium-rich micas, and tourmaline. Examples of this group are the greisen deposits of the Erzgebirge and several deposits, such as the Anchor mine, in Tasmania and Australia.

5. Pegmatites that form tin deposits are commonly large discrete bodies that may or may not be directly associated with granite plutons. They characteristically occur in high-grade metamorphic terranes and are Precambrian in age. The grade of these deposits is low but their value may be increased by the presence of minerals other than cassiterite. In fact, columbite-tantalite is distinctly more common in cassiterite-bearing pegmatites than in any other type of tin deposit. Important tin-bearing pegmatites occur in the shield areas of Africa and Brazil.

Most of the world's tin deposits fall into the above groups but not all of them. An important exception is the "geosynclinal" deposits (Baumann, 1970, p. B68) that are stratabound and associated with submarine volcanic rocks.

The role of depth in determining the nature of the first two groups is rather clear: deposits formed at the surface in rhyolite flows and domes are essentially the result of *in-situ* processes that are lacking in significant tin-concentrating mechanisms, and deposits formed in near-surface environments can have all the complexities that characterize an essentially open magmatic-hydrothermal system. In the next two deeper groups the depth of formation influences the mobility of the residual melt and/or aqueous phase system. In deposits formed exterior to the parent granites, dynamic instability exists in the vicinity of the crystallizing pluton and late intrusions commonly accompany expulsion of the evolved aqueous phase. In deposits formed within the parent granites the evolved aqueous phase may be mobile within the host intrusive complex, where it is commonly localized in structural traps, but the increased pressure regime in the vicinity of the evolved aqueous phase does not exceed the confining abilities of surrounding rocks and its escape to higher levels is prevented. In the deeper levels where tin-bearing pegmatites are formed, the aqueous phase is a medium that facilitates transfer of materials in the residual environment, but it is not physically separated from the silicate components of the final residual system.

The above five-fold subdivision is arbitrary. Even though its purpose is to help clarify differences between tin deposits, it also helps to show that continuity exists among them. All gradations of spatial and structural relationships, from those of the surface environment to those of pegmatites, are to be expected. For example, the deposit at Mt. Bischoff, Tasmania (Groves and others, 1972) is associated with a radially oriented dike system and may have formed at a depth intermediate

between the near-surface environment and that of most deposits formed exterior to granite plutons. Some mineralized cupolas or cusps on granite plutons may be examples of deposits intermediate between those formed exterior and those formed interior to the parent granites. This would appear to be the case if the cupola represents mobile residual melt that is structurally trapped at the pluton-country rock contact, and if stockworks and greisen develop both within it and in adjacent country rocks. Unfortunately, it is not always clear whether mineralized cusps are developed in residual facies or simply represent localization of the mineralizing aqueous phase in a structural trap formed by the contact between earlier granite facies and the country rocks. The deposit at Lost River, Alaska (Sainsbury, 1964), is a possible example of a deposit that is intermediate between those formed interior and those formed exterior to the parent granite pluton.

The above emphasis on the role of depth in determining major spatial and structural differences between tin deposits is not unique to this discussion. Itsikson (1960) uses the depth of formation as one useful aspect of a categorization of regional relationships in tin-mineralized belts. Rudakova and Tikhomirov (1970, p. 89) state the "The reason for diversity of the types of tin deposits associated with intrusives is the formation of the latter at different depths in the earth," and Varlamoff (1974) has sketched out a rather complete classification of tin deposits that is based primarily upon their depth of formation. But even though depth of formation may be the most important single factor responsible for spatial and structural differences among tin deposits, it is not the only factor. Some others are the pre-emplacement physical nature of the country rocks, the influence of

tectonic displacements unrelated to the crystallizing pluton, and the absolute amount of water and other volatiles contained in the granite melt. The interaction of factors such as these and others helps to create an element of uniqueness for each deposit and, in light of the actual complexities of the magmatic-hydrothermal environments that form tin deposits, it is remarkable that so many similarities and indications of continuity among them exist. Because of this continuity, further clarification of the spatial and structural nature of tin deposits is likely to result in important steps toward understanding the dynamic nature of epizonal magmatic environments.

REFERENCES

Barker, D. S., 1970, Compositions of granophyre, myrmekite, and graphic granite: Geol. Soc. America Bull., v. 81, p. 3339-3350.

Barker, F., Wones, D. R., Sharp, W. N., and Desborough, G. A., 1975, The Pikes Peak batholith, Colorado Front Range, and a model for the origin of the gabbro-anorthite-syenite-potassic granite suite: Precambrian Res., v. 2, p. 97-160.

Barnes, D. F., 1971, Preliminary Bouguer anomaly and specific gravity maps of Seward Peninsula and Yukon flats, Alaska: U. S. Geol. Survey open-file map.

Barth, T. F. W., 1969, Feldspars: New York, John Wiley and Sons, 261 p.

Baumann, Ludwig, 1970, Tin deposits of the Erzgebirge: Inst. Mining Metall. Trans., v. 79, no. 762, p. B68-B75.

Boyle, R. W., 1970, The source of metals and gangue elements in hydrothermal deposits, *in* Pouba, Zdeněk, and Štemprok, Miroslav, eds., Problems of hydrothermal ore deposition: Internat. Union Geol. Sci., Ser. A, no. 2, p. 3-6.

Bradshaw, P. M. D., 1967, Distribution of selected elements in feldspar, biotite, and muscovite from British granites in relation to mineralization: Inst. Mining Metall. Trans., v. 76B, p. 137-148.

Burnham, C. W., and Davis, N. F., 1971, The role of H_2O in silicate melts, I. P-V-T relations in the system $NaAlSi_3O_8$-H_2O to 10 kilobars and 1000°C: Am. Jour. Sci., v. 270, p. 54-79.

Collier, A. J., 1902, A reconnaissance of the northwestern portion of the Seward Peninsula, Alaska: U. S. Geol. Survey Prof. Paper 2, 70 p.

———— 1904a, Tin deposits of the York region, Alaska: U. S. Geol. Survey Bull. 225, 61 p.

———— 1904b, The tin deposits of the York region, Alaska: U. S. Geol. Survey Bull. 229, 61 p.

Collier, A. J., Hess, F. L., Smith, P. S., and Brooks, A. H., 1908, The gold placers of parts of Seward Peninsula, Alaska: U. S. Geol. Survey Bull. 328, 343 p.

Csejtey, Béla, Jr., Patton, W. W., Jr., and Miller, T. P., 1971, Cretaceous plutonic rocks of St. Lawrence Island, Alaska--a preliminary report: U. S. Geol. Survey Prof. Paper 750-D, p. D68-D76.

Dalrymple, G. B., and Lanphere, M. A., 1969, Potassium-argon dating--principles, techniques, and applications to geochronology: San Francisco, W. H. Freeman and Co., 258 p.

Deer, W. A., Howie, R. A., and Zussman, J., 1967, An introduction to the rock-forming minerals: New York, John Wiley and Sons, 528 p.

Dewey, Henry, 1925, The mineral zones of Cornwall: Geologists' Assoc. Proc., v. 36, p. 107-135.

Dines, H. G., 1956, The metalliferous mining region of southwest England: Great Britain Geol. Survey Mem., 2 v., 795 p.

Duffield, W. A., and Jahns, R. H., 1975, Depth of emplacement of the El Pinal pluton, Baja California, Mexico [abs.]: Geol. Soc. America Abs. with Programs, Los Angeles.

Emmons, W. H., 1934, On the origin of certain systems of ore-bearing fractures: Am. Inst. Mining Metall. Engineers Tech. Pub. 561, 26 p.

Groves, D. I., 1972, The geochemical evolution of tin-bearing granites in the Blue Tier batholith, Tasmania: Econ. Geology, v. 67, p. 445-447.

Groves, D. I., Martin, E. L., Murchie, H., and Wellington, H. K., 1972, A century of tin mining at Mt. Bischoff, 1871-1971: Geol. Survey Tasmania Bull., no. 54, 310 p.

Hietanen, Anna, 1967, On the facies series in various types of metamorphism: Jour. Geology, v. 75, no. 2, p. 187-214.

Hopkins, D. M., and others, 1955, Permafrost and ground water in Alaska: U. S. Geol. Survey Prof. Paper 264-F, 146 p.

Hosking, K. F. G., 1967, The relationship between primary deposits [of tin] and granitic rocks: Internat. Tin Council, 1st Tech. Conf. on Tin, London, 1967, v. 1, p. 267-311.

Hutchinson, R. M., 1956, Structure and petrology of Enchanted Rock batholith, Llano and Gillespie Counties, Texas: Geol. Soc. America Bull., v. 67, p. 763-806.

Itsikson, M. I., 1960, The distribution of tin-ore deposits within folded zones: Internat. Geol. Rev., v. 2, p. 397-417.

Johnson, G. R., and Sainsbury, C. L., 1974, Aeromagnetic and generalized geologic map of the west-central part of the Seward Peninsula, Alaska: U. S. Geol. Survey Geophys. Inv. Map GP-881.

Keppel, David, 1940, Concentric patterns in the granites of the Llano-Barnet region, Texas: Geol. Soc. America Bull., v. 51, p. 971-1000.

Knopf, Adolph, 1908a, The Seward Peninsula tin deposits: U. S. Geol. Survey Bull. 345, p. 251-267.

———— 1908b, Geology of the Seward Peninsula tin deposits, Alaska: U. S. Geol. Survey Bull. 358, 71 p.

Krauskopf, K. B., 1970, The source of ore metals: Geochim. et Cosmochim. Acta, v. 35, p. 643-659.

Laves, Fritz, 1954, The coexistence of two plagioclases in the oligoclase composition range: Jour. Geology, v. 62, p. 409-411.

Lovering, T. G., 1972, Distribution of minor elements in biotite samples from felsic intrusive rocks as a tool for correlation: U. S. Geol. Survey Bull. 1314-D, p. D1-D29.

Meyers, A. T., Havens, R. G., and Dunton, P. J., 1961, A spectrochemical method for the semiquantitative analysis of rocks, minerals, and ores: U. S. Geol. Survey Bull. 1084-I, p. 207-229.

Miller, T. P., 1970, Preliminary correlation of Mesozoic plutonic rocks in the Bering Sea region [abs.]: Am. Assoc. Petroleum Geologists Bull., v. 54, no. 12, p. 2496.

———— 1972, Potassium-rich alkaline intrusive rocks of western Alaska: Geol. Soc. America Bull., v. 83, p. 2111-2127.

Miller, T. P., Barnes, Ivan, and Patton, W. W., Jr., 1975, Geologic setting and chemical characteristics of hot springs in west-central Alaska: U. S. Geol. Survey Jour. Res., v. 3, no. 2, p. 149-162.

Mitchell, A. H. G., and Garson, M. S., 1972, Relationship of porphyry copper and circum-Pacific tin deposits to paleo-Benioff zones: Inst. Mining Metall. Trans., v. 81, no. 786, p. B10-B25.

Moxham, R. M., and West, W. S., 1953, Radioactivity investigations in the Serpentine-Kougarok area, Seward Peninsula, Alaska: U. S. Geol. Survey Circ. 265, 11 p.

Noble, J. A., 1970, Metal provinces of the western United States: Geol. Soc. America Bull., v. 81, p. 1607-1624.

Nockolds, S. R., 1954, Average chemical composition of some igneous rocks: Geol. Soc. America Bull., v. 65, p. 1007-1032.

Norman, M. B., II, 1974, Improved techniques for selective staining of feldspar and other minerals using amaranth: U. S. Geol. Survey Jour. Res., v. 2, no. 1, p. 73-79.

Odihadze, G. L., 1967, Distribution of tantalum, niobium, tin, and fluorine in micas from granitoids of the greater Caucasus and Dzirula crystalline massif: Geochem. Internat., v. 4, p. 754-763.

Orville, P. M., 1963, Alkali ion exchange between vapor and feldspar phases: Am. Jour. Sci., v. 261, p. 201-237.

Phillips, E. R., 1964, Myrmekite and albite in some granites of the New England batholith, New South Wales: Geol. Soc. Australia Jour., v. 11, p. 49-60.

Phillips, W. J., 1973, Mechanical effects of retrograde boiling and its probable importance in the formation of some porphyry ore deposits: Inst. Mining Metall. Trans., v. 82, p. 90-98.

Ragland, P. C., Billings, G. K., and Adams, J. A. S., 1967, Chemical fractionation and its relationships to the distribution of thorium and uranium in a zoned granite batholith: Geochim. et Cosmochim. Acta, v. 31, no. 1, p. 17-33.

———— 1968, Magmatic differentiation and autometasomatism in a zoned granitic batholith from central Texas, U.S.A., *in* Ahrens, L. H., ed., Origin and distribution of the elements: New York, Pergamon, 1178 p.

Ramberg, H., 1962, Intergranular precipitation of albite formed by unmixing of alkali feldspar: Neues Jahrb. Mineralogie Abh., v. 98, p. 14-34.

Rattigan, J. H., 1964, Geochemical characteristics of Australian granitic rocks in relation to the occurrence of tin: Univ. of New South Wales, Sydney, Ph.D. thesis.

Rayment, B. D., Davies, G. R., and Willson, J. D., 1971, Controls to mineralization at Wheal Jane, Cornwall: Inst. Mining Metall. Trans., v. 80, p. B224-B237.

Reesor, J. E., 1958, Dewar Creek map area with special emphasis on the White Creek batholith, British Columbia: Canada Geol. Survey Mem. 292, 78 p.

Rudakova, Zh. N., and Tikhomirov, N. I., 1970, On sources of hydrothermal solutions and the depth of formation of the Transbaikalian tin deposits, *in* Pouba, Zdeněk, and Štemprok, Miroslav, eds., Problems of hydrothermal ore deposition: Internat. Union Geol. Sci., Ser. A, no. 2, p. 87-89.

Sainsbury, C. L., 1964, Geology of the Lost River mine area, Alaska: U. S. Geol. Survey Bull. 1129, 80 p.

———— 1969a, Geology and ore deposits of the central York Mountains, western Seward Peninsula, Alaska: U. S. Geol. Survey Bull. 1287, 101 p.

———— 1969b, The A. J. Collier thrust belt of the Seward Peninsula, Alaska: Geol. Soc. America Bull., v. 80, p. 2595-2596.

———— 1972, Geologic map of the Teller quadrangle, western Seward Peninsula, Alaska: U. S. Geol. Survey Misc. Geol. Inv. Map I-685.

———— 1975, Geology, ore deposits, and mineral potential of the Seward Peninsula, Alaska: U. S. Bur. Mines open-file report.

Sainsbury, C. L., and Hamilton, J. C., 1968, Geology of lode tin deposits: Internat. Tin Council, 1st Tech. Conf. on Tin, London, 1967, v. 1, p. 314-349.

Sainsbury, C. L., Hamilton, J. C., and Huffman, Claude, Jr., 1968, Geochemical cycle of selected trace elements in the tin-tungsten-beryllium district, western Seward Peninsula, Alaska--a reconnaissance study: U. S. Geol. Survey Bull. 1242-F, 42 p.

Sainsbury, C. L., Hedge, C. E., and Bunker, C. M., 1970, Structure, stratigraphy, and isotopic composition of rocks of the Seward Peninsula, Alaska [abs.]: Am. Assoc. Petroleum Geologists Bull., v. 54, no. 12, p. 2502-2503.

Sainsbury, C. L., Hudson, Travis, Kachadoorian, Reuben, and Richards, Thomas, 1970, Geology, mineral deposits, and geochemical and radiometric anomalies, Serpentine Hot Springs area, Seward Peninsula, Alaska: U. S. Geol. Survey Bull. 1312-H, 19 p.

Sainsbury, C. L., Kachadoorian, Reuben, Smith, T. E., and Todd, W. C., 1968, Cassiterite in gold placers at Humbolt Creek, Serpentine-Kougarok area, Seward Peninsula, Alaska: U. S. Geol. Survey Circ. 565, 7 p.

Sainsbury, C. L., Mulligan, R. R., and Smith, W. C., 1969, The circum-Pacific "tin belt" in North America: Internat. Tin Council, 2nd Tech. Conf. on Tin, Bangkok, 1969, v. 1, p. 123-148.

Sainsbury, C. L., and Reed, B. L., 1973, Tin: U. S. Geol. Survey Prof. Paper 820, p. 637-651.

Schuiling, R. D., 1967, Tin belts around the Atlantic: some aspects of the geochemistry of tin: Internat. Tin Council, 1st Tech. Conf. on Tin, London, 1967, v. 2, p. 529-550.

Shapiro, Leonard, 1967, Rapid analysis of rocks and minerals by a single solution method: U. S. Geol. Survey Prof. Paper 575-B, p. 187-191.

Shapiro, Leonard, and Brannock, W. W., 1962, Rapid analysis of silicate, carbonate, and phosphate rocks: U. S. Geol. Survey Bull. 1144-A, 56 p.

Sigafoos, R. S., 1958, Vegetation of northwestern North America, as an aid in interpretation of geologic data: U. S. Geol. Survey Bull. 1061-E, p. 165-185.

Spry, Alan, 1969, Metamorphic textures: New York, Pergamon, 350 p.

Steidtmann, Edward, and Cathcart, S. H., 1922, Geology of the York tin deposits, Alaska: U. S. Geol. Survey Bull. 733, 130 p.

Štemprok, Miroslav, 1967, The origin of tin-tungsten mineralization in the Erzgebirge: Mineralium Deposita, v. 2, p. 102-118.

———— 1971, Petrochemical features of tin-bearing granites in the Krušne Hory Mountains, Czechoslovakia: Japan Soc. Mining Geol. Spec. Issue 2, p. 112-118.

Štemprok, Miroslav, and Škvor, Premysl, 1974, Composition of tin-bearing granites from the Krušne Hory metallogenic province of Czechoslovakia: Loziskova Geologie Mineralogie, v. 16, p. 7-79.

Štemprok, Miroslav, and Sulcek, Zdenek, 1969, Geochemical profile through an ore-bearing lithium granite: Econ. Geology, v. 64, no. 4, p. 392-404.

Tischendorf, G., 1973, The metallogenetic basis of tin exploration in the Erzgebirge: Inst. Mining Metall. Trans., v. 82, p. B9-B24.

Tischendorf, G., Hosel, G., Lange, H., and Bolduan, H., 1971, The geochemical and structural control of the tin mineralization in the Erzgebirge: Japan Soc. Mining Geol. Spec. Issue 3, p. 15-19.

Turekian, K. K., and Wedepohl, K. H., 1961, Distribution of the elements in some major units of the earth's crust: Geol. Soc. America Bull., v. 72, p. 175-192.

Turner, F. J., 1968, Metamorphic petrology--mineralogical and field aspects: San Francisco, McGraw-Hill, 403 p.

Tuttle, O. F., and Bowen, N. L., 1958, Origin of granite in the light of experimental studies in the system $NaAlSi_3O_8$-$KAlSi_3O_8$-SiO_2-H_2O: Geol. Soc. America Mem. 74, 153 p.

Vance, J. A., 1961, Zoned granitic intrusions--an alternative hypothesis of origin: Geol. Soc. America Bull., v. 72, p. 1723-1728.

Varlamoff, N., 1974, Classification and spatio-temporal distribution of tin and associated mineral deposits, *in* Štemprok, M., ed., Metallization associated with acid magmatism: Acad. Sci. Czechoslovak, v. 1, p. 137-144.

Wahrhaftig, Clyde, 1965, Physiographic division of Alaska: U. S. Geol. Survey Prof. Paper 482, 52 p.

Wright, T. L., 1968, X-ray and optical study of alkali feldspar, II. An X-ray method for determining the composition and structural state from measurement of 2θ values for three reflections: Am. Mineralogist, v. 53, p. 88-104.